SNOW-PACK DEVELOPMENT AND GROUND-FROST PENETRATION IN THE BLACKSTONE UPLANDS, YUKON TERRITORY, CANADA.

by

Pascale Roy-Léveillée, B.Sc.

A thesis submitted to

the Faculty of Graduate Studies

in partial fulfillment of the requirements

of the degree of

Master of Science

Carleton University

Ottawa, Ontario

Your file Votre référence
ISBN: 978-0-494-33712-7
Our file Notre référence
ISBN: 978-0-494-33712-7

ABSTRACT

This thesis investigates snow-pack development and frost penetration in the Blackstone Uplands, Y.T. The purpose is to assess the use of an accessible reference site as an index of these conditions throughout the area. The project responds to local interest in improving management of snowmobile access to the region. Sixteen transects were monitored for snow depth in fall and winter 2006-07. Active-layer temperature was monitored by data logger during freeze-up. Below-normal snowfall permitted examination of snow-pack development with marginal conditions for snowmobile traffic. Prior to snow redistribution by wind, snow depth was controlled by elevation and the reference site had more snow than all valley-bottom sites. After the onset of blowing snow in the valley bottom, vegetation structure controlled snow depth and all sites had more snow than the reference site. Under conditions of little snowfall, ground-frost penetration at the reference site was slower than at all the monitored sites.

ACKNOWLEDGEMENTS

This project was funded by the NSERC Northern Research Chair at Carleton University. The Northern Scientific Training Program assisted with the costs of summer field work. The fall and winter data collection were funded through an NSERC Northern Internship at the Dawson office of the Government of Yukon Department of Environment.

Chris Burn provided guidance and support at every stage of this academic project. I am grateful to him for accepting to be my teacher and ensuring I never ran out of intellectual challenges. Dan Patterson generously helped me resolve numerous GIS puzzles while Jon Pasher, Ian Olthof, Sylvain Leblanc, and Junhua Li provided satellite-derived vegetation maps of the Blackstone Uplands. Jill Johnstone provided technical advice for vegetation characterisation and for the analysis of the collected data. Thank you also to Sean Carey for broadening my understanding of environmental modelling.

During my internship at the Department of Environment, Dorothy Cooley ensured I had the necessary logistical support, and Martin Kienzler provided welcome technical advice and assistance. Thank you to both for sharing their enlightening perspective on the relation between scientific research and resource management. I am also grateful to numerous helping hands in the field: Geoff Crammond, Geneviève Hétu, Julian Kanigan, Alice McCullough, Thai-Nguyen Nguyen, Seth Plunkett, Troy Pretzlaw, and André Zadrazil. During the final writing stage, the Yukon Geological Survey provided me with a peaceful and supportive work space.

Finally, thank you to Tr'ondek Hwech'in and Na-Cho Nyak Dun First Nations for allowing me to conduct research within their traditional territory.

TABLE OF CONTENTS

LIST OF TABLES

LIST OF FIGURES

CHAPTER 1
INTRODUCTION

1.1 Introduction

The purpose of this research is to investigate how topography and vegetation structure affect snow-pack development during early winter and to examine the rate of active-layer freezing under different snow packs in the Blackstone Uplands, Y.T. (Fig. 1.1a). The project was designed in response to local interest in improving management of snowmobile access to the region during the fall hunting season. Snowmobile traffic before ground freezing and in the absence of a protective snow cover may result in mechanical damage to vegetation, soil compaction, and changes in the ground thermal regime (Greller et al. 1974; Caissie 1999). Snow-pack thickness and the presence of frozen ground at a reference site (Fig. 1.1b) are currently used by local conservation officers in the decision to open the Blackstone Uplands to snowmobile access during the fall hunting season. This research examines whether snow-pack development and ground-frost penetration in the portion of the Blackstone Uplands which receives a high intensity of snowmobile traffic (Fig. 1.1b) can be effectively monitored using this reference site.

1.2 Spatial variability of the snow cover

Figure 1.2 summarises the environmental system and the processes affecting the development and erosion of the snow pack. Snow-pack development depends on time-dependent variables such as precipitation, wind speed and direction, air temperature, and relative humidity, as well as time-independent variables such as topography and vegetation structure (Pomeroy et al. 1997; Liston and Sturm 1998; Marks et al. 2002;

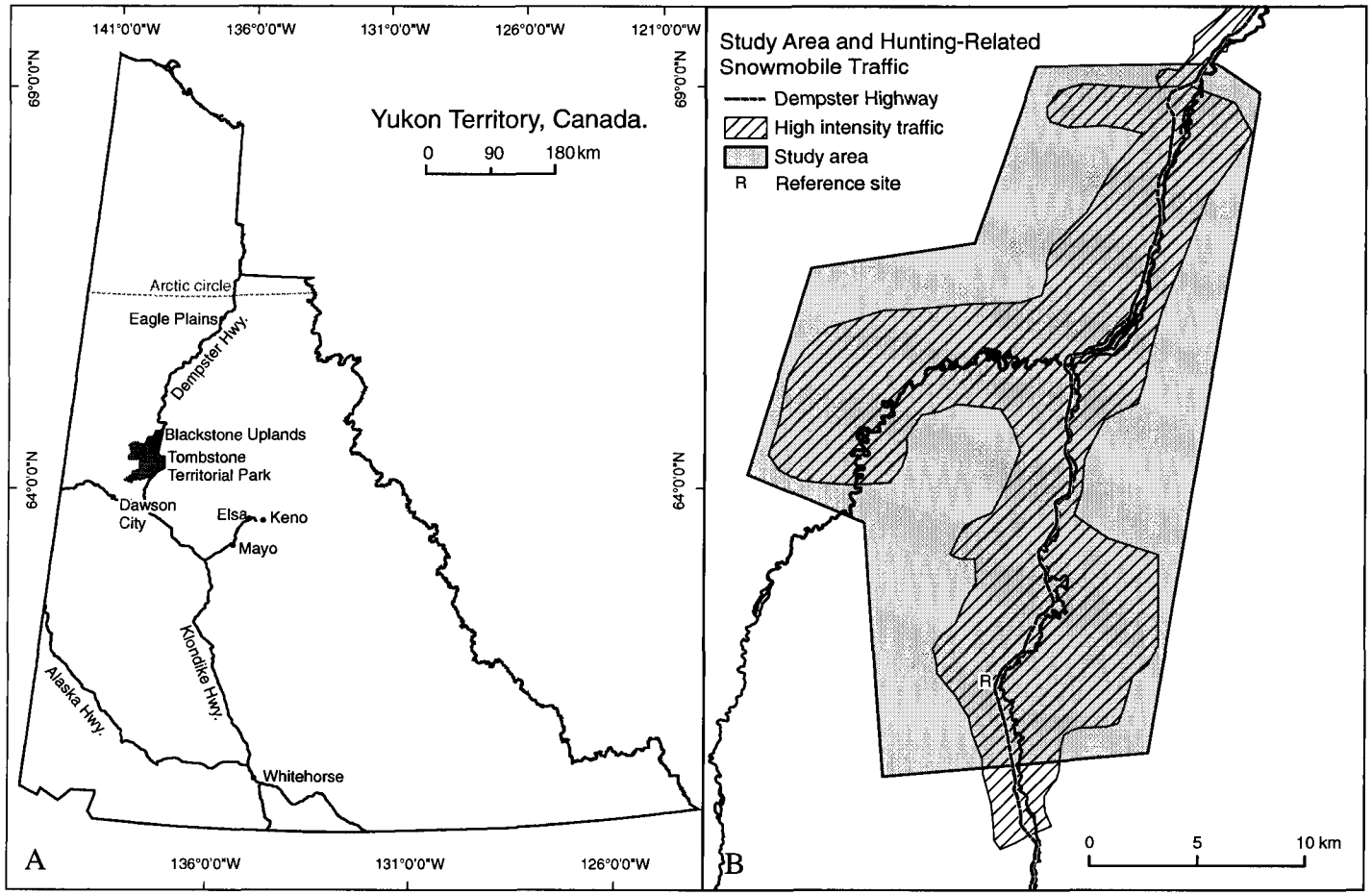

Fig. 1.1 (A) Location of the Blackstone Uplands within the Yukon Territory, and (B) study area boundaries in relation to the zone of high-intensity snowmobile traffic during the fall hunting season, in the Blackstone Uplands (Dorothy Cooley, personal communication 2006). Data sources: Geomatics Yukon, Government of Yukon; Geobase®; Department of Natural Resources Canada.

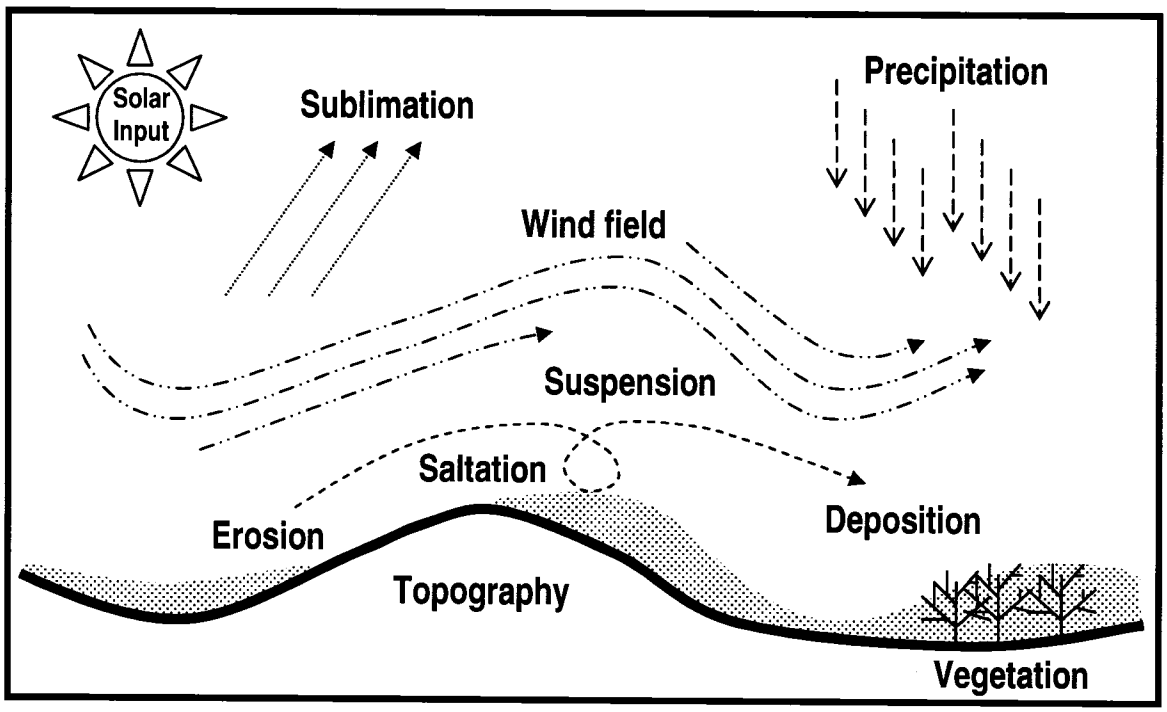

Figure 1.2 Key processes affecting snow-pack development and erosion.

Winstral and Marks 2002; Durand et al. 2004). This project focuses on the relative effects of vegetation cover and topography on the evolution of the snow pack in late fall.

1.3 Frost penetration

The ground above permafrost which thaws during the summer and freezes in the winter is called the active layer (Mueller 1947; Burn 1998). In the fall, freezing proceeds from the ground surface downwards and from the top of the permafrost upwards. Previous research has shown that the timing and rate of active layer freeze-back depends on air temperature, active-layer thickness, soil moisture, soil thermal properties, mean annual permafrost surface temperature, and development of the snow cover (Zhang et al. 1996; Osterkamp and Romanovsky 1997; Romanovsky and Osterkamp 1997). Few studies have investigated the timing of freezing in the discontinuous permafrost zone (Carey and Woo 2005). This thesis examines the relations among the timing of active-layer freezing, snow depth, topography, and vegetation cover in an alpine area underlain by discontinuous permafrost (Brown 1967).

1.4 Thesis objectives

The objectives of this research were to 1) investigate the effects of topography and vegetation structure on snow-pack development during early winter in the Blackstone Uplands, Y.T., 2) examine the rate of active-layer freezing under different snow packs, and 3) compare and relate snow-pack development and frost penetration over the high-intensity snowmobile-traffic corridor to snow-pack development and frost penetration at the reference site, for the fall and early winter 2006.

1.5 Methods

Fifteen transects for measurement of vegetation and snow characteristics were located through the study area to represent four vegetation structure classes and four elevation classes. A transect was also established at the reference site currently used by local conservation officers. Most sites were located in open, flat areas such as wide valleys, long benches, and broad plateaus which characterize the local landscape and constitute favourite travel corridors for snowmobile-assisted hunting. Vegetation structure and composition was characterised during summer 2006. The depth of the active layer was measured in early September 2006, and temperature sensors were installed through the active layer and connected to a data logger at nine sites, including the reference site. Snow depth was monitored along the transects from October 2006 to January 2007. Ground temperature measurements were recovered in December 2006. The descriptors showing the strongest relation to snow depth were identified using correlation analysis. Variations in the rate of ground freezing between the nine sites equipped with temperature sensors were examined in relation to snow depth, vegetation cover, and topography.

1.6 Thesis structure

The thesis is presented in six chapters. The following chapter presents the factors controlling spatial variability in snow accumulation and frost penetration in mountainous terrain. Chapter three introduces the biophysical setting of this study, and discusses the geomorphology, climate, and vegetation structure across the study area. It also presents the criteria used in selecting the location of the transects and sampling stations and the

methods used for data collection. Chapter four describes the transects in relation to vegetation cover and topography. Chapter five presents snow-pack development and active-layer freezing along the transects. It examines the development of the snow pack and the timing of active-layer freeze-back in relation to topography and vegetation structure, and effectiveness of the reference site is discussed. The final chapter concludes this thesis with a summary of results and discusses implications for the management of snowmobile traffic in early winter in the Blackstone Uplands.

CHAPTER 2
SNOW-PACK DEVELOPMENT AND FROST PENETRATION IN MOUNTAINOUS TERRAIN

2.1 Introduction

This chapter discusses the main factors controlling snow-pack development and ground freezing in mountainous terrain. To understand the influence of topography and vegetation structure on the snow pack, the factors affecting precipitation and redistribution of snow by wind must be examined. Specifically, the influence of elevation on precipitation, and the influence of topographic features and vegetation structure on the erosion and deposition of snow will be discussed. Similarly, to understand the relations between topography, snow cover, and ground freezing, the process of frost penetration in the ground will be reviewed, and the influence of the snow-cover on surface temperatures will be discussed.

2.2 Snow-pack development in mountainous terrain

The snow pack consists of layers of snow and ice on the ground. The rate of snow-pack development can be described according to the snow accumulation flux ($Q_{surface}$) at the surface of a given homogenous landscape element (Pomeroy et al. 1997):

$$Q_{surface} = Q_p - \frac{dQ_t}{dx}(x) - Q_s \qquad (2.1)$$

The snow precipitation flux, Q_p (kg/m^{2}s), varies over short distances in mountainous areas, and is largely controlled by orographic effects. The change in the rate of snow transport, Q_t (kg/ms), over horizontal distances, x (m), results in the erosion and deposition of snow as wind accelerates and decelerates over a heterogeneous surface.

Finally, Q_s (kg/m^{2}s) represents the portion of the snow pack lost to sublimation during snow transport by wind.

2.3 Precipitation in mountainous terrain

The response of airflow to the presence of orography sets the three-dimensional pattern of condensation from which precipitation results (Roe 2005). Commonly, the forced ascent of an air mass encountering mountainous terrain results in cooling of the air mass, a decreased capacity to hold moisture, and a general increase in precipitation on the windward side. Descent of the air mass on the lee side leads to warming and drying, and precipitation is suppressed (Roe 2005). In the Blackstone Uplands, weather systems travelling from the Pacific Ocean generally result in increased precipitation on southeast slopes (Wahl 2004). Weather systems travelling from the north or the east can result in increased precipitation on northern and eastern slopes, but this is less frequent (Wahl 2004). In the Yukon, the general rate of precipitation increase with elevation has been estimated as 8% per 100 m, up to a maximum near 1500 m to 2000 m elevation, above which precipitation tends to slowly decrease (Wahl 2004).

As elevation increases, a greater fraction of the precipitation occurs as snowfall due to the lower temperatures (Barry 1992). In central Yukon, for instance, the mean annual precipitation and the mean fraction of precipitation occurring as snowfall increase between Mayo (Fig. 1.1), elevation 504 m, and Keno (Fig. 1.1), elevation 1472 m (Table 2.1). The number of days with snowfall and the duration of the snow cover also increase with elevation (Yoshino 1975; Jackson 1978; Slatyer et al. 1984). However, the relation between elevation and depth of snow on the ground is not straightforward (Meiman 1970;

Table 2.1 Mean annual precipitation and fraction of precipitation occurring as snow in Mayo, Elsa, and Keno from 1974 to 1982 (modified from Côté 2002, Table 3.1)

Location	**Mayo**	**Elsa**	**Keno**
Elevation (m)	504	914	1472
Total precipitation (mm)	324	393	552
Snow fraction (%)	35	46	52

Caine 1975; Anderton et al. 2004), as it is complicated by the effects of wind and lower temperatures on snow deposition, metamorphism, and erosion.

2.4 Deposition and metamorphism of snow

During snowfall, wind speed affects how snow will be packed when it lands on the surface. In light winds, dendritic crystals may form floccular aggregates and accumulate in a layer of very low density snow (10 kg m^{-3}) (Langham 1981). In turbulent conditions, snow crystals may bounce or be dragged along the surface, resulting in comminution of the crystals (Langham 1981). The simplified shapes created through this process can be packed much more closely and result in a denser snow surface (400 kg m^{-3}) than would otherwise occur (Langham 1981).

During the first few hours after new snow is deposited, the snow pack begins to consolidate (Langham 1981). Dendritic and needle-like crystals decompose into fragments. When the air and ground temperatures are similar, the temperature gradient across the snow pack is minimal. These conditions result in slow crystal growth (Colbeck 1983). Under equi-temperature conditions, water tends to evaporate from convex surfaces and condense on concave surfaces, as water vapour pressure tends to decrease from a convex surface to a concave surface (Li and Pomeroy 1997). This causes the rounding of particles. Water vapour also condenses in the concave surfaces resulting from contact between the particles, thus causing sintering of the snow pack. Sintering increases mechanical continuity in the snow pack, and is responsible for the increased strength and hardness of the snow (Colbeck 1997). The rate of sintering is low in the cold and dry snow conditions typical of northern continental climates (Colbeck 1997).

Cold air temperatures may result in a steep temperature gradient between the warmer ground surface and the snow surface. There is a net transfer of vapour from the warmer parts of the snow pack where saturated vapour pressure is relatively high to the colder parts where saturated vapour pressure is low (Langham 1981). Grain growth is fed by water vapour transport through the pores of the snow. Water vapour condenses on the bottom of the snow grain, and sublimates from the top (Yosida 1955). The rates of condensation and sublimation are much higher than the rate of grain growth, thus allowing the grains to change form readily (Sturm and Benson 1997). One out of ten grains grows by a factor 2 or 3, while the other grains shrink and disappear in order to supply water vapour for growth (Sturm and Benson 1997). This process dominates at the base of the snow pack, near the ground surface. The snow crystals developing under these conditions have angular, facetted shapes (Schaerer 1981) and grow to become vertically aligned, striated, cup-shaped crystals called, in aggregate, depth hoar. In the subarctic, depth-hoar crystals commonly form a significant portion of the snow pack. Depth-hoar crystals are large, poorly bonded, and loosely spaced, thus creating a weak layer in the snow cover (Schaerer, 1981).

Solar radiation can result in the occurrence of melt-freeze cycles leading to accelerated densification of the snow pack (Langham 1981). Melt–freeze grains are amorphous, multicrystalline, solid within, and well-bonded to their neighbours (Colbeck 1997). Melt-freeze metamorphism is most significant in warmer conditions, possibly during the spring prior to the period of active melt.

2.5 Redistribution of snow by wind

In windswept environments, snow transport by wind controls the spatial distribution of snow-pack thickness (Pomeroy et al. 1993; Liston and Sturm 1998; Anderton 2004). The erosion of snow in some areas and formation of drifts in others reflect the effects of the surface on wind speed. As wind speed increases, so does the ability to erode and transport snow, while a decrease in wind velocity results in partial deposition of the transported load (Liston and Sturm 1998). The rates of erosion, deposition, and sublimation are controlled by aspects of the topography and vegetation which affect wind speed near the surface.

2.5.1 Snow erosion

Erosion and transport of snow begin when the force exerted on the snow particles by the wind exceeds the forces holding the particles in the snow pack. This occurs when the shear velocity of the wind at the snow surface, μ_* (m/s), exceeds the threshold shear velocity μ_{*_t} (m/s) of the snow cover. The shear velocity μ_* is given by :

$$\mu_* = \mu_r \frac{\kappa}{\ln\left(\frac{Z_r}{Z_0}\right)} \tag{2.2}$$

where μ_r (m/s) is the wind speed at reference height Z_r, κ is von Karman's constant, and Z_0 is the roughness length of the surface (see below) (Liston and Sturm 1998). The threshold shear velocity μ_{*_t} depends on the temperature, size, shape, density, and cohesion of the snow particles.

Spatial variations in forces driving and resisting snow erosion in the field are complicated by topography, vegetation cover, and snow crystal form, and it is difficult to

predict the occurrence of blowing snow on a deterministic, physical basis (Li and Pomeroy 1997a). Li and Pomeroy (1997b) used hourly wind speed at 10 m height, snow age, and air temperature to examine the occurrence of blowing snow on a probabilistic basis at manned weather stations in the prairies or western Canada. They found that the probability of occurrence of blowing snow increases with wind speed, and decreases with air temperature and age of the snow pack. The effect of an increase in wind speed on the probability of blowing snow is greater at lower temperature, when the snow pack is less cohesive and hence less resistant to erosion. At very cold temperatures however, this sensitivity to changes in wind speed begins to decrease. Similarly, the probability of occurrence of blowing snow declines when air temperature descends below -25°C. Typical μ_{*_t} values range from 0.15 to 0.25 m/s (0.54 to 0.9 km/hr) for fresh, loose, dry snow, and from 0.25 to 1.0 m/s (0.9 to 3.6 km/hr) for consolidated, wind-hardened, dense, or wet snow (Kind 1981; Pomeroy et al. 1993).

2.5.2 Snow transport

There are two distinct modes of transport for blowing snow: saltation and suspension. In saltation, snow particles bounce along the surface in a layer rarely exceeding a few centimetres in thickness (Takeuchi 1980; Kikuchi 1981; Kind 1981), dislodging other particles as they land and return to the surface. The proportion of snow transported above any specific height increases with mean wind speed (Pomeroy et al. 1993). When μ_* is greater than approximately $5\,\mu_{*_t}$ the vertical component of turbulent air flow near the surface exceeds the terminal fall velocity of the particles (Kind 1981). Snow particles are lifted above the saltation layer, and become part of the suspended snow load which extends to the top of the boundary layer (Pomeroy et al. 1993). Transported snow

increases with fetch length, which is the distance from a topographic obstacle, until saturation of the snow-transport capacity (Takeuchi 1980). Broad valleys running parallel to dominant wind directions, such as the Blackstone River valley, provide optimal conditions for snow transport. While the rate of saltation increases linearly with wind speed, the capacity of an airflow to transport snow is proportional to the fourth power of its speed. The difference between the rate of saltation and the rate of total snow transport implies that saltation represents a decreasing proportion of snow transport as wind speed increases (Pomeroy et al. 1997).

2.5.3 Sublimation

Sublimation is the transfer of snow-crystal mass to water vapour (Pomeroy et al. 1997). Blowing-snow events create optimum conditions for high sublimation rates due to a high particle surface area to volume ratio, ventilation of blowing snow particles, and an atmospheric water vapour deficit (Pomeroy et al. 1997). Fifteen to forty-five percent of the snow cover can be removed through sublimation during snow transport by wind (Marsh 1999). The snow surface can also exchange moisture with the atmosphere by sublimation under stable conditions, but at a greatly reduced rate (Liston and Sturm 1998).

2.6 Effects of topography on snow-pack erosion and deposition

2.6.1 Elevation

The lower air temperatures at high elevations imply increased snow precipitation and reduced melt losses, which combine to increase snow accumulation. On the other hand, low temperature also reduces the rate of sintering, retarding consolidation of the snow

pack. This increases the vulnerability of the snow pack to erosion, as μ_{*_t} is lower for an unconsolidated snow pack (Pomeroy et al. 1997). Higher elevations are also generally subject to increased wind speeds (McKay and Gray 1981; Wahl et al. 1987). Thus, as elevation increases, snow and wind conditions become more favourable to high rates of erosion of the snow pack. As a result, after redistribution by wind, snow depth is weakly correlated to elevation alone, but is better associated with indices combining several terrain parameters (Meiman 1970; McKay and Gray 1981; Winstarl and Marks 2002; Anderton 2004).

2.6.2 Topographic sheltering

Compression of air flow over a convex microtopographic feature, such as a ridge or a hill, causes acceleration of the air, increased snow transport capacity, and increased scour rates (Barry 1992). Downwind of a feature, the expansion of the airflow results in decreased air speed, reduced snow-transport capacity, and snow deposition (Windstral et al. 2002). Higher wind speed and steep slope breaks such as cliffs may cause separation of the airflow from the surface and the development of a lee eddy (Fig 2.1). These conditions commonly result in the formation of snow drifts (Winstral and Marks 2002). Flow separation sometimes also occurs upwind of steep obstacles (Whiteman 2000).

Lapen and Martz (1993) developed a series of indices to quantify the level of wind sheltering or exposure provided by topography in the prairie landscape. These indices allow the directional representation of relief and fetch. For modelling the effect of topography in mountainous terrain, Purves et al. (1998) used a simple sheltering index based on slope and dominant wind direction to produce a map of shelter zones in their study area, Aonach Mor, in Scotland. Winstral et al. (2002) tested three terrain

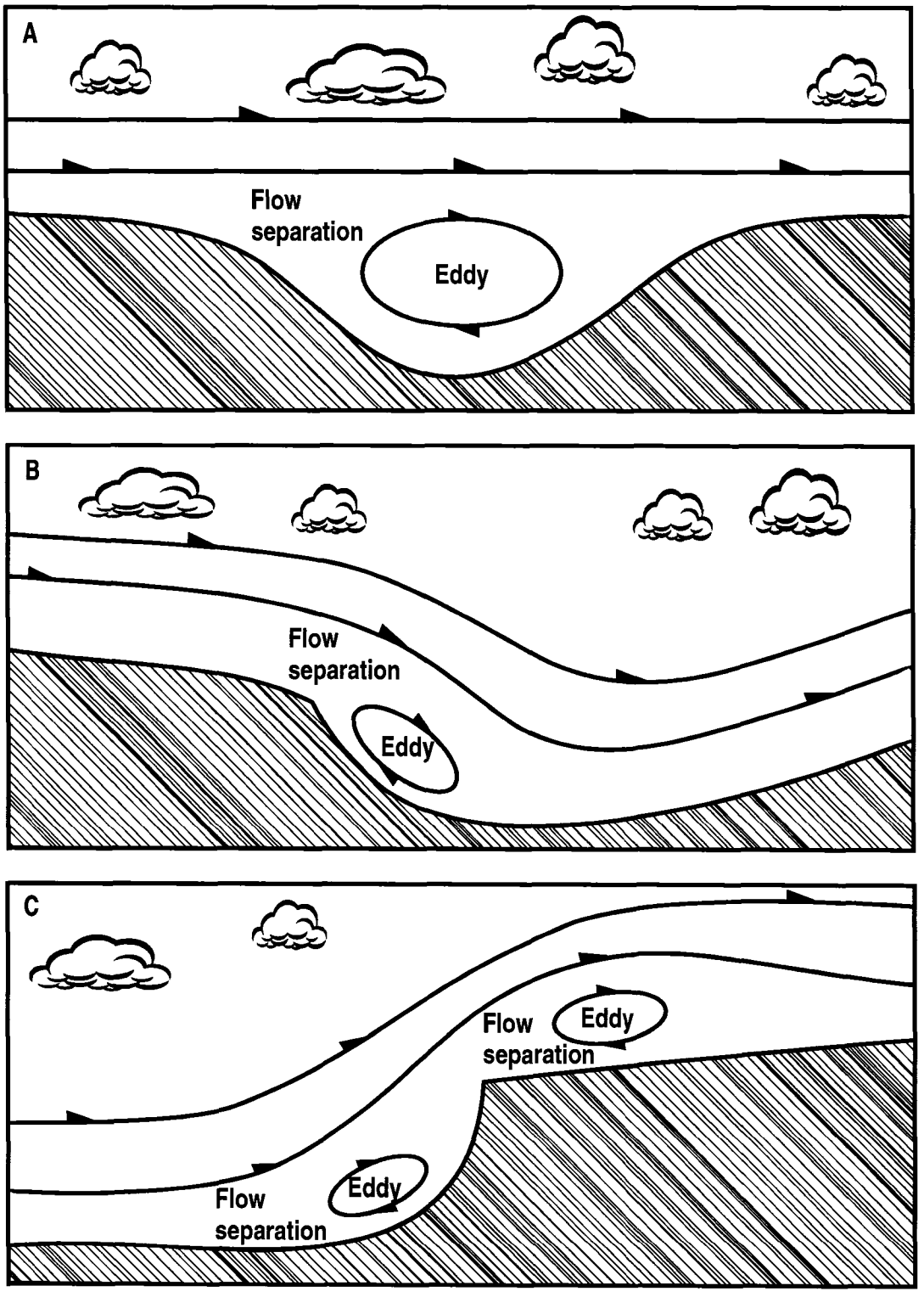

Fig. 2.1 Flow separation (A) over a lee slope in a valley, (B) below a steep slope break, and (C) above an obstacle and on the upwind side of a steep slope break. Modified from Scorer (1978), Fig. 5.18i, 5.18ii, and 5.18iii, pp.207-208.

parameters based on upwind terrain characteristics. These parameters quantified: (1) topographic sheltering/exposure to prevailing winds, (2) potential for upwind flow separation, and (3) exposure of potential flow separation zones located upwind of each cell in a digital elevation model. They found that sheltering provided by upwind terrain within 100 m was the strongest predictor for snow distribution at Green Lakes Valley, Colorado. Sheltering was based on a calculation of the maximum slope S_x, in the upwind direction A, for every point defined by (x_i,y_i), and was calculated according to:

$$S_{x_A}(x_i, y_i) = \max\left[\tan\left(\frac{E(x_v, y_v) - E(x_i, y_i)}{\sqrt{\left[(x_v - x_i)^2 + (y_v - y_i)^2\right]}}\right)\right] \quad (2.3)$$

where E is the elevation, and (x_v,y_v) represents all sets of cell coordinates along the vector defined by (x_i,y_i), A, and the maximum distance of 100 m. Using a similar sheltering index in Izas Catchement, Spain, Anderton (2004) found that performance of the index was increased by averaging for every direction rather than focussing on the angle of the prevailing winds.

2.6.3 Aspect

Due to the sheltering effect of ridges, leeward slopes accumulate snow while exposed windward slopes are subject to higher rates of erosion. Aspect also affects incoming solar radiation, with south-facing slopes receiving the highest amount of radiation in the northern hemisphere (Wahl et al. 1987). Shading from the surrounding topography can also greatly reduce the amount of solar radiation reaching a portion of the landscape. Variations in incoming solar radiation result in different melting rates. Increased solar radiation on south slopes can also result in instability effects and the resulting airflow increases the rate of sublimation from the snow pack (Barry 1992). In the present case,

the impact of solar radiation on development of the snow pack is limited by the rapid decrease in solar radiation in the subarctic in late fall and early winter and by prevailing cold air temperatures.

2.6.4 Microtopography

Similar to larger topographic features, convex or concave microtopography alters the wind speed by causing the concentration and expansion of the airflow at the ground surface. Drifts can form on the downwind side of banks, cliffs, rocks, and similar features representing a significant break in slope along the surface. The size of the resulting drift is proportional to the disruption in wind flow, with very small drifts forming near grass tussocks and large drifts forming below steep river banks. Beyond their individual influence on the wind flow, the general distribution of microtopographic features over the landscape increase surface friction and constitute surface roughness, similar to the effect of vegetation cover.

2.7 Effects of the vegetation cover on snow-pack development

2.7.1 Aerodynamic properties of the vegetation cover

Vegetation increases surface roughness, causes frictional drag between the landscape and the lower atmosphere, and causes a general reduction of wind speed near the surface by changing the aerodynamic properties of the ground. This reduces the effective shear stress applied to snow particles at the surface (Liston and Sturm 1998). An increase in surface roughness caused by a shrubby area in the tundra, for example, results in a decrease in wind speed near the surface, and in deposition of part of the transported snow load in and behind the shrubs (Sturm et al. 2001).

The roughness length Z_0 is used to describe the aerodynamic property, or roughness, of a given surface. It is the calculated height above the ground surface at which the extrapolated wind speed would equal zero (Dong et al. 2001). Z_0 is a key parameter of many snow distribution models, representing the effect of the vegetated surface on wind speed and snow deposition (Liston and Sturm 1998; Essery et al. 1999; Essery and Pomeroy 2004). The roughness length of a vegetation cover depends on the geometry of the vegetation structure (Lettau 1969), and increases with canopy height and vegetation density (Dong et al. 2001).

Estimates of roughness length can be obtained from measurements of canopy height and leaf-area index (Raupach 1994). Leaf-area index (LAI) is the integral of the area of leaf surface through the entire canopy depth (Kaimal and Finnigan 1994). LAI measurements recorded with a LiCor LAI-2000 optical canopy analyser, as in this study, rather correspond to the plant area index, as all plant parts are included in the reading. LiCor LAI-2000 measurements of LAI have shown good correlation with total above-ground plant biomass in the foothills of the Brooks Range, Alaska (Shippert et al.1995), an area with a vegetation cover structurally similar to the Blackstone Uplands. Allometric relations between leafy biomass and woody biomass have been identified for various shrubs (Brown 1976; Niklas 1994; Martínez and López-Portillo 2003) and it is likely that LAI measured under shrubs during leaf-out provides an indication of the perennial canopy structure affecting surface roughness in winter. LAI is a convenient variable for estimation of roughness length as it is easily obtained with a plant canopy analyser (Welles and Norman, 1991), and may also be derived by calibration of satellite imagery for the study area as a whole (Shippert et al. 1995; Olsson and Pilesjö 2002).

2.7.2 Snow-holding capacity

Snow accumulates in a vegetated area until it exceeds the snow-holding capacity of the vegetation structure. Any additional snow is available for wind transport (Liston and Sturm 1998). The protection from wind erosion offered by vegetation depends on canopy height, vegetation density, and wind speed (Pomeroy et al. 1997). For uniform and closely planted agricultural crops snow-holding capacity is generally 1 cm to 5 cm below the maximum stem height (Pomeroy et al. 1997). Natural vegetation covers often have irregular structures with multiple layers and the snow-holding capacity can be more difficult to assess. For modelling purposes, natural vegetation has been assigned a static snow-holding capacity based on mean vegetation height, or based on a subjective evaluation of the properties of the vegetation cover (Liston et al. 1998; Prasad et al. 2001; Liston et al. 2002). Areas covered with taller, denser shrubs are assigned a higher snow-holding capacity than areas where vegetation structure is minimal, such as open areas dominated by mosses and graminoids (Table 2.2) (Liston et al. 2002).

2.7.3 Vegetation and snow stratigraphy

The deeper snow associated with tall and dense vegetation covers contains a higher percentage of depth hoar (Sturm et al. 2001). In comparison to other snow types, depth hoar often has a very low density, a very low thermal conductivity (Sturm and Johnson 1992; Zhang et al. 1996), and is a good insulator of the ground. This contributes to higher ground temperatures in shrubby areas. In an arctic tundra landscape in Alaska, Sturm et al. (2001) found that snow–ground interface temperatures measured in April were 3°C higher in shrub areas than in non-shrub areas, contributing to higher ground temperatures in shrub-covered areas (Sturm et al. 2001).

Table 2.2 Snow-holding capacity for various vegetation covers (Liston and Sturm, 1998).

Vegetation cover	Mean canopy height (m)	Snow-holding capacity (m)
No vegetation	0	0.05
Tussock tundra	0.15	0.10 – 0.30
Shrubland	0.40	0.40

2.8 Freezing of the active-layer

Most of the Blackstone Uplands is underlain by permafrost (Brown 1967). The active layer above permafrost is frozen in winter, thaws during the spring and summer, and begins to freeze again during fall when the ground surface temperature drops to near 0°C. Freezing progresses both downwards from the ground surface and upwards from the top of the permafrost (Romanovsky and Osterkamp 1997). Over relatively "warm" permafrost, up-freezing may account for less than 10% of the active layer while it could account for 25% or more in areas underlain by "cold" permafrost (Burn 2004).

The soil between the two progressing freezing fronts remains isothermal at a temperature just below 0°C for the duration of the phase change. This interruption in cooling is called the zero curtain, and is caused by the release of latent heat as soil moisture freezes. The end of the zero curtain at a specific point below the surface is generally marked by a rapid decrease in ground temperature (Osterkamp and Romanovsky 1997), marking the passage of the freezing front past this point (Fig. 2.2). The rate of active-layer freezing in the fall is controlled by air and ground surface temperatures, snow depth, water content, depth of active layer, the thermal properties of the ground, and the thermal conditions below the active layer.

2.9 Stefan's solution for the freezing of the active layer

Stefan's solution for the progression of a freezing front (Carslaw and Jaeger 1959) has been applied in various forms to model penetration of frost into the ground as a function of time (Nelson and Outcalt 1983; Riseborough, 2001; Carey and Woo 2005). It allows for a simple representation of ground freezing based on one-dimensional heat transfer, but has several limitations. Stefan's solution assumes a constant ground surface

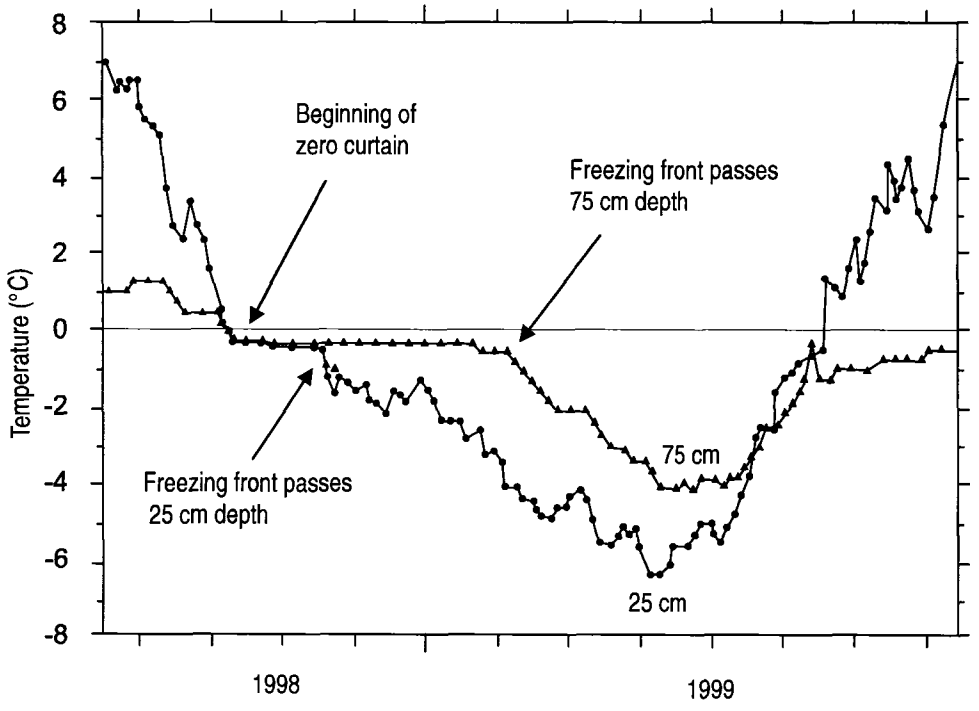

Fig. 2.2 Soil temperature series at depths of 25 cm and 75 cm from the Illisarvik experimentally drained lake on Richards Island, western Arctic coast, August 1998-1999. The active-layer depth is up to 1 m at this site (modified from Burn 2004, Fig. 3.3.6, p.402).

temperature during freezing and uniform soil thermal properties. It also assumes all freezing takes place at 0°C, which implies that all heat flow is used to extract heat from the freezing front, and that the temperature gradients in both layers are linear (Riseborough 2001). This assumption is acceptable if the amount of latent heat released is much greater than the sensible heat of the ground, a condition more easily fulfilled by soils with a high moisture content (Lunardini 1981; Carey and Woo 2005). Stefan's solution also ignores convective effects and assumes all heat transfer is through conduction, which is problematic when groundwater flow is involved (Mackay 1997).

Stefan's solution relates the depth of freezing Z_t (m) to the amount of time t (s) elapsed since the beginning of freezing as follows :

$$Z_t = \sqrt{\frac{2\lambda T_s t}{L}} \tag{2.4}$$

where L (Jm^{-3}) is the volumetric latent heat of fusion, T_s (°C) is the temperature at the surface, and λ ($Wm^{-1}{}^{o}C^{-1}$) is the thermal conductivity of the soil. The rate at which the freezing front progresses downwards is given by:

$$\frac{dZ_t}{dt} = \frac{1}{2}\sqrt{\frac{2\lambda T_s}{tL}} \tag{2.5}$$

which indicates that the rate of freezing will decrease with time.

2.10 Thermal properties of the ground

The thermal conductivity (λ) of the soil is the ability of a material to transmit heat by conduction (Carslaw and Jaeger 1959; Andersland and Anderson 1978). Table 2.3 presents the thermal conductivity and heat capacity of various ground materials. In the case of a very porous soil material such as peat, the thermal properties of the ground

reflect, mostly, the thermal properties of the material which fills the pore spaces. The thermal conductivity of ice is four times that of water, and one hundred times that of air (Table 2.3). As a result, the presence of ground moisture and whether it is in a solid or liquid phase at a given temperature is an important control on the thermal conductivity of the ground.

During freezing of the active layer, the release of latent heat from soil moisture dominates thermal conditions in the soil. Due to its heat capacity, water must release 4.2 x 10^6 J m^{-3} to reduce its temperature by one degree. At the freezing point however, an additional 3.33 x 10^8 J m^{-3} of latent heat must be removed before the temperature can decrease (Williams and Smith 1989). The latent heat released by soil moisture during freezing thus reduces the rate of frost penetration, and prolongs the duration of the zero curtain.

Though most of the groundwater freezes during the zero curtain, a portion of soil moisture is prevented from freezing at 0°C in organic soils and soils with high silt or clay content. This depression of the freezing point is due to high solute content, confinement in restricted pore space, or adsorption by charged soil particles (Burn 2004). Large amounts of soil moisture in fine-grained soils may result in a very slow decrease of ground temperatures following the freeze-up of the active layer (Osterkamp and Romanovsky 1997), as the apparent thermal diffusivity is still affected by the release of latent heat.

2.11 Air and ground surface temperatures

The ground surface temperature is governed by air temperature, but has greater spatial variability due to site-specific factors which may influence the microclimate (Klene et al.

Table 2.3 Thermal properties of some ground materials (data from Burn, 2004, Table 3.3.1 and Berry, 1981, Table 2.6). Wet peat has a volumetric water content of 0.8, while wet sand and clay have volumetric water contents of 0.4.

	Thermal conductivity λ (W m^{-1o} C^{-1})	**Volumetric heat capacity** C (10^6 J $°C^{-1}$ m^{-3})	**Thermal diffusivity** K (m^2 s^{-1})
Air	0.022	0.00086	26 x 10^{-6}
Water	0.56	4.2	0.13 x 10^{-6}
Ice	2.2	1.9	1.2 x 10^{-6}
Peat (dry)	0.060	0.5	0.10 x 10^{-6}
Peat (wet)	0.50	3.9	0.12 x 10^{-6}
Peat (frozen)	1.1	1.6	0.68 x 10^{-6}
Sand (dry)	0.29	1.3	0.22 x 10^{-6}
Sand (wet)	2.2	2.9	0.76 x 10^{-6}
Clay (dry)	0.25	1.3	0.19 x 10^{-6}
Clay (wet)	1.6	2.9	0.55 x 10^{-6}
Limestone	2.9	2.5	1.2 x 10^{-6}
Granite	2.0	2.1	0.95 x 10^{-6}

2001; Taras et al. 2002). Snow is the most important factor controlling ground surface temperatures in winter, and local differences in the snow cover can cause significant variations in the ground thermal regime (Smith 1975). Compared to other surface materials, snow has low thermal conductivity and its presence on the ground surface reduces heat flow from the ground to the atmosphere (Goodrich 1982; Sturm et al. 1997). Areas that are windblown such as ridges, plateaus, and broad open valleys, have the lowest ground temperatures in winter (Mackay and Mackay 1974). During the freezing season, the difference between air temperature and surface temperature is controlled by the timing, thickness, and stratigraphy of the snow cover (Zhang et al. 1996; Karunaratne and Burn 2003).

2.12 Timing and rate of snow-cover build-up

The development of the snow cover shortly after the initiation of active-layer freezing reduces the loss of latent heat from the ground. A thinner snow cover in late fall and early winter results in an accelerated freeze-up of the active layer. Once freeze-up is completed, the surface temperature drops sharply as the latent heat source in the active layer is much reduced (Goodrich 1982).

2.13 Snow stratigraphy

As a result of high wind-speeds and low air temperatures, the snow cover in the tundra typically consists of high-density wind-packed layers (wind slabs) above coarse low-density depth hoar (Benson and Sturm 1993). The depth-hoar layer frequently represents over 50% of the snow-cover volume (Sturm and Johnson 1992) and increases in

proportion in areas with shrubby vegetation cover where the upper wind-slab layer may be nearly absent (Sturm et al. 2001).

The low thermal conductivity of snow results from its microstructure, and variations in grain size, grain type, and bonding can result in an order of magnitude range in thermal conductivity (Table 2.4). Depth hoar appears to have a consistently lower thermal conductivity, and variations in the depth-hoar fraction of the snow pack have an important effect on the insulating properties of the snow pack. Zhang et al. (1996) modelled the influence of the depth-hoar fraction on the ground thermal regime with a one-dimensional finite difference conductive heat transfer model. A change in the depth hoar fraction from 0.0 to 0.6 delayed the freeze-up of the active layer by several months. The model ignored convective heat flow in the snow.

2.14 Vegetation cover and thermal regime of the active layer

Variations in the vegetation cover of an area may reflect changes in factors controlling the thermal regime of the active layer. Soil moisture availability is a control on species composition (Billings and Mooney 1968; Zinko et al. 2005), total live above ground biomass (Gross et al. 1990), leaf area index (Tenhumen et al. 1992), and distribution of biomass among growth forms (Tenhumen et al. 1992). The distribution of vegetation communities may reflect geomorphic factors which also control soil material (Gill 1973). In subarctic tundra, deeper snow is frequently associated with shrubby vegetation through a positive feedback interaction (Sturm et al. 2001; Schimel et al. 2004; Geddes et al. 2005).

In light of these relations, vegetation has been used as a surface indicator in the investigation of aspects of the thermal regime of the active layer, such as the depth of

Table 2.4 Mean thermal conductivity for four types of snow. Data from a 12-year study including 488 thermal conductivity measurements of 13 types of snow (Sturm et al. 1997).

	n	Thermal conductivity ($W\ m^{-1}\ °C^{-1}$) [SD*]	Density ($g\ cm^{-3}$) [SD]	Temperature (°C) [SD]
Chains of depth hoar	171	0.072 [0.025]	0.225 [0.055]	-14.4 [8.9]
Recent snow	21	0.128 [0.050]	0.254 [0.068]	-13.5 [2.8]
Small rounded grains	51	0.169 [0.111]	0.320 [0.078]	-12.9 [6.5]
Hard drift snow	77	0.359 [0.084]	0.444 [0.034]	-18.4[8.9]

*SD represents the standard deviation.

thaw at various points through the summer (Peddle and Franklin 1993; Leverington and Dugay 1996; McMicheal et al. 1997; Nelson et al. 1997).

2.15 Concluding remarks

Several studies have been conducted concerning snow-pack variations in mountainous terrain, but few consider areas where both topography and vegetation structure vary. Most snow distribution studies in mountainous terrain were conducted within hydrological studies, and as a result few studies have examined the redistribution and spatial variability of shallow snow packs in the fall and first months of winter. Similarly, few studies have investigated the freezing of the active-layer in subarctic mountainous terrain. This project proposes to examine the effects of topography and vegetation cover on both snow-pack development and active-layer freezing in the Blackstone Uplands, Y.T.

CHAPTER 3
BIO-PHYSICAL SETTING AND DATA COLLECTION

3.1 Introduction

This research investigates the relation between topography, vegetation cover, snow-pack development, and frost penetration in the Blackstone Uplands, Y.T. This chapter describes the location, physiography, climate, and ecology of the area. It discusses the criteria used for the selection of transect locations, and the methods used to characterize vegetation, topography, and active-layer depth at each study site in summer 2006. The techniques used to monitor ground temperatures during freeze-up and to measure the depth of the snow pack between October 2006 and January 2007 are also presented.

3.2 Location

The study area (Fig. 3.1) is located in central Yukon (Fig. 3.2), and is contained within the quadrangle defined by 64° 58'N, 138° 40'W and 64° 39'N, 138° 04'W. It is located 135 km from Dawson City, and extends over 506 km^2 of alpine terrain. The elevation varies between 1000 m and 1800 m above sea level.

3.3 Physiography

3.3.1 Geomorphology

The study area is located on the boundary between the Mackenzie Mountains and the North Ogilvie Mountains ecoregions (Yukon Ecoregions Working Group 2004) (Fig. 3.2) and the boundaries of the study area mostly follow the limits of the Taiga Valley physiographic subdivision (Bostock 1961). Taiga Valley extends east-west between the southern and central Ogilvie ranges and is characterised by hilly plateaus and long, undulating northward-draining slopes. The relief is lower and the topography is

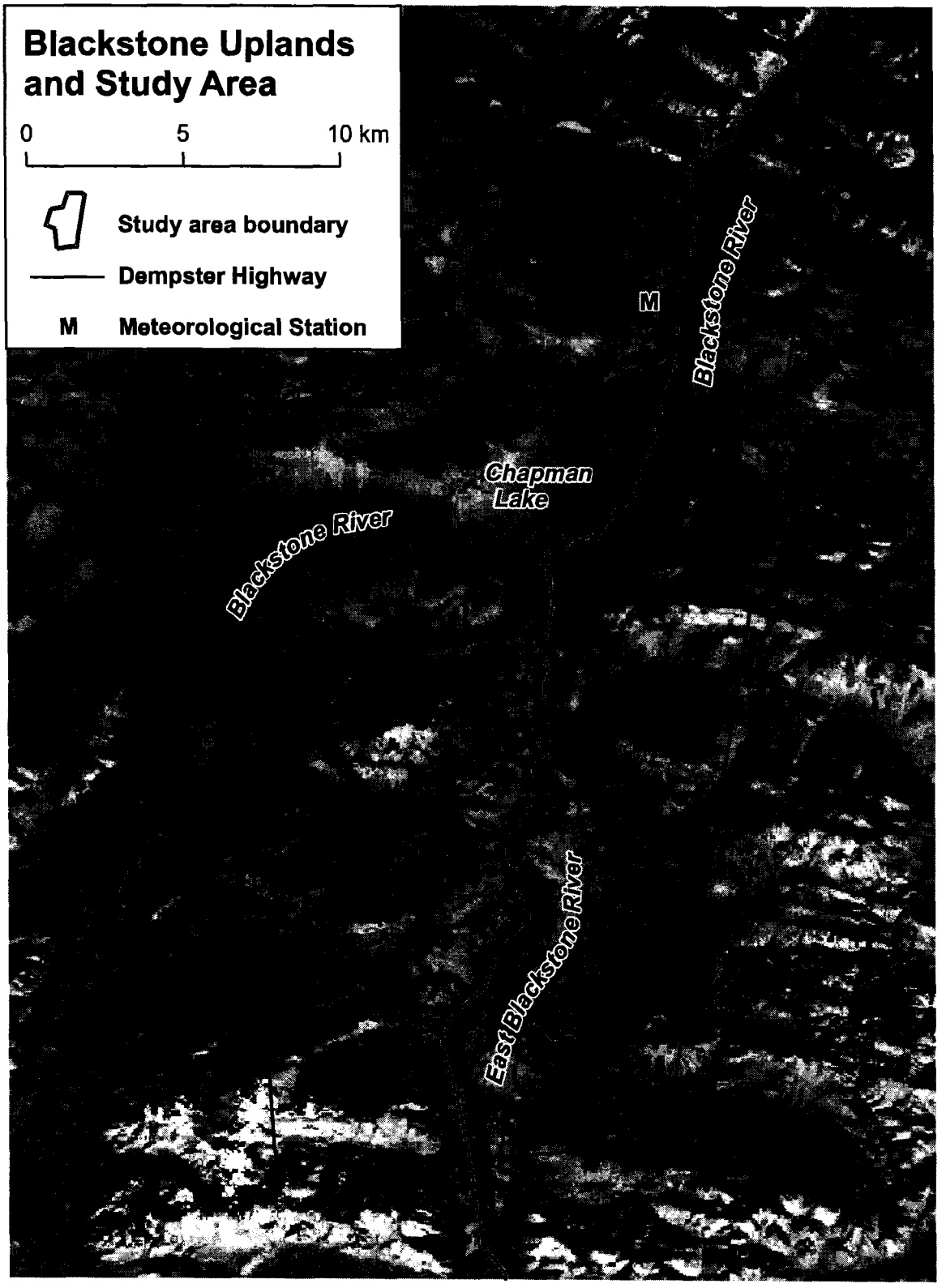

Fig. 3.1 Landsat-7 image of the Blackstone Uplands and study area.

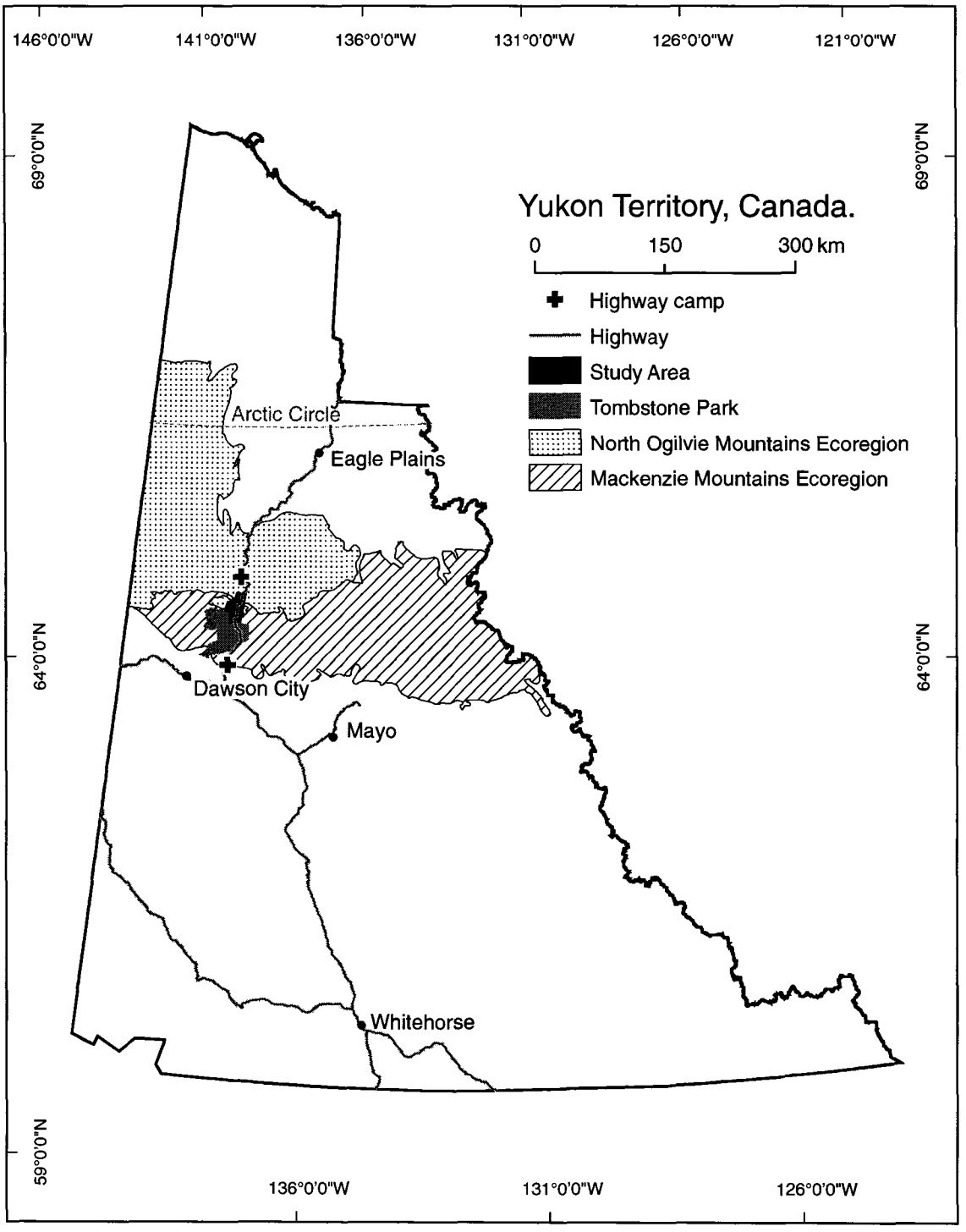

Fig. 3.2 Location of study area in relation to Mackenzie Mountains Ecoregion, North Ogilvie Mountains Ecoregion, and associated sources of climatic data.

noticeably less rugged than that of the surrounding Ogilvie Mountains. Small portions of the central Ogilvie Ranges are included near the southern and western boundaries of the study area. In contrast to most of the Ogilvie Ranges, the hillslopes and summits in the study area are generally vegetated, and talus slopes and rocky outcrops are rare.

The area is underlain by strongly folded Proterozoic sediments (Norris and Dyke 1966) overlain by easily eroded Paleozoic sediments including black shale, slate, siltstone, platy limestone, chert, and chert pebble conglomerate of mid-Devonian to Carboniferous age (Ricker 1959; Gordey and Makepeace 2000). Since the formation and final uplift of Ogilvie Mountains in the Cretaceous, subaerial erosion resulted in the development of a northward-sloping pediment over the area. This pediment has been dissected by streams and overridden by glaciers, so very little of the original surface remains (Thomas and Rampton 1982).

3.3.2 Surficial geology

Glacial deposits cover 32% of the study area (Fig 3.3). These deposits are characterised by unsorted silt, sand, and clay with abundant pebbles, cobbles, and boulders. Dominant glacial landforms in the area include sloping and hummocky moraines, straight and sinuous ridge moraines, till veneer (0-2 m thick) conforming to the underlying topography, and broad mounds with 10-20 m relief where the till is less than 20 m thick (Duk-Rodkin 1996). These deposits are generally attributed to the Reid glaciation (middle to late Pleistocene), but recent evidence from relict fluvial channels and lake sediments suggest that the Chapman Lake Moraine Complex is associated with the younger McConnell glaciation (late Wisconsin) (Beierle 2002). This would imply that a

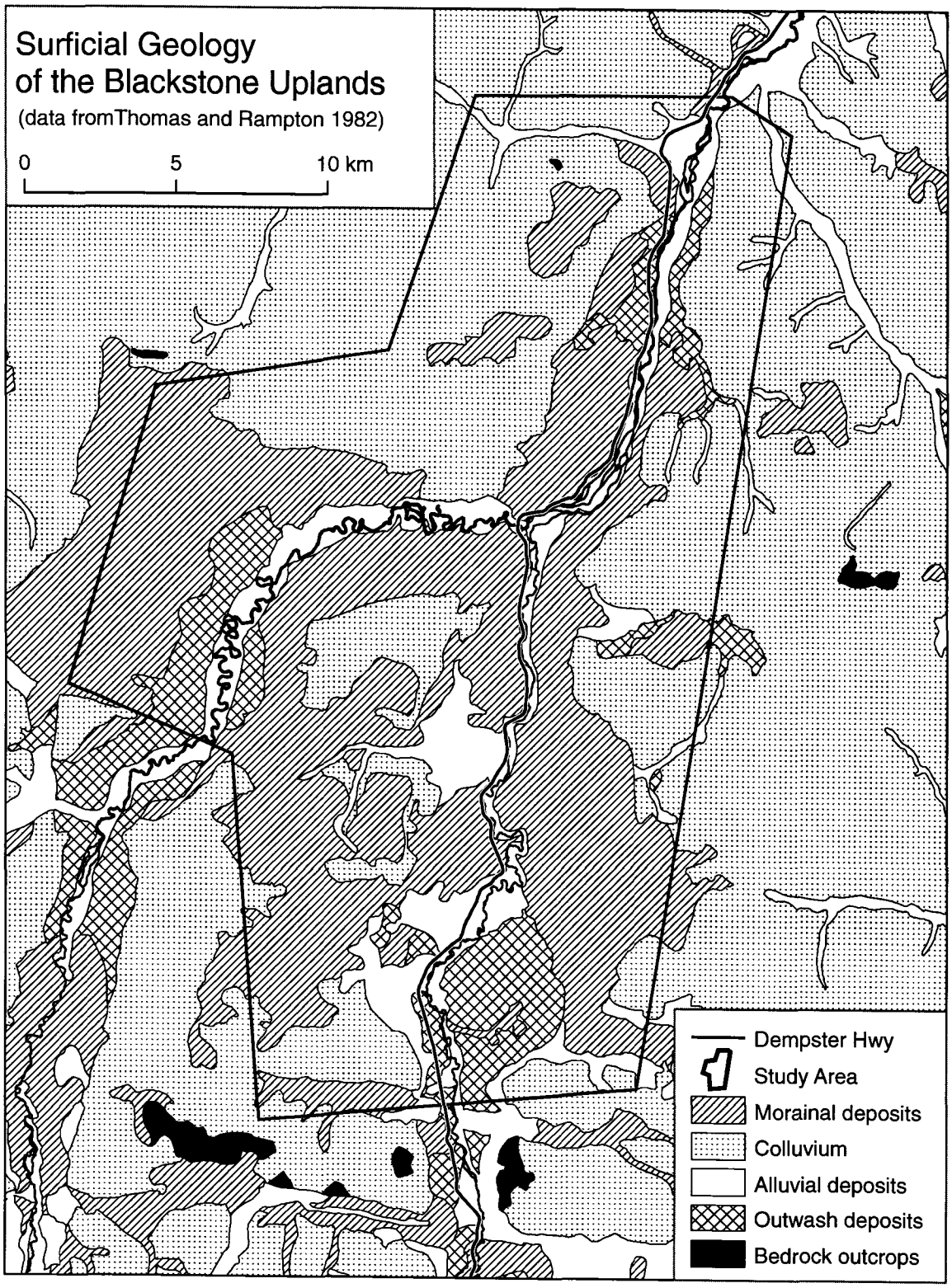

Fig. 3.3 Surficial geology of the Blackstone Uplands.

significant portion of the surficial material in the Blackstone Uplands is much younger than previously thought, and associated with the Late-Wisconsinan period. These morainal deposits generally support cryosols, due to the prevalence of permafrost in the area (Yukon Ecoregions Working Group 2004).

A colluvial veneer (1-2 m thick) or blanket (≥3 m thick) conforming to the bedrock topography covers 32% of the study area. Soil development on colluvial deposits is generally poor.

The Blackstone and East Blackstone River valley bottoms are covered with alluvial deposits up to 12 m in thickness, characterized by coarse sand and gravel. This constitutes approximately 10% of the study area (Duk-Rodkin 1996). Alluvial sediments along the Blackstone River may be without near-surface permafrost, and support gravely brunisols (Yukon Ecoregions Working Group 2004).

3.3.3 Permafrost

The Blackstone Uplands straddle the boundary between the zones of extensive discontinuous permafrost and continuous permafrost (Fig. 3.4) (Heginbottom et al. 1995). Permafrost is likely 100 m thick throughout most of the area (Thomas and Rampton 1982) with taliks present beneath large lakes and rivers. Unfrozen areas can also be expected on south-facing exposures or unvegetated coarse-grained material (Foothills Pipe Lines Yukon Ltd. 1979). The depth to permafrost varies from 40 cm to 75 cm under the ice-wedge polygon tundra (Tarnocai 1993), and can increase to 1 m in areas where gravel is perennially frozen (Yukon Ecoregions Working Group 2004).

In the Blackstone Uplands, ground ice occurs in the form of small ice lenses in peat, stratified ice layers up to 3 cm thick in ice-rich till, and several meters of massive

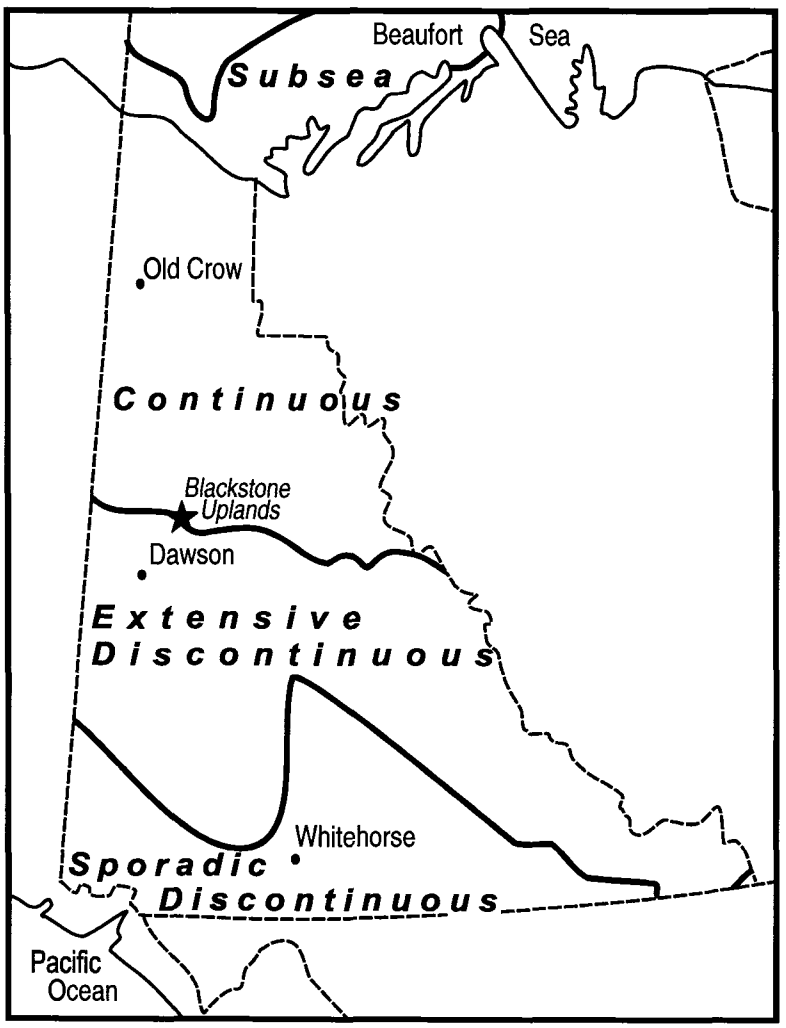

Fig. 3.4 Distribution of subsea permafrost, continuous permafrost (90-100%), extensive discontinuous permafrost (50-90%), and sporadic discontinuous permafrost (10-50%) in the Yukon Territory (after Heginbottom et al. 1995).

ice in some morainal units located in low-lying areas (Klohn Lenoff Consultants Ltd. 1979). Ice-wedge polygons are found throughout the study area in moderately to poorly drained fine-grained sediments. Several closed-system pingos occur on the low alluvial terraces along the Blackstone River Valley (Thomas and Rampton 1982). Ground ice was also exposed in a retrogressive thaw slump near Chapman Lake (Lacelle et al. 2007), and in a network of tunnels likely formed by thermal erosion of ice wedges near the southern boundary of the study area. Active-layer detachment slides are commonly observed in late August through the area (Thomas and Rampton 1982), and suggest the presence of an ice-rich layer near the top of permafrost. The abundant small lakes found along the Blackstone River have been attributed to thermokarst processes (Thomas and Rampton 1982).

Other landforms typical of periglacial terrain are abundant within the study area, including various types of patterned ground, and well developed solifluction lobes on steeper slopes. Frost blisters develop in the nearby North Fork Pass (Pollard and French 1983; Michel 1984; Pollard and French 1984) and icings form on a number of rivers in the area, including on the East Blackstone where the ice can persist until mid-July.

3.3.4 Drainage

North Fork Pass, approximately 15 km south of the study site, marks the divide between the Pacific and Arctic drainages. The study area is located in the Peel River Watershed. The main rivers of the area are the northward flowing East Blackstone and Blackstone Rivers, whose confluence is just south of Chapman Lake (Fig. 3.1).

3.4 Vegetation cover

The Blackstone Uplands are generally located above tree line, with small pockets of spruce trees near the East Blackstone river and the northern limit of the study area. The vegetation cover is structurally varied, including diverse tall or dwarf shrub associations, cotton-grass tussocks, and lichen-dryas associations (Kennedy and Smith, 1999).

The Blackstone and East Blackstone valleys are characterized by extensive areas of eriophorum tussocks and sphagnum hummocks. Communities of *Betula glandulosa, Ledum groenlandicum, Rubus chamaemorus* with *Sphagnum* and lichens are widespread over the broad valleys. Communities of *Betula glandulosa/Cladina* or *Betula glandulosa/Salix* are found in areas with better drainage (Kennedy and Smith, 1999). At intermediate elevations, *Betula glandulosa/Salix* communities are frequent on hillslopes and low elevation ridges, and shrub-tussock tundra is common on pediment slopes with near-surface permafrost (Yukon Ecoregions Working Group 2004). Well-drained morainal deposits support a low-shrub community of *Betula glandulosa, Vaccinium vitis-idea* and *Empetrum nigrum* (Kennedy and Smith, 1999). At higher elevations, low-shrub communities of prostrate willows and lichens dominate where the soil is more acidic, while *Dryas* communities are common on slopes and ridges with calcareous substrate (Yukon Ecoregions Working Group 2004).

3.5 Climatic setting

3.5.1 Climatic controls

The climate of the Yukon is sub-arctic continental. It is relatively dry with large annual, day to day, and daily ranges in temperature (Wahl et al. 1987). The study area is part of the Ogilvie – Mackenzie Mountains Climatic Division. The mountainous topography of

the area, with abundant topographic barriers, creates small mesoclimatic subdivisions in the landscape, and every climate element is also affected by elevation. Weather data are available from Klondike Camp, located 30 km south of the study area, and from Ogilvie Camp located 65 km north of the study area (Fig. 3.2).

3.5.2 Temperature

In the North Ogilvie Ecoregion, mean annual temperatures range between -7°C and -10°C, and vary considerably with elevation (Yukon Ecoregions Working Group 2004). The warmest month is July and the coldest month is January (Fig. 3.5). Mean July temperatures range from 12°C on the valley floors to 6°C at the higher elevations (Wahl 2004). These summer lapse conditions are reversed in winter as temperature inversions develop. Cold air sinks towards lower elevations and accumulates in valley bottoms. Under clear and calm conditions, temperature inversions can intensify and last for days (Barry 1992). Diurnal heating is unlikely to break the temperature inversions during the winter when incoming solar radiation is limited (Bradley et al. 1992). In the North Ogilvie Ecoregion, mean January temperatures in the lower valleys are near -30°C with minima between -50°C and -60°C. At higher elevations, January means are approximately 10°C higher at -20°C with warmer windy weather more common (Yukon Ecoregions Working Group 2004).

3.5.3 Precipitation

Weather systems travelling north and eastward from the Gulf of Alaska lose most of their moisture before they reach the area, but some moist air masses reach Ogilvie Mountains

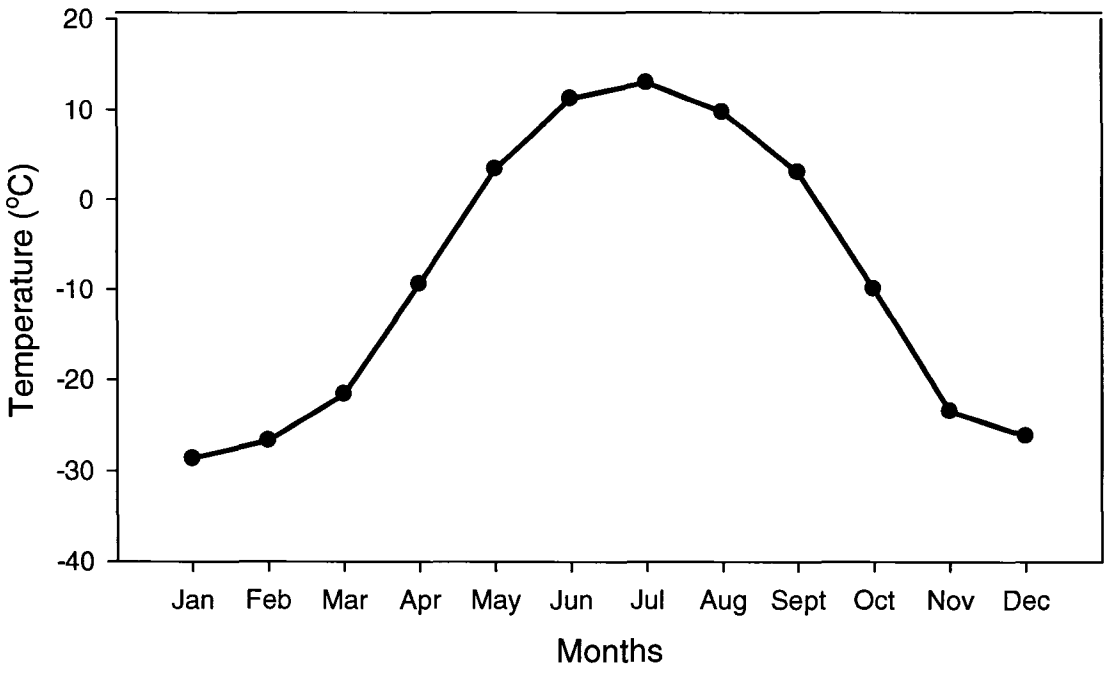

Fig. 3.5 Mean monthly air temperature (1973-2005) at Ogilvie Camp Meteorological Services of Canada, 2007).

(Yukon Ecoregions Working Group 2004). The high peaks of the southern Ogilvie Mountains located to the south of the study area form a significant orographic barrier to maritime influences, resulting in reduced precipitation to the north. Figure 3.6 shows monthly precipitation at Klondike Camp, located in the southern Ogilvie Mountains, and at Ogilvie Camp, located in the North Ogilvie Mountains Ecoregion. The mountains between these sites result in a 34% decrease in total annual precipitation between them. The North Ogilvie Mountains receive moderate precipitation, ranging annually from 300 mm to 450 mm. Summer is the wettest period (June to August) with mean monthly precipitation between 50 and 60 mm (Fig. 3.6). Snow is the main form of precipitation from September to May, with the heaviest amounts in the fall (Yukon Ecoregions Working Group 2004). In March, mean snow depths measured near the highway in the Ogilvie Mountains range between 35 cm and 65 (Yukon Territorial Government 2006).

3.5.4 Wind

No long-term wind data have been collected in the area. In the mountainous areas of the Yukon, topography is a greater control than pressure gradients on wind direction (Kendrew 1955; Wahl 1987). In the study area, dominant wind directions are expected to reflect the north-south alignment of the two major valleys dissecting the Blackstone Uplands.

A meteorological station was installed near Chapman Lake airstrip in July 2006. A weather logger recorded wind speed and direction bi-hourly. Figure 3.7 presents wind roses based on mean hourly wind speed and direction measured from July 2006 to April 2007. Lower winds from the north dominated during the summer and fall (Fig. 3.7a and

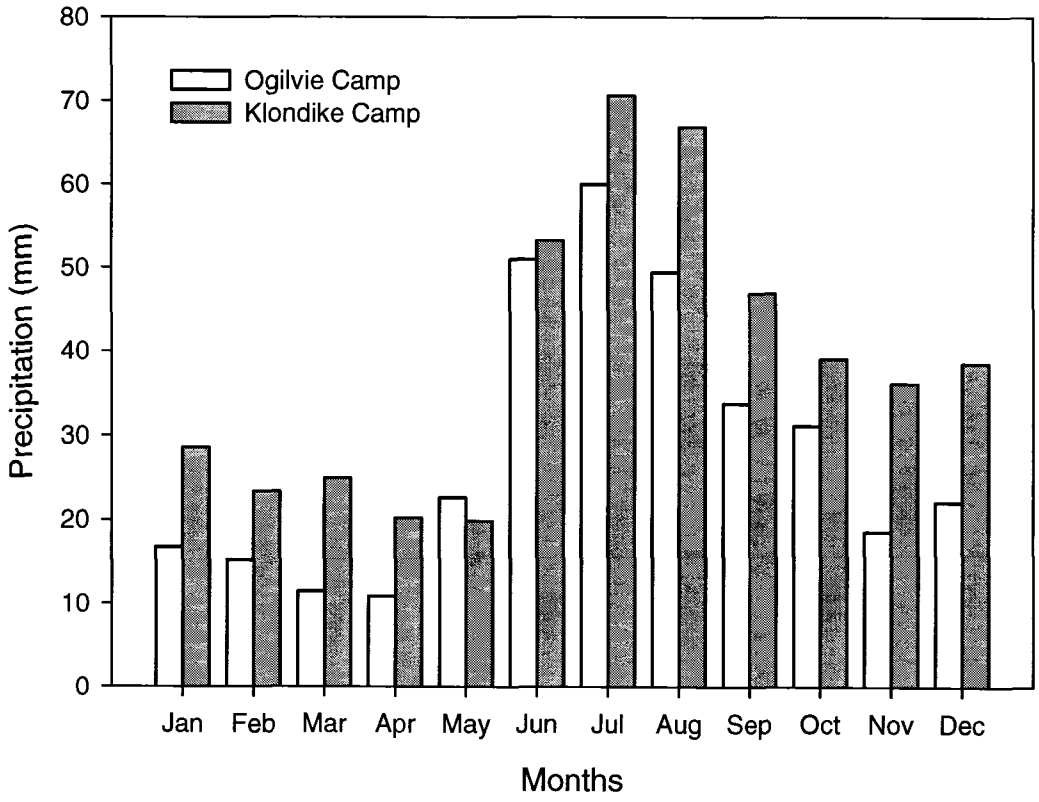

Fig. 3.6 Mean monthly total precipitation at Ogilvie and at Klondike camps (Fig. 3.2), 1973-2005.

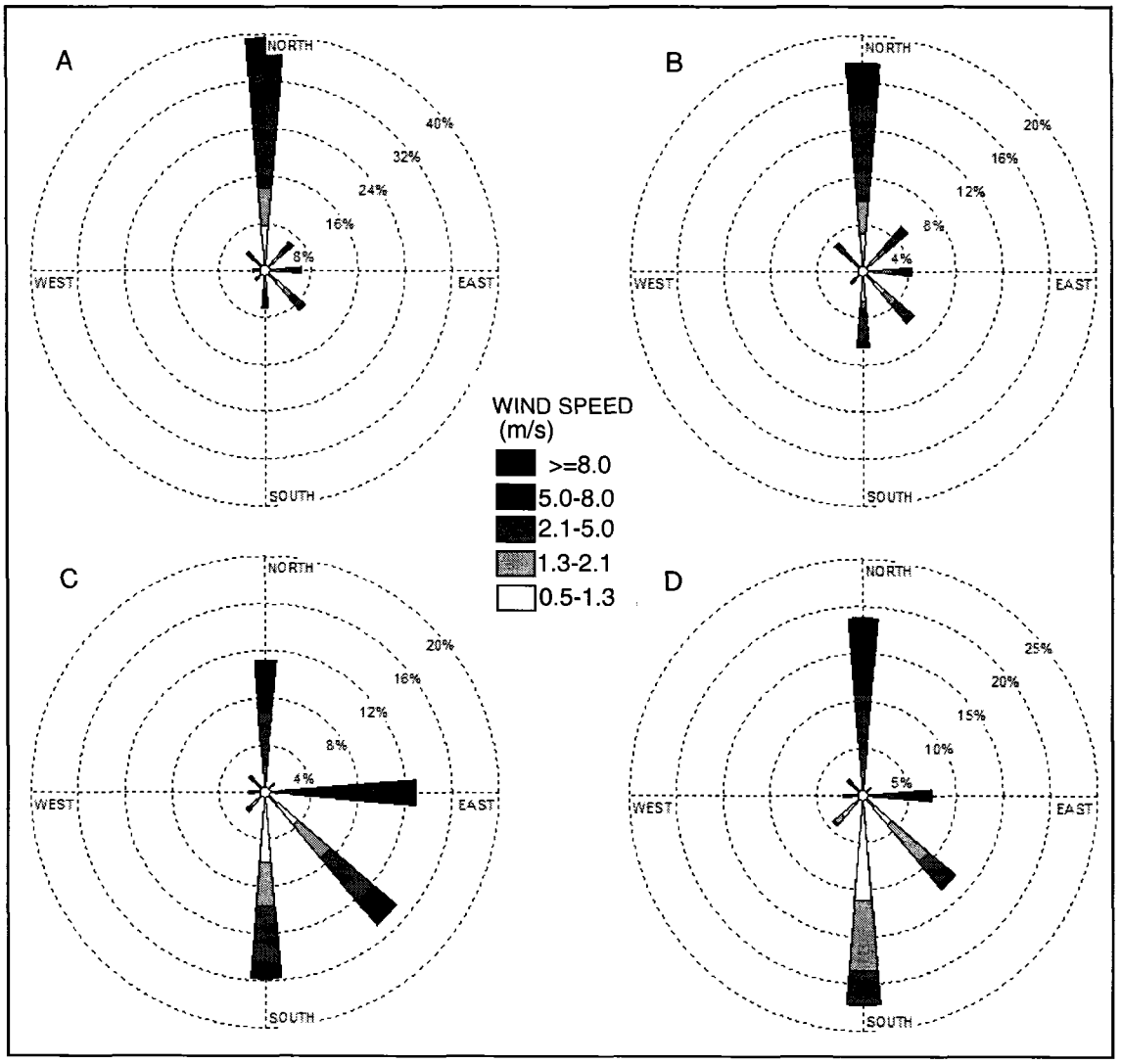

Fig. 3.7 Frequency distribution of wind speed and direction for the months of (A) July to September 2006, (B) October and November 2006, (C) December 2006 and January 2007, and (D) February to April 2007. Calm periods (winds below 0.5 m/s) are not included in the graphs and represent 35% of the entire period.

3.7b), while stronger winds from the east, south-east, and south blew in December and January (Fig 3.7c). Winds were concentrated along the Blackstone River valley corridor for the rest of the winter, with stronger winds mostly coming from the north (Fig 3.7d).

3.6 Temperature and precipitation during the study period

Precipitation and air temperature are key controls on snow-pack development and ground freezing. Comparison of conditions during the study period and the mean climatic conditions for the area provides an assessment of whether the study period was representative of normal conditions. Freezing of the active layer and redistribution of snow by wind were monitored from September 1st, 2006, to January 27th, 2007.

At Ogilvie Camp, monthly mean air temperatures during the study period were 3°C, 5°C, and 4°C above average in September, October and December respectively, but 3°C below average in November (Fig. 3.8). While the first snowfall to persist on the ground in the Blackstone Uplands generally occurs in early September (Dorothy Cooley, personal communication), in fall 2006 this occurred in late October. Total monthly precipitation was 10 mm below average that month, and 86% of the monthly precipitation fell prior to October 23rd, when temperatures still rose daily above 0°C. Only 3 mm of precipitation were recorded at Ogilvie Camp between October 23rd and 31st, when the air temperature remained below 0°C. Monthly total precipitation was 1 mm above average in November, 14 mm below average in December, and 15 mm above average in January. Total precipitation at Ogilvie Camp was only 1.8 mm below average for the study period, mostly due to abundant snowfall in January. Snow precipitation and accumulation occurred later than usual in fall 2006, and the thin snow cover and cold November temperatures combined to create ideal conditions for rapid freeze-up of the active layer.

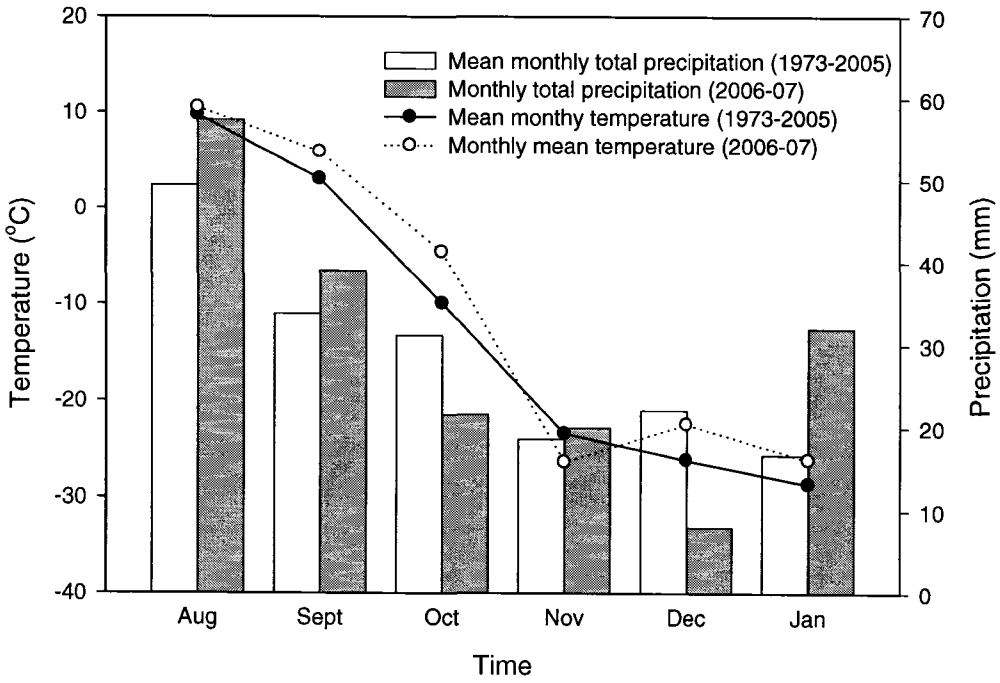

Fig. 3.8 Mean monthly air temperature and total precipitation (1973-2005) at Ogilvie Camp, and monthly mean air temperature and monthly total precipitation for study period (September 2006 to January 2007).

3.7 General sampling scheme and selection of transect locations

Sixteen sampling sites were established across the study area (Fig. 3.9). At each site, sampling stations were established along a transect to facilitate rapid retrieval of the stations under any conditions. Transects ranged from 100 to 250 m in length, and included four to twelve sampling stations located at 25-m intervals (Fig. 3.10), each marked with a stake. The location of each station was recorded using a hand-held GPS unit. Table 3.1 presents a summary of the criteria used for the selection of the transect locations.

Ten transects were located in flat, open areas between 900 m and 1200 m elevation. These transects were characterised by different vegetation cover structures, and were referred to as the "valley-bottom" transects. The 900 m to 1200 m elevation range represents 66% of the study area. Transect V1 and V2 are respectively located on a lake and on a pond. Sparse dwarf and low shrubs with a canopy height below 0.25 m, a dominant vegetation cover in the area, was represented by transect V3, V4, and V5. Shrubs with a canopy height between 0.35 m and 0.60 m were classified as medium shrubs and were represented by transects V6, V7, V8, and V9. In this study, tall shrubs have a canopy height above 0.70 m and were represented by transect V10.

Five transects (T1 to T5) were located above the valley floor in areas with relatively uniform topography and a vegetation cover characterized by dwarf and low shrubs with a mean canopy height below 0.25 m. These transects were referred to as the hill transects, and were located in three ranges of elevation. Three transects (T1, T2, and T5) were established between 1200 m to 1400 m. This elevation range represents 28% of the study area. The two last elevation classes, 1400 m to 1600 m (5% of the study area),

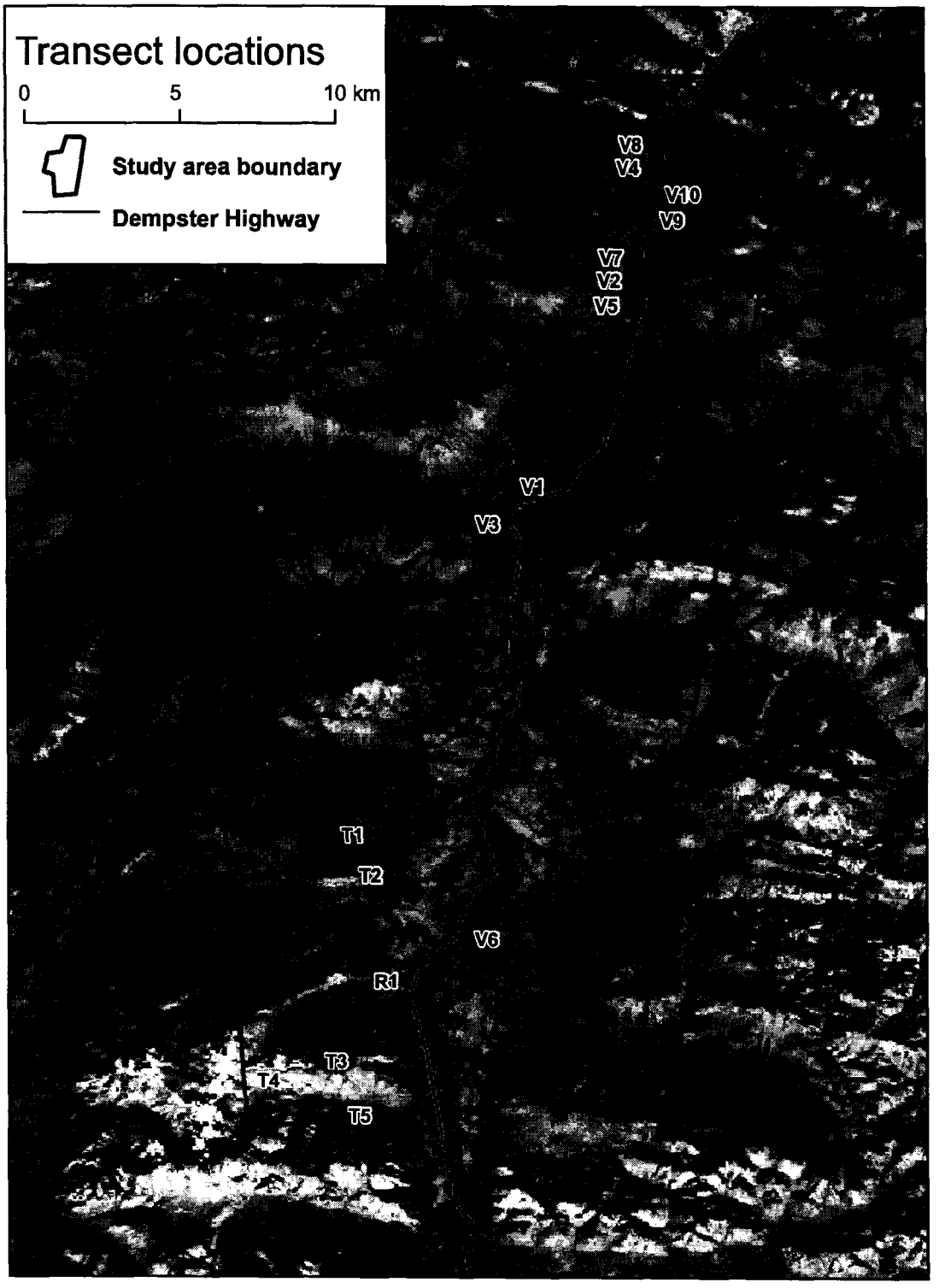

Fig. 3.9 Map of transect locations.

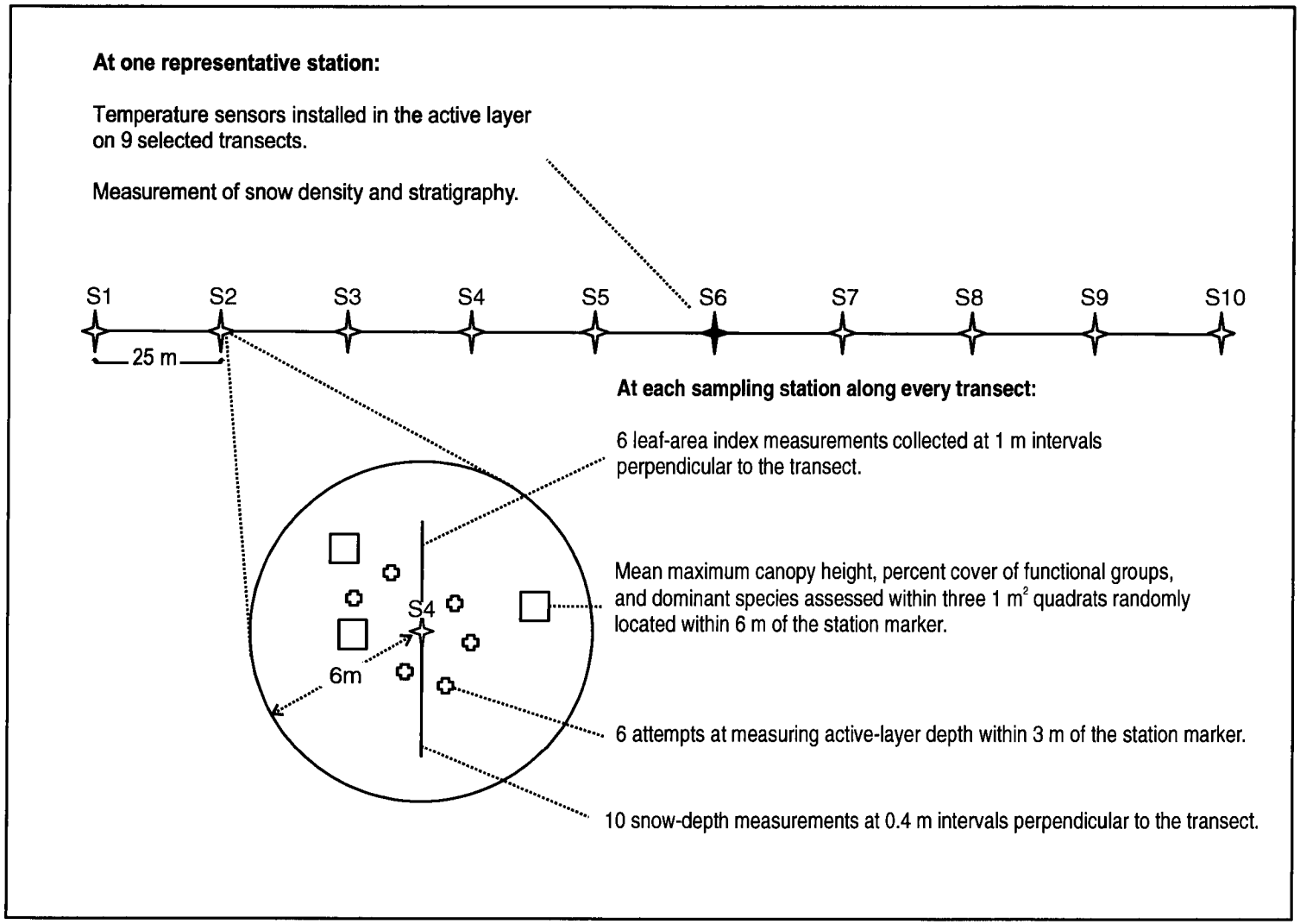

Fig. 3.10 Diagram of general sampling scheme.

Table 3.1 Summary of selection criteria used to determine transect locations. Elevation classes: (1) 900-1200 m, (2) 1200-1400 m, (3) 1400-1600 m, (4) above 1600 m. Vegetation cover categories: (0) uniform surface with no vegetation, (1) graminoids, (2) dwarf shrubs over thin soil, median canopy height below 0.25 m (3) dwarf and low shrubs over thick moss, mean canopy height below 0.25 m, (4) medium shrubs with mean canopy height between 0.35 and 0.60 m, (5) tall shrubs with mean canopy height between 0.70 m and 1.80 m.

Site	Elevation Class	Vegetation Cover Category	Selection Criteria
V1	1	0	Vegetation cover
V2	1	0	
V3	1	3	
V4	1	3	
V5	1	3	
V6	1	4	
V7	1	4	
V8	1	4	
V9	1	4	
V10	1	5	
T1	2	3	Elevation
T2	2	3	
T3	3	3	
T4	4	2	
T5	2	3	
R1	1	3	Locally used reference site.

and 1600 m and above (0.6% of the study area) were represented by one transect each (respectively T3 and T4). Hill transects were located in open flat areas with the exception of T5, which was located on the sloping floor of a broad valley.

A transect was also established at the reference sites currently used by local conservation officers to assess snow depth and ground freezing prior to the opening of the snowmobile season (R1).

Potential transect locations were initially identified with the help of aerial photos, LandsatTM 7 satellite imagery and a digital elevation model. Broad, open, relatively flat areas with apparently uniform conditions were identified, and uploaded to a hand-held GPS to facilitate subsequent location and assessment in the field. Final transect locations were selected on-site to ensure uniform conditions within the transect.

Information on vegetation cover type, canopy height, and snow depth was also recorded at 59 locations through the study area (Fig. 3.11). This secondary dataset was collected to be used as "ground-truth" when extrapolating observed field relations to the landscape scale.

3.8 Description of vegetation based on species composition and growth forms

At each station along a transect, three 1 m^2 quadrats were used for vegetation characterization (Fig. 3.10). These quadrats were randomly located within 6 m of the station marker. A set of four dice were used to determine the exact location of each quadrat (distance and azimuth) in relation to the station marker. For each quadrat associated with a station, the four species representing the largest portions of canopy cover were identified and recorded.

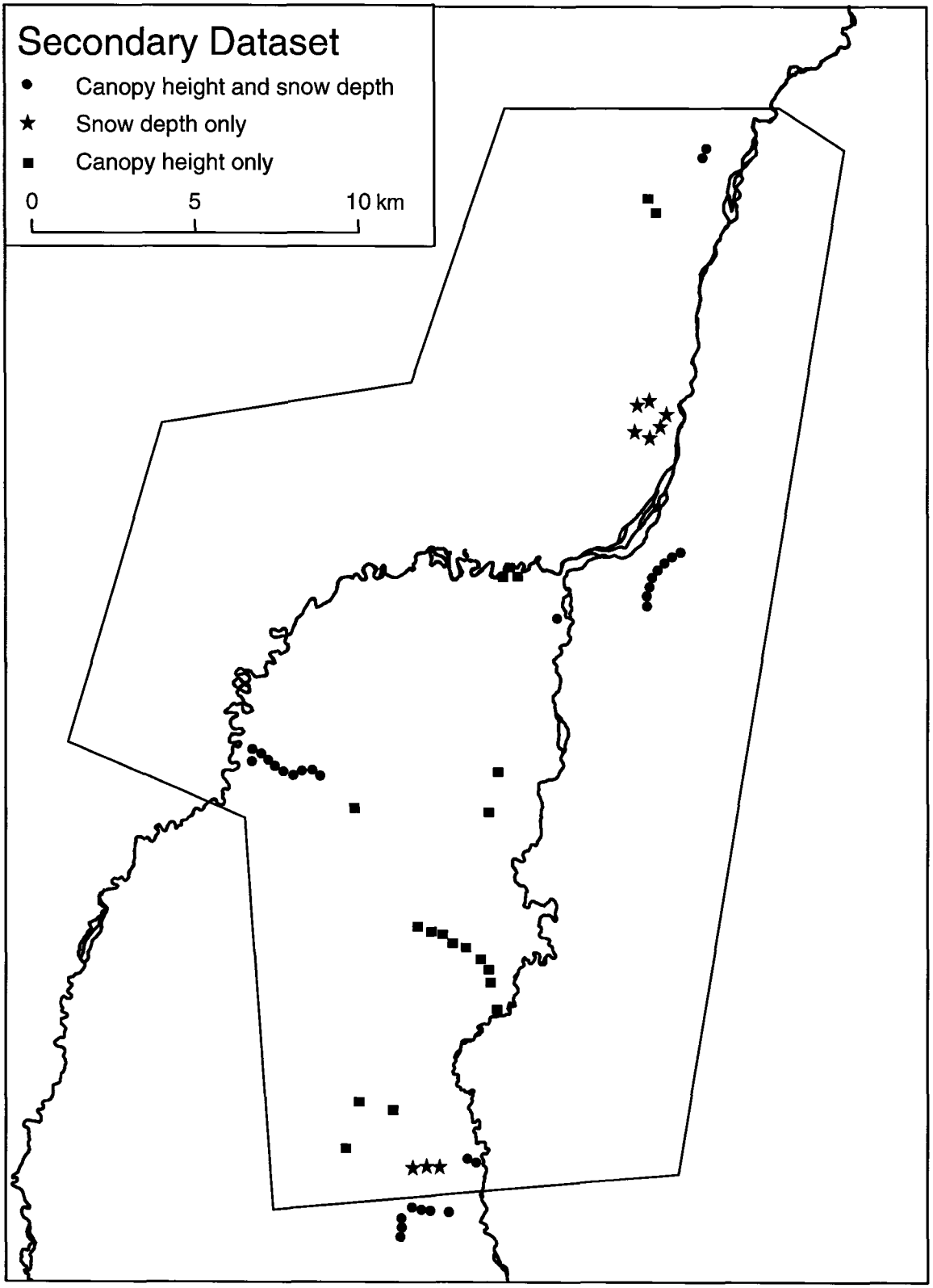

Fig. 3.11 Distribution of the secondary dataset.

Six major growth forms were considered for percentage cover, including lichens, mosses, graminoids, forbs, evergreen shrubs, and deciduous shrubs. Shrubs included all woody plants. All shrubs with evergreen leaves or tardily deciduous leaves were considered evergreen shrubs, including *Andromeda polifolia*, *Cassiope tetragona*, *Vaccinium vitis-idea*, *Empetrum nigrum*, *Rhododendron lapponicum*, *Ledum* spp., and all *Dryas* spp. Growth form composition of the vegetation cover can give information on the response of a community to particular environmental factors (Mueller-Dombois and Ellenberg 1974).

The percentage cover represented by the canopy cover of each growth form was measured in the three quadrats associated with each station. The canopy cover was taken to be the vertical projection of the crown or shoot area of a functional group to the ground expressed as a percent of the 1 m^2 area represented by the quadrat (Mueller-Dombois and Ellenberg 1974). Cover classes were assigned using a semi-logarithmic cover scale with eight classes of cover ranging from 0 to 100% (Johnstone and Kasischke 2005). Broad classes were used to minimize the impact of human error (Daubenmire 1959), and a finer breakdown in the lower-scale values ensured the capture of diagnostic differences in less abundant functional groups (Mueller-Dombois and Ellenberg 1974). Table 3.2 lists the classes used in this study. Percent-cover estimations were conducted by two different observers. To minimize systematic errors due to bias in cover assessment, the two observers assessed up to six training quadrats together every time a significant change in vegetation structure was assessed. Twenty-six quadrats were also assessed separately by both observers at the beginning, middle and end of the field season to

Table 3.2 Classes used for the estimation of canopy cover.

Class number	Percent cover range
1	0-1%
2	2-3%
3	4-5%
4	6-10%
5	11-20%
6	21-35%
7	36-60%
8	61-100%

evaluate observer bias. Though results differed in a number of quadrats, observer bias was not consistent over the whole range of cover values and could not be calibrated. Human error resulting in differences in assessment will be considered as noise reducing the accuracy of the percent cover data.

The mean percent-cover values at the station level and at the transect level were calculated using the midpoint of each class range, and translated back to the corresponding cover classes. This method assumes that the actual cover values within each class tend to be symmetrically dispersed about these mid-points (Daubenmire 1959).

3.9 Description of vegetation structure

The structure of the vegetation cover was assessed on the basis of the mean maximum canopy height and leaf area index. These two variables allow estimation of the roughness length of a vegetated surface, and provide a good indication of the snow-holding capacity of a vegetation stand.

Mean maximum canopy height was measured in the three quadrats associated with each station. The three tallest stems contained within the quadrat were identified. The height of the three tallest stems was measured from the apical bud to the ground surface directly below the tip of the stem. The ground surface was defined as the level where the moss cover is continuous. All stems whose vertical projection on the ground was included in the quadrat were considered. Mean maximum canopy height for a station was obtained by averaging the nine height measurements collected in the three quadrats. The mean maximum canopy height for a transect is the average of all 90 measurements collected over 30 quadrats.

Leaf area index (LAI) measurements were made in the last three weeks of July using a LICOR LAI-2000 Plant Canopy Analyzer. The instrument uses measurements made above and below the plant canopy to determine the gap fraction at five angles around the zenith. It combines multiple measurements made in one area by averaging the logarithm of the gap fractions to compute a mean LAI value (Welles and Norman 1991). Although "LAI" means leaf area index, the LICOR LAI-2000 estimates include all opaque objects, such as stems, fruit, and branches. Foliage area index is a better description of the measurement (Welles and Norman 1991).

At each sampling station along a transect, one reading was taken above the canopy and six readings were collected on the moss layer at 1-m intervals on a line perpendicular to the main transect (Fig. 3.10). To obtain the mean LAI value for a transect, the average of all LAI values along a transect was computed (Weiss et al. 2004).

The LICOR LAI-2000 uses inverted gap fraction data to compute LAI, which implies the following assumptions: (1) all radiation striking the foliage is absorbed, and the sensor perceives only sky radiation, (2) foliage is randomly positioned in the canopy, (3) foliage elements are small, (4) foliage is randomly oriented with respect to azimuth (Welles and Norman 1991).

To address the first assumption, the LI-COR LAI includes a filter to limit sensitivity of the optical lens to radiation below 490 nm, as leaf reflectance and transmittance are minimal below this value (LI-COR Inc. 1990). Yet, below canopy readings are increased by scattering from sunlit foliage and it is best if the sun is obscured while the measurements are taken (Welles 1990). The LAI readings should ideally be taken on cloudy days, but this was not always possible. On sunny days an umbrella was

used to shade the sensor from direct sunlight. When an umbrella was used, a reading was taken above the canopy prior to each of the six below canopy readings to minimize variations due to shifts in the position of the umbrella from one reading to the next. A 90° field-of-view shield was attached to the optical lens to prevent interference from the observers.

The second and fourth assumptions are problematic for the assessment of most natural plant canopies, as clumping of the foliage elements leads to significant gaps in the cover (Weiss et al. 2004). Clumping is frequent in natural canopies, and large gaps often separate patches of dense vegetation in shrubby areas. When the optical sensor perceives portions of both dense vegetation and a large gap in a single reading, the leaf area index is generally underestimated (Welles and Norman 1991). To address this, view caps were used to ensure the canopy perceived by the lens in each reading was relatively uniform. Readings were taken below both wide gaps and dense vegetation "clumps". When the field of view is reduced by a view cap, the required minimal distance to foliage elements increases (LI-COR inc., 1992). As a result view caps obstructing no more than 90° were used with dwarf and low shrubs. An attempt was made to reduce the effect of clumping and gaps by locating each measurement in relatively uniform areas.

The third assumption can be accommodated by ensuring that the distance between the instrument lens and the foliage is equivalent to at least four times the size of the foliage elements. This is generally easily achieved under medium and tall shrubs, but constitutes an important limitation in areas characterized by extremely low-growing prostrate or decumbent vegetation common in the high arctic and in wind-blown areas. Avoiding foliage in proximity to the lens may result in the lens perceiving no foliage at

all. This is particularly problematic for studies concerned with the estimation of biomass (Walker et al. 2003). In this study however, LAI is used to provide a measure of plant structure. The assumption that extremely low growing vegetation has "no structure" because it was not perceived by the LICOR LAI-2000 optical lens was considered acceptable, as very low vegetation indeed has a very low snow-holding capacity.

3.10 Description of topography

3.10.1 Elevation, slope, and aspect

The elevation value of each station was obtained by plotting the coordinates of each station on a digital elevation model (DEM) of the area. The DEM was produced by Geomatics Yukon and had a horizontal resolution of 30 m and a vertical resolution of 10 m.

The spatial analyst tools of ArcMap 9.1 were used to calculate the slope and aspect at each station. Slope was calculated as the maximum rate of change in elevation between the grid cell comprising the location of the station and the neighbouring cells. The mean slope value for each transect is the median of the distribution of slopes along the transect. Slope values extracted from the DEM were compared with field notes and measurements taken with an inclinometer. When there was disagreement between measured and extracted slope values, measurements collected with the inclinometer were used. Aspect was identified as the steepest downslope direction within a radius of 24 m around the station. The aspect of each transect is the mode of the distribution of aspect values along the transect.

3.10.2 Sheltering index

In this study, calculation of the sheltering index for a given point on the digital elevation model was the maximum elevation change per unit distance between the cell comprising the location of this point (x_i,y_i) and the neighbouring cells (x_j,y_j) found in a specified direction (A) and within a radius of 90 m, according to:

$$S_{x_i,y_i} = \max_A \left[\frac{E_{x_j,y_j} - E_{x_i - x_j}}{\sqrt{(x_j - x_i)^2 + (y_j - y_i)^2}} \right] \quad (3.1)$$

where E is the elevation of the points considered. The directions considered for the assessment of sheltering were south-east, south, north, and east, and which respectively represent 28%, 25%, 20% and 11% of the mean hourly wind directions recorded in the study area between October 2006 and January 2007.

3.10.3 Microtopography

Terrain features likely to affect surface wind flow and snow distribution but too small to be perceived by the digital elevation model were described for each quadrat. Notes were taken on surface features such as hummocks or tussocks, drainage channels, rocks on the ground surface, as well as on the position of the sampling station in relation to nearby slope breaks, embankments, or ridge crests.

3.11 Active-layer depth measurements and installation of thermistors

3.11.1 Active-layer depth

At each station, six attempts to measure active-layer depth were made with a graduated metal probe of length 1.20 m. Though less accurate than the measurement of the 0°C isotherm, probing is adequate for surveying extensive areas (Burn 1998), such as the one

considered in this study. Probing for active-layer depth is most accurate in icy peat, or sandy soils, but leads to a great level of uncertainty in silty clays and clays (Mackay 1977). In this study, most stations are located on morainal, alluvial, and glacio-fluvial outwash units with silty sand, sand, or gravel matrix sometimes covered with peat. Only three transects are included in colluvial units with silty clay to silty sand matrix (Thomas and Rampton 1982).

The probe was pushed in the ground to the depth of refusal, which was assessed to be rock or ice according to the sound made at contact and the texture of the obstruction. In areas where it appeared difficult to determine whether passage of the probe was obstructed by the frost table, rock strata, or a firm clay unit, the active-layer depth was noted as "undetermined". In areas where rocks impeded penetration of the probe, ten attempts were made before also noting active-layer depth as "undetermined". When the depth of refusal was greater than 1.20 m for the first four measurements, the active layer depth was automatically noted as >1.20 m.

Measurements were made between the 3rd and the 21st of September 2006. Active-layer depth was measured along transect T1 on both September 5th and September 21st to assess the effect of up-freezing (Osterkamp and Romanovsky 1997) on active-layer depth between the beginning and the end of the measurement period. No difference was found at a 0.05 significance level.

3.11.2 Monitoring of ground temperature

Temperature sensors were installed in the active layer at nine stations representing the four elevation classes (900-1200 m, 1200-1400 m, 1400-1600 m, 1600 m and above), three vegetation structure classes (sphagnum and dwarf shrubs, medium shrubs, and tall

Table 3.3 Summary description and selection criteria used to determine temperature sensor locations. Vegetation cover categories: (0) uniform surface with no vegetation, (1) graminoids, (2) dwarf shrubs over thin soil, mean canopy height below 0.25 m (3) dwarf and low shrubs over thick moss, mean canopy height below 0.25 m, (4) medium shrubs with mean canopy height between 0.35 and 0.60 m, (5) tall shrubs with mean canopy height between 0.70 m and 1.80 m.

Site	Longitude	Latitude	Elevation	Vegetation	Selection Criteria
V3	-138.369	64.835	1007	3	Vegetation
V4	-138.279	64.946	934	3	Vegetation
V6	-138.377	64.717	1090	4	Vegetation
V7	-138.287	64.911	949	4	Vegetation
V10	-138.267	64.933	929	5	Vegetation
T1	-138.457	64.742	1284	4	Elevation
T3	-138.451	64.677	1568	3	Elevation
T4	-138.498	64.675	1679	2	Elevation
R1	-138.415	64.701	1104	3	Reference site

shrubs), and the area currently used by local conservation officers to assess snow depth and ground freezing prior to the opening of the snowmobile season. Table 3.3 gives the coordinates and main site selection criteria for the nine stations.

At each location, temperature sensors (Onset Computing, TMC6-HD) were installed at depths of 5 cm, 15 cm, 30 cm, and at the top of the permafrost (Fig 3.12). Temperature was recorded at 2-hour intervals with HOBO^{TM} four-channel data loggers (Onset Computing, H08-006-04). The thermistors had a range of -40°C to 100°C, an accuracy of ±0.5°C, and a resolution of ±0.41°C at 20°C.

3.12 Monitoring the development of the snow pack

Transects were surveyed for snow accumulation from October 2006 to January 2007. Table 3.4 presents snow survey dates for all transects. Transects located in proximity to the highway were surveyed more frequently, while transects located in more remote locations were surveyed monthly. On October 1st, the study area was surveyed visually from the road and from the highest site, and a snow depth of zero was recorded for all sites.

At each station, ten snow-depth measurements were collected at 0.40 m intervals on either side of the station marker, perpendicular to the main transect direction. A snow probe graduated every 0.5 cm was used. A walking path was established to prevent trampling of the sampling areas.

A snow pit was excavated near each of the stations equipped with temperature sensors in January 2007. Snow density was measured every 10 cm starting at the top of the snow pack. A volume of 100 cm^3 was extracted and weighed to the nearest 1 g using an Homs Model 100g Instrument and Laboratory spring scale. For each stratigraphic unit

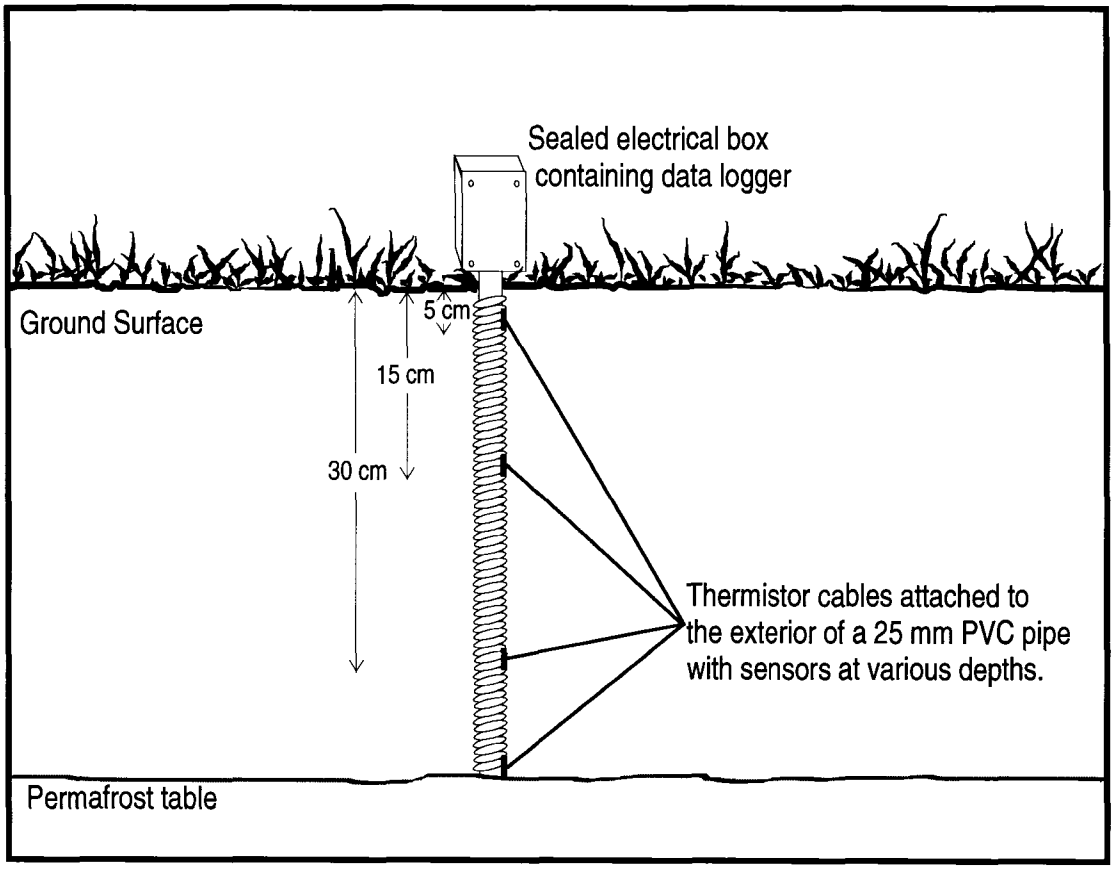

Fig. 3.12 Ground temperature monitoring station.

Table 3.4 Dates on which data were collected along each transect.

Site	Oct. 06	Nov. 06	Dec. 06	Jan. 07
V1	1, 9, 29	5, 15	2, 9	23
V2	1, 9, 23, 27	15	12	23
V3	1, 9, 27	5, 15	2, 12	21
V4	1, 9, 23, 27	15	12	23
V5	1, 9, 23, 27	15	12	23
V6	1, 9, 15, 24, 27	6, 15	2, 12	21
V4	1, 9, 23, 27	5	2, 12	23
V7	1, 9, 23, 27	15	12	23
V8	1, 9, 23, 27	15	12	23
V9	1, 9, 23, 27	5	2, 12	23
V10	1, 9, 23, 27	5	2, 12	23
T1	1, 10, 25	16	13	22
T2	1, 10, 25	16	13	22
T3	1, 10, 15, 26	17	10	27
T4	1, 10, 15, 26	17	10	27
T5	1, 24	18	5	26
R1	1, 9, 10,15, 24, 25, 26, 27, 29	5, 7, 15, 16, 18, 22	2, 5, 7, 13	26

of the snow pack, the thickness of the layer, as well as snow crystal shape and size were recorded.

Chapter 4
PHYSICAL CHARACTERISTICS OF THE STUDY SITES

4.1 Introduction

This chapter describes the transects according to topography and vegetation cover. The first part describes the ten valley-bottom sites (V1 to V10) established near the Blackstone or East Blackstone rivers and which represent different ground covers, and includes a description of the reference site (R1). The second part of this chapter describes the six hill sites (T1 to T6) located at various elevations in the uplands surrounding the two rivers. The last part of this chapter summarises the location of the temperature sensors.

4.2 Description of valley-bottom sites

4.2.1 Topography

The valley-bottom transects were established on the floor of the Blackstone and East Blackstone river valleys, between elevations of 900 m and 1200 m. They are located on flat to gently sloping terrain with a slope of 3° or less (Table 4.1). All the valley-bottom transects are located on the west side of either the East Blackstone river or the Blackstone river, and as a result most sites are on east-facing slopes (Table 4.1). The reference site (R1) is located higher than the other valley-bottom sites.

All valley-bottom transects are located in open areas, and as a result there is little shelter provided by the surrounding topography (Table 4.2). Transects are generally positively sheltered to the west and negatively sheltered to the east, following the general gradient on the west side of the Blackstone and East Blackstone valleys.

Table 4.1 Elevation, slope, aspect, and microtopography at valley-bottom sites.

Site	Elev. (m)	Slope (°)	Aspect (°)	Microtopography
V1	996	0	-	Lake
V2	952	0	-	Pond
V3	995	2	S	Hummocky
V4	927	3	N	Hummocky
V5	952	2	E	Hummocky
V6	1103	1	E	Hummocky
V7	953	2	E	Hummocky
V8	926	1	E	Marshy depression
V9	926	1	E	Hummocky
V10	925	1	E	Planar
R1	1117	3	E	Hummocky

Table 4.2 Median sheltering index (eq. 3.1) in five directions for all valley-bottom transects, calculated based on a radius of 30 m, 60 m, and 90 m. Negative values indicate that elevation decreases away from the transect.

Site	n	North	East	South	South-East
V1	8	0.03	-0.05	-0.02	-0.04
V2	4	-0.02	-0.01	-0.04	-0.04
V3	8	0.03	0.00	-0.02	-0.02
V4	4	-0.03	-0.02	0.05	0.02
V5	8	0.03	-0.03	0.01	-0.02
V6	10	0.01	-0.01	-0.01	-0.01
V7	4	-0.01	-0.01	0.04	0.02
V8	4	0.03	0.00	0.01	0.00
V9	8	0.00	0.00	0.00	0.00
V10	12	0.00	-0.01	0.00	0.00
R1	7	0.01	-0.03	-0.01	-0.04

Transect V9 is the only transect located on even ground, with very little microrelief. All other transects were established on hummocky ground with surface features varying from 0.3 m to 1.25 m in diameter, and from 0.15 m to 0.35 m in height. Site V3 and R1 have only subtle hummocks, with most of the microtopography resulting from grass tussocks.

4.2.2 Vegetation structure

Vegetation structure was a determining criterion for the selection of transect locations (Table 3.1). Table 4.3 summarizes the structure of the vegetation cover along each valley-bottom transect according to median maximum canopy height and leaf area index (LAI). Transects can be grouped in structural classes on the basis of their vegetation structure. This is most easily done using canopy height, considering that LAI is strongly correlated with maximum canopy height at the transect level (Fig. 4.1). The range of vegetation structures represented in the valley-bottom sites is apparent in Fig 4.2, which presents box and whisker diagrams of canopy heights, including the reference site (R1), and excluding the two transects located on water bodies (V1 and V2).

Three transects (V3, V4, V5) have a median canopy height below 0.2 m and are structurally very similar to the reference site (Fig 4.3). The upper layer of the canopy at these sites can be described as low shrubs and tussocks. Transects V6, V7, V8, and V9 have similar median canopy heights, resulting in the classification of these sites as medium height shrubs. These sites differ considerably in terms of the variability of their canopy heights. Site V6 and V7 appear to have relatively uniform canopies, while V8 and V9 include a wide range of canopy heights, indicating a more patchy vegetation cover (Fig 4.4). Finally, site V10 represents the tallest vegetation cover, also exhibiting a high

Table 4.3 Median of maximum canopy height and LAI measurements for all valley-bottom transects and for the reference site.

Site	Canopy Height (m)			Leaf Area Index		
	median	n	IQR	median	n	IQR
V1	0.00	72	0.00	0.00	8	0.00
V2	0.00	36	0.00	0.00	4	0.00
V3	0.12	71	0.08	0.44	8	0.25
V4	0.14	36	0.05	0.38	4	0.06
V5	0.17	72	0.07	0.50	8	0.25
V6	0.46	90	0.24	0.93	10	0.56
V7	0.43	36	0.30	1.25	4	0.47
V8	0.49	36	0.40	1.55	4	0.28
V9	0.47	72	0.45	1.12	8	0.39
V10	0.71	108	1.15	2.17	12	0.77
R1	0.11	63	0.1	0.49	7	0.19

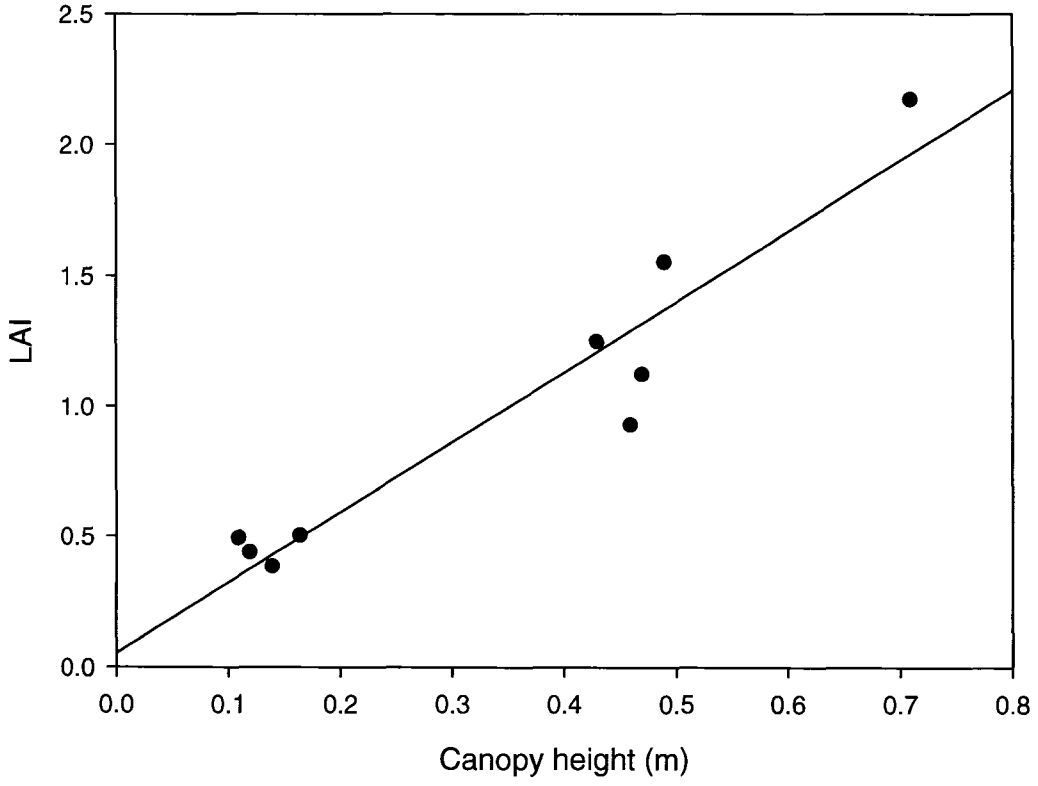

Fig. 4.1 Scattergram of LAI against maximum canopy height for valley-bottom transects. Transects with no vegetation were omitted as their values of 0 for both variables were assigned, not measured. The principal axis $y = 2.69x + 0.05$ has a r^2 value of 0.91.

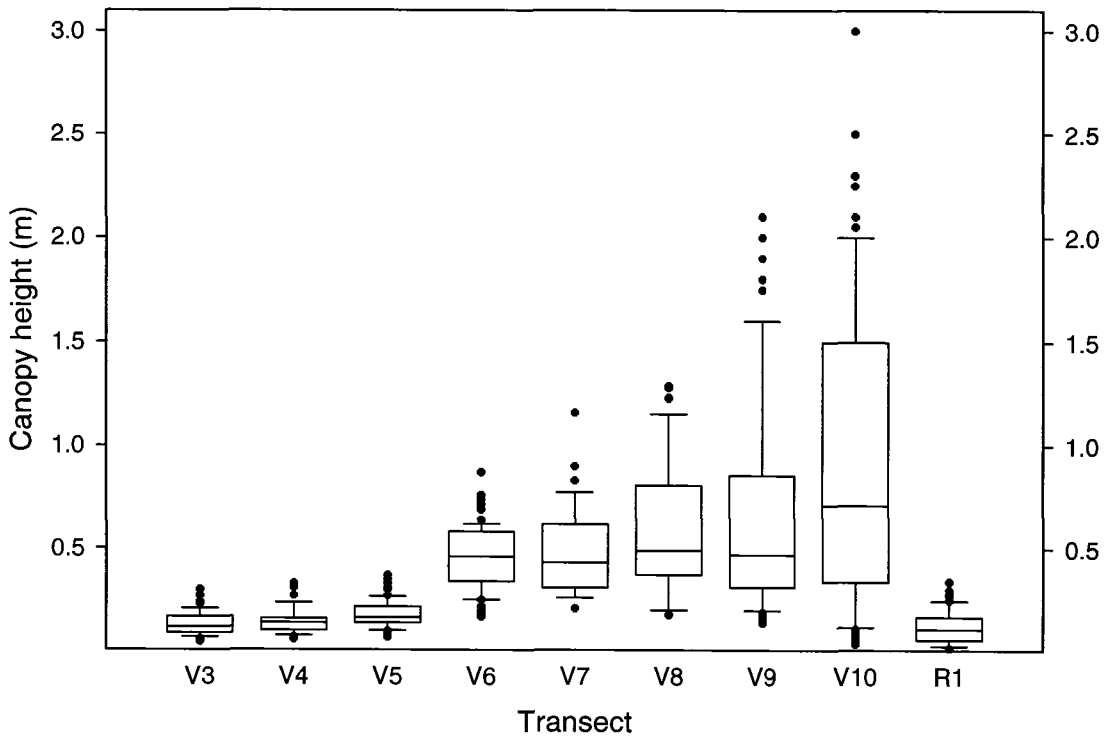

Fig. 4.2 Maximum canopy height at valley-bottom transects.

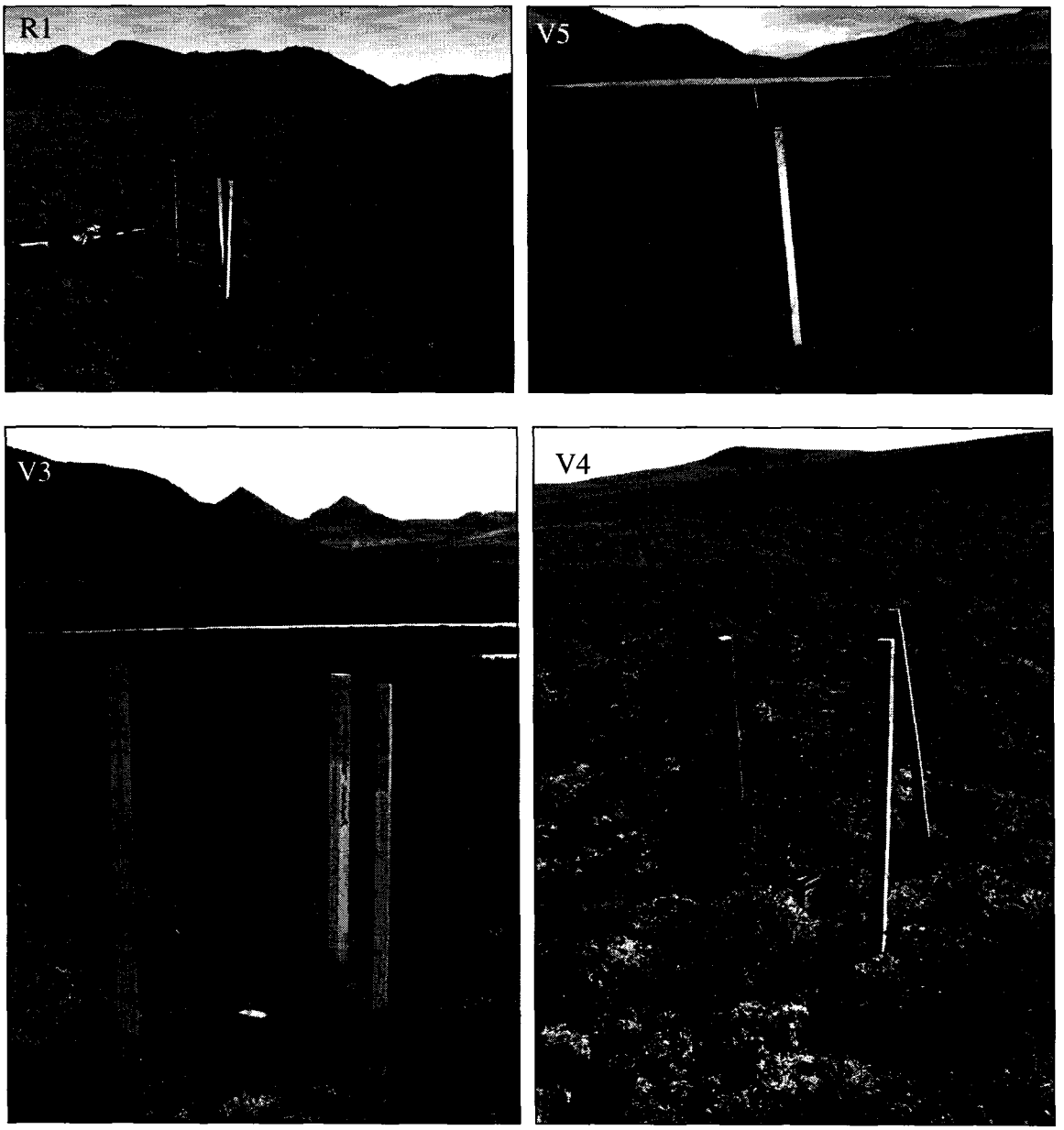

Fig. 4.3 Four sites with similar vegetation covers of low shrubs and tussocks.

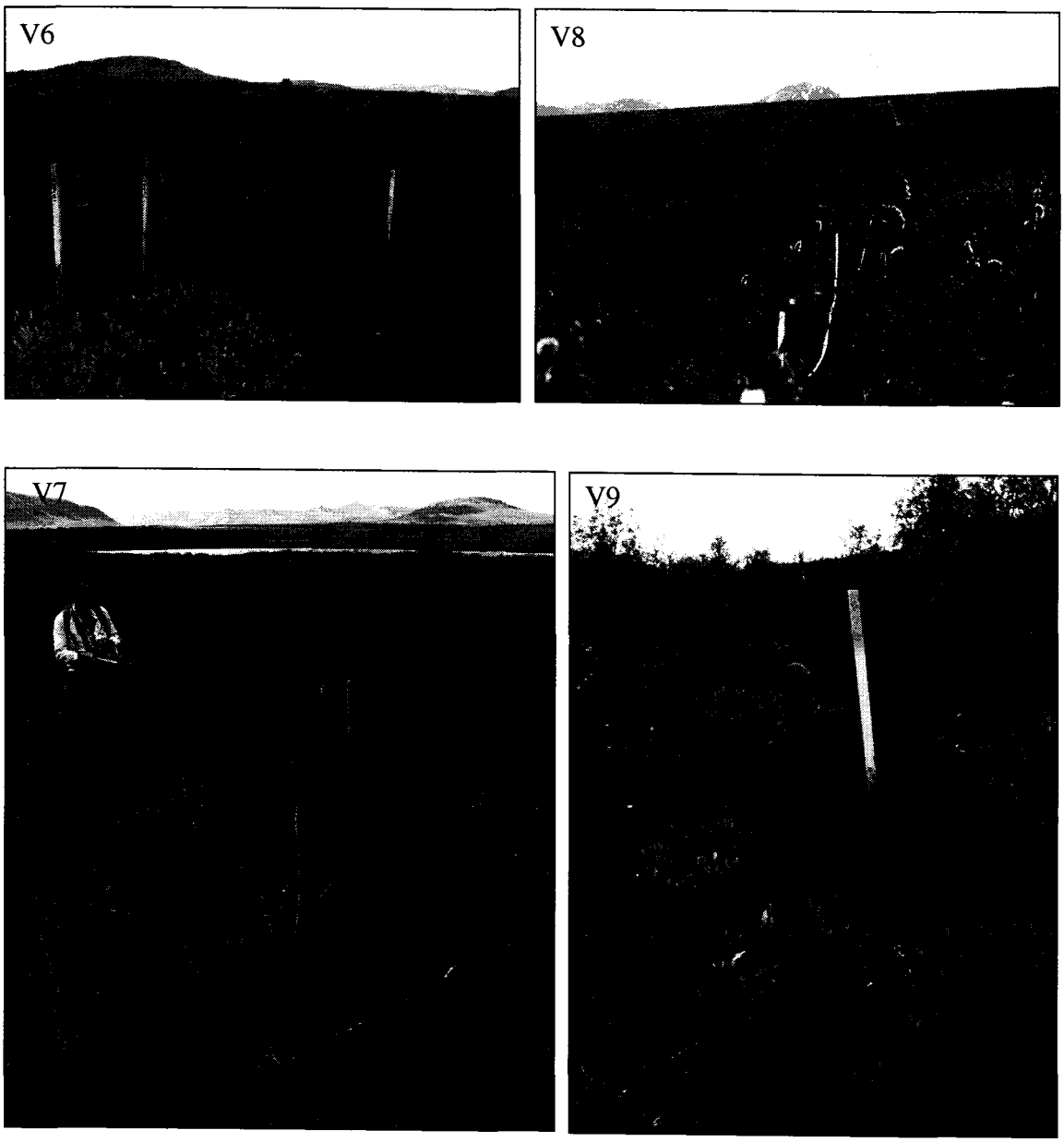

Fig. 4.4 Vegetation cover at four sites with medium height shrubs.

level of variability. The vegetation at this site generally constitutes a sparse tall shrub layer over a patchy medium shrub layer, with some prostrate shrubs and a nearly continuous moss cover beneath (Fig 4.5).

4.2.3 Species composition

Despite similar vegetation structure, species composition at each site varies according to growing conditions. Table 4.4 lists dominant species at the valley-bottom sites and at the reference site. Species are grouped according to the stratification of the vegetation cover at each site. Table 4.5 presents percent cover for shrubs, graminoids, mosses, lichens, bare ground, and water for each of the valley-bottom transects (V1 to V10) and for the reference site (R1). The shrub cover class includes woody plants of all heights. Shrub cover provides an indication of the amount of woody biomass at each site, which is the portion of the vegetation structure most susceptible of influencing snow-pack development. Sites with a dwarf and low shrub vegetation have a varying shrub cover with 5-10% cover at site V3, 10-20% cover at sites V4 and V5, and 20-35% at site R1. At all these sites, the shrub cover constitutes of *Betula glandulosa* and *Ledum decumbens*, with *Empetrum nigrum* at V3, *Vaccinium uliginosum* at V4, and *Vaccinium vitis-idaea* at V5. These species indicate acidic bog conditions, and suggest slightly better drainage at V5, where *Vaccinium vitis-idaea* is abundant. Sites with medium height shrubs have 20-35% shrub cover, with the upper canopy layer constituting of *Betula gandulosa* and *Salix* spp. Site V9 is an exception to this with a shrub cover between 35% and 60% and an upper layer of tall and medium *Salix* spp. with *Potentilla fruticosa* dominating in some sections. The site with the tallest shrubs, V10 has a canopy constituting of *Salix* spp. representing a 20-35% canopy cover.

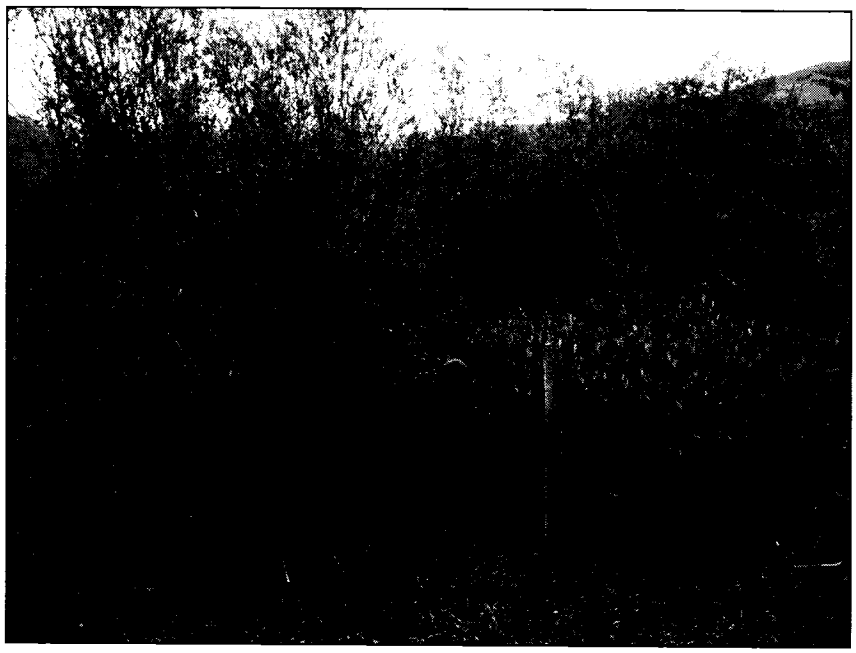

Fig. 4.5 Tall shrub vegetation cover at V10.

Table 4.4 Summary of dominant species at valley-bottom sites and at the reference site.

Site	Upper Layer	Intermediate Layer	Lower layer
V1	Lake		
V2	Pond		
V3	Low shrubs: *Betula glandulosa, Ledum decumbens, Empetrum nigrum.*	Small tussocks: *Eriophorum* spp.	Mosses: *Sphagnum* spp. Diverse lichens: *Cetraria* spp., *Cladina* spp.
V4	Low shrubs: *Betula glandulosa, Vaccinium uliginosum, Salix* spp.	Tussocks: *Eriophorum* spp. Forbs: *Rubus chamaemorus*	Mosses: *Sphagnum* spp. Lichens: *Cetraria* spp.
V5	Low shrubs: *Betula glandulosa, Ledum decumbens, Vaccinium vitis-idaea*	Tussocks: *Eriophorum* spp. Forbs: *Rubus chamaemorus*	Mosses: *Sphagnum* spp. Lichens: *Cetraria* spp.
V6	Med. shrubs: *Betula glandulosa, Salix* spp.		Mosses: pleurocarpous and acrocarpous Abundant lichen: *Cladina* spp.
V7	Med. shrubs: *Betula glandulosa, Salix* spp.	Low shrubs: *Vaccinium vitis-idaea* Forbs: *Rubus chamaemorus*	Mosses: *Sphagnum* spp., acrocarpous mosses.
V8	Med. shrubs: *Salix* spp., *Betula glandulosa*	Graminoids: *Carex* spp. Forbs: *Equisitum* spp. Low shrubs: *Vaccinium uliginosum*	Mosses: pleurocarpous
V9	Tall shrubs: varied *Salix* spp.	Med. shrubs: *Potentilla fruticosa, Salix* spp.	Mosses: acrocarpous and pleurocarpous Dwarf shrubs: *Salix reticulata* and *Dryas* spp.
V10	Tall shrubs: varied *Salix* spp.		Mosses: acrocarpous and pleurocarpous Dwarf shrubs: *Salix reticulata*
R1	Low shrubs: *Betula glandulosa, Ledum decumbens*	Tussocks: *Eriophorum* spp.	Mosses: *Sphagnum* spp. Dwarf shrubs: *Salix reticulata* Lichens: *Cetraria* spp. *Cladina,* spp.

Table 4.5 Summary of vegetation structure and ground cover (%) data for valley-bottom transects.

Site	Shrub cover	Graminoid cover	Moss cover	Lichen cover	Bare ground	Water
V1	0	0	0	0	0	100
V2	0	0	0	0	1-3	100
V3	5-10	10-20	10-20	20-35	0-1	0
V4	10-20	10-20	60-100	5-10	0-1	0
V5	10-20	10-20	60-100	10-20	0	0
V6	20-35	5-10	35-60	10-20	0-1	3-5
V7	20-35	10-20	60-100	0-1	1-3	5-10
V8	20-35	20-35	35-60	0	0-1	0
V9	35-60	1-3	20-35	5-10	1-3	0
V10	20-35	3-5	60-100	1-3	0-1	0
R1	20-35	35-60	35-60	10-20	0-1	0

Graminoid cover in the sites with low shrubs generally consists of *Eriophorum* and *Carex* spp. in tussock formations. These are densest and most abundant at the reference site, R1. At the sites with a medium height shrub cover, graminoids are associated with wet environments such as drainage channels (V6), proximity to a water body (V7), or poor drainage (V8).

Most sites are covered with a continuous moss layer over a thick organic mat. Despite the reduced apparent moss cover, site V3 also has a thick layer of sphagnum moss largely covered with lichens and dense tussocks. Site V9 is an exception to this, with a sparse moss and lichen cover over a rocky substrate.

4.2.4 Active-layer depth

Table 4.6 presents the median depth of thaw at each transect, measured in September 2006. The depth of thaw varies from 33 cm at the reference site (R1) to over 120 cm near the Blackstone River (V9). It was not possible to survey transect V9 with the active layer probe, as boulders prevented penetration. A pit was dug to a depth of 1.30 m, where the water table was encountered. No frozen ground was found. The pond found at site V2 had partly drained by September, and eleven thaw-depth measurements were collected on the exposed pond bottom. Active-layer depth showed no obvious linear relation to vegetation structure as described by canopy height or LAI.

Table 4.6 Median depth of thaw and interquartile range (IQR) at valley-bottom transects in September 2006.

Site	Thaw depth (m)	n	IQR
V1	N/A	0	N/A
V2	0.95	11	N/A
V3	0.38	48	0.05
V4	0.41	24	0.08
V5	0.42	48	0.16
V6	0.35	54	0.10
V7	0.38	24	0.23
V8	0.70	24	0.26
V9	>1.30	1	N/A
V10	0.55	72	0.23
R1	0.33	42	0.06

4.3 Description of the hill sites

4.3.1 Topography

The hill transects were established in small valleys, on plateaus, benches, and ridges between 1265 m and 1675 m elevation (Table 4.7). Most sites were located on flat or gently sloping terrain with a median slope below 3°. Transect T4 is located on a small plateau, and the slope value obtained from the 30 m resolution DEM was exaggerated as it included portions of the hillslope surrounding the plateau in the transect. The value measured on site with an inclinometer was used instead. Site T5 is located on sloping terrain in a valley providing a higher level of topographic sheltering.

Topographic sheltering (Table 4.8) at the hill sites is more variable than at the valley-bottom sites. Sites located on plateaus and ridges (T1, T2, T3, and T4) are on high points in the landscape and receive very little sheltering from the surrounding terrain. At site T5, the sloping terrain and surrounding valley walls provide substantial sheltering, and the site is only exposed on the north and east sides.

Transect T2, and T4 are located on planar ground with very little microtopography. The ground surface at sites T1, T3, and T5 is hummocky. The hummocks are small and sparse at site T3, rarely greater than 15 cm in height. Hummocks at T5 vary between 0.3 m and 1.5 m in diameter and are up to 0.3 m in height. At site T1, surface features are up to 0.6 m in diameter and up to 0.5 m in height.

4.3.2 Vegetation cover

All hill sites have a maximum canopy height below 0.2 m (Table 4.9), suggesting that their structure is similar to reference site R1 and to valley-bottom sites V3, V4, and V5. In contrast with these sites, the graminoid cover is generally lower on the hill slopes

Table 4.7 Elevation, slope, aspect and microtopography at hill sites.

Site	Elev. (m)	Slope (°)	Aspect (°)	Microtopography
T1	1296	3	E	Hummocky
T2	1310	3	E	Planar
T3	1568	1	E	Hummocky
T4	1675	3	S	Planar
T5	1266	7	N	Hummocky

Table 4.8 Median sheltering index (eq. 3.1) in five directions for all hill transects, calculated based on a radius of 30 m, 60 m, and 90 m. Negative values indicate that elevation decreases away from the transect.

Site	n	North	East	South	South-East
T1	10	0.00	-0.02	-0.01	-0.02
T2	7	0.03	-0.03	-0.02	-0.05
T3	10	0.00	-0.06	-0.04	-0.05
T4	11	-0.03	0.00	-0.33	-0.20
T5	10	-0.09	-0.08	0.09	0.01

Table 4.9 Median of maximum canopy height and LAI measurements for all hill transects.

Site	Canopy Height (m)			Leaf Area Index		
	median	n	IQR	median	n	IQR
T1	0.09	90	0.09	0.12	10	0.14
T2	0.19	63	0.25	0.81	7	0.27
T3	0.10	90	0.11	0.50	10	0.47
T4	0.06	72	0.05	0.09	11	0.09
T5	0.17	90	0.17	0.35	10	0.44

(Table 4.10), and tussocks are rare. Sites T2 and T4 have a low moss cover and a high lichen cover, and both have thin soil. Site T2 has a high percentage of bare ground cover as a result of extensive patterned ground over the area (Fig. 4.6).

Figure 4.7 presents a box and whisker diagram of maximum canopy height for the six hill sites and the reference site R1. Site T1 and T3 appear structurally similar to the reference site, while T4 has a lower vegetation cover. The vegetation cover of the latter transect is characterised by an extensive lichen cover (Table 4.10), with sparse graminoids forming the upper canopy and dwarf shrubs underneath (Table 4.11). Sites T2 and T5 (Fig. 4.6 and 4.8) have a higher canopy cover , including low to medium height *Betula glandulosa* (T2) or *Betula glandulosa* and *Salix* spp. (T6) (Table 4.11).

4.3.3 Active-layer depth

Table 4.12 presents the median depth of thaw at each transect, as measured in September 2006. The depth of thaw varied from 0.38 cm at site T6 to over 1.20 m at site T2, and showed no obvious relation to elevation.

4.4 Temperature-sensor locations

Table 4.13 summarizes conditions at the nine locations equipped with data loggers. Elevation ranged from 927 m to 1676 m. Most sites are located on gentle slopes, and the data logger at site T3 is located on the steepest terrain with a slope of 4°. Six of the sites are located between 900 m and 1200 m, and represent a range of vegetation structures with maximum canopy heights from 0.08 m to 0.84 m, and LAI from 0.39 to 1.66.

Table 4.10 Ground cover (%) by functional group at hill sites.

Site	Shrub cover	Graminoid cover	Moss cover	Lichen cover	Bare ground	Water
T1	10-20	5-10	35-60	20-35	0-1	1-3
T2	20-35	0-1	5-10	60-100	10-20	0
T3	5-10	5-10	20-35	35-60	1-3	0-1
T4	5-10	3-5	5-10	60-100	1-3	0
T5	10-2	1-3	60-100	10-20	0-1	0

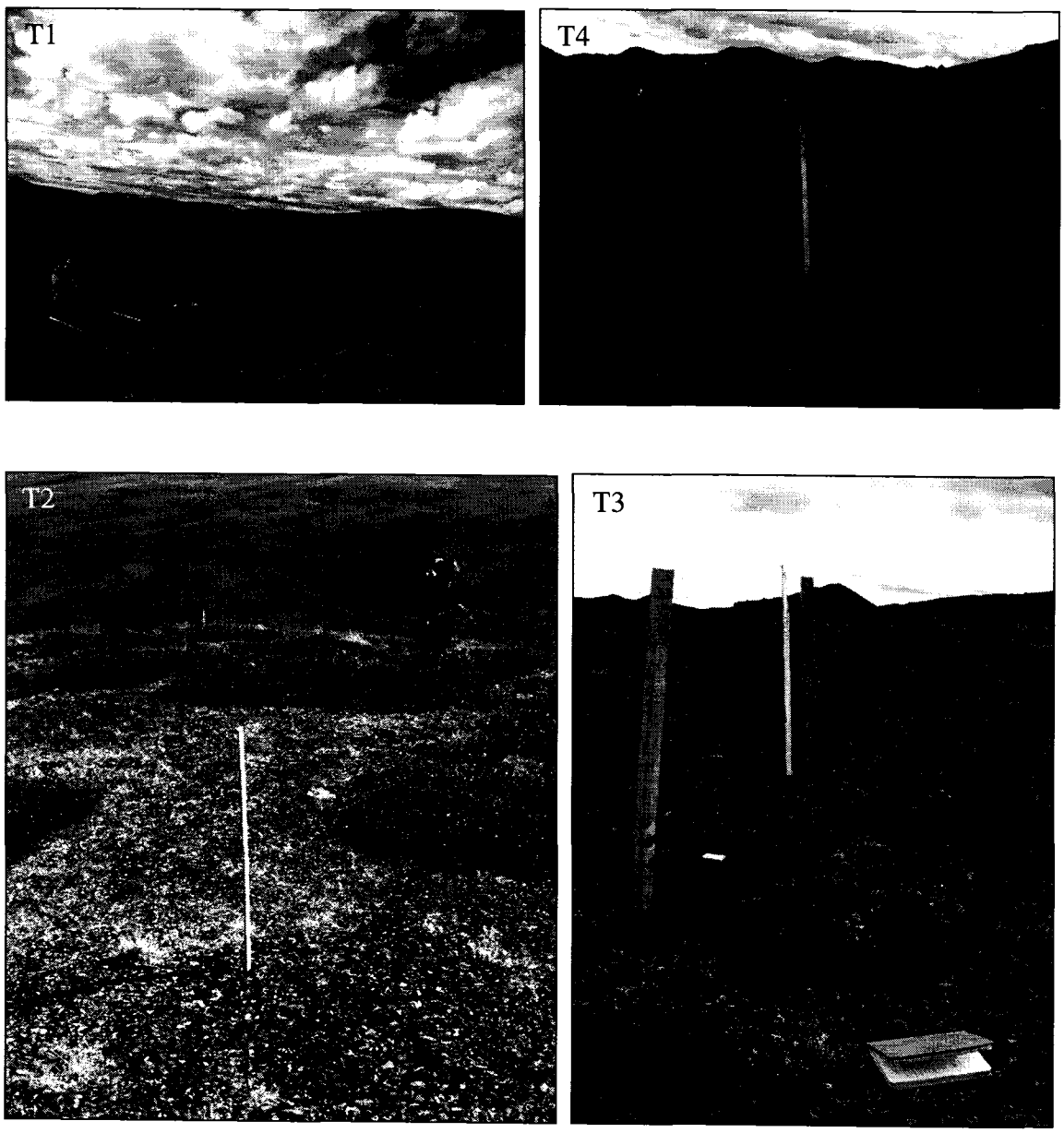

Fig. 4.6 Photographs of hill sites T1, T2, T3, and T4.

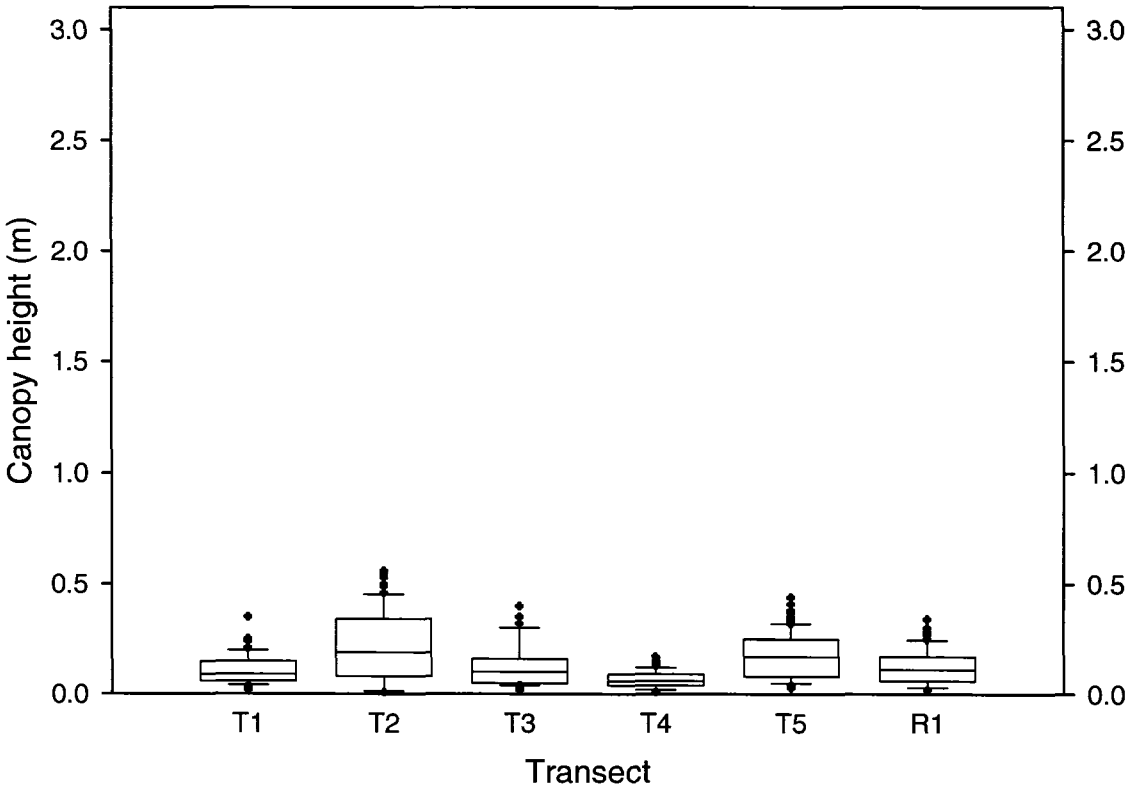

Fig. 4.7 Maximum canopy height at the hill transects (T1 to T5) and at the reference site (R1).

Table 4.11 Summary of dominant species for the hill transects. Dominant species are grouped according to the stratification of the vegetation cover.

Site	Upper Layer	Intermediate Layer	Lower layer
T1	Low shrubs: *Vaccinium uliginosum, Cassioppea tetragona.*	Tussocks: *Carex* spp.	Mosses: acrocarpous Dwarf shrubs: *Salix reticulata, Dryas* spp.
T2	Patches of low to medium shrubs: *Betula glandulosa.*		Dwarf shrubs: *Dryas* spp. *Salix reticulata, Salix arctica* Lichens: *Cetraria* spp., *Cladina* spp., *Flavocetraria* spp., *Stereocaulon* spp.
T3	Sparse low shrubs: *Betula glandulosa, Salix* spp., *Cassioppea tetragona*		Mosses: acrocarpous Lichens: *Cladina* spp., *Cetraria* spp.
T4	Sparse graminoids: *Hierochloe alpina, Carex* spp.		Dwarf shrubs: *Dryas* spp., *Salix* spp. Lichens: *Cladina* spp., *Cetraria* spp., *Flavocetraria* spp.,
T5	Low shrubs: *Ledum decumbens, Cassioppea tetragona, Salix* spp., *Betula glandulosa, Vaccinium vitis-idaea*		Mosses: acrocarpous and pleurocarpous Dwarf shrubs: *Dryas* spp. Lichens: *Cetraria* spp.

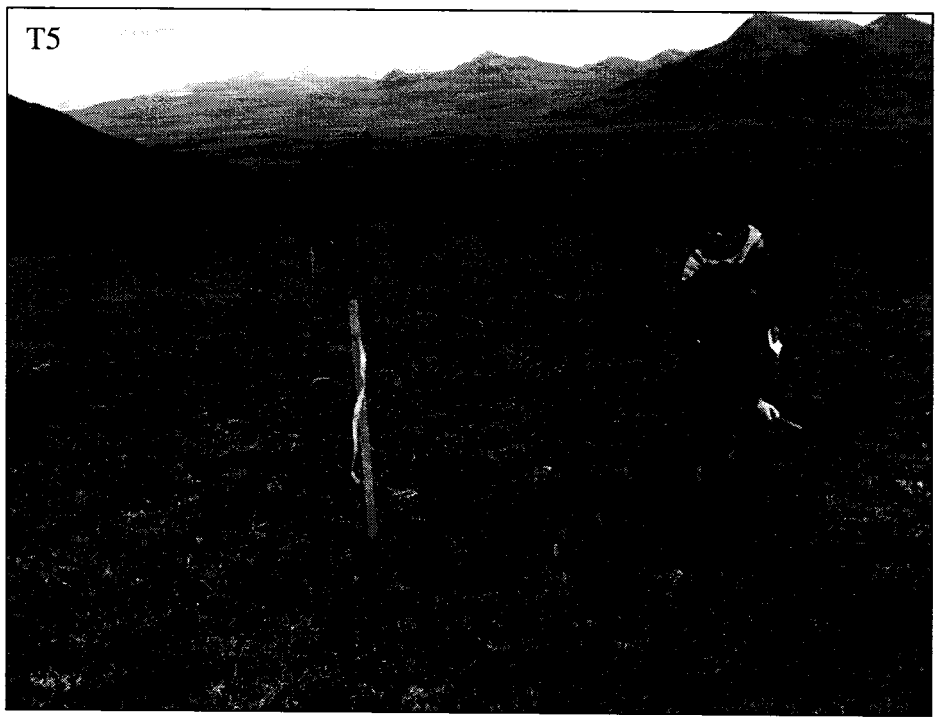

Fig. 4.8 Photograph of hill site T5.

Table 4.12 Mean depth of thaw measured along the hill transects in September 2006.

Site	Thaw depth (m)	n	IQR
T1	0.51	50	0.30
T2	>1.20	18	0
T3	0.48	64	0.21
T4	0.78	33	0.35
T5	0.38	55	0.10

Table 4.13 Summary of topography, maximum thaw depth, and ground cover at each location equipped with ground temperature sensors.

Site	Elev. (m)	Aspect	Slope (°)	Max. Thaw Depth (m)	Canopy Height (m)	LAI	Ground Cover Classes (%)			
							Shrub	Graminoid	Moss	Lichen
V3	995	S	2	0.41	0.08	0.64	11-20	6-10	21-35	11-20
V4	927	N	3	0.35	0.14	0.39	6-10	11-20	36-60	6-10
V5	955	N	3	0.42	0.54	1.66	21-35	11-20	61-100	0
V6	1106	E	1	0.43	0.43	0.64	36-60	0-1	61-100	11-20
V10	925	E	1	0.73	0.84	1.53	4-5	4-5	61-100	4-5
T1	1300	E	1	0.79	0.07	0.03	11-20	11-20	36-60	21-35
T3	1566	N	4	0.49	0.06	0.12	11-20	2-3	21-35	36-60
T4	1676	E	3	0.81	0.05	0.04	6-10	2-3	6-10	61-100
R1	1114	E	2	0.34	0.18	0.25	11-20	21-35	36-60	21-35

4.5 Concluding remarks

The fifteen sites presented in this chapter differ according to the characteristics of their topography and vegetation cover. This research investigates the effect of these characteristics on snow-pack development and ground freezing.

Chapter 5
SNOW-PACK DEVELOPMENT AND FROST PENETRATION IN THE BLACKSTONE UPLANDS

5.1 Introduction

This chapter describes the development of the snow pack between October 15th and January 23rd at each site, and summarizes the freezing of the active layer at the nine sites equipped with ground-temperature sensors. The main controls on snow-pack development are identified, and the relations between ground freezing, snow, elevation, and vegetation structure are discussed. Finally, the effectiveness of the reference site as an indicator of snow-pack development and ground freezing over the study area is assessed.

5.2 Snow-pack development at the valley-bottom sites

Table 5.1 presents monthly median snow depth at each transect. In October, median snow depth in the valley bottom ranged from 2 cm to 5 cm, and in November from 6 cm to 11 cm. In the following two months, snow depth increased and became more variable, ranging from 7 cm to 21 cm in December and 8 cm to 42 cm in January.

The variability of the snow cover within each transect increased between November and December, as reflected in the greater interquartile ranges (IQR) (Table 5.1). These increases in IQR were between 200% and 500% and exceeded the increases in snow depth observed during the same period. Exceptions to this are the reference site, where the IQR remained at the same level while the snow pack decreased by 30%, and sites V1, V2, and V9 which are all characterized by a planar ground surface. Figure 5.1 presents the evolution of the median snow depth and IQR at three valley-bottom sites with a vegetation cover characterised by low shrubs and grass tussocks. An increase in

Table 5.1 Monthly median snow depth at the reference site and at all valley-bottom transects. The number of measurements over each transect and the interquartile range of the data are presented.

	October Snow Depth (cm) [n, IQR]	**November Snow Depth (cm) [n, IQR]**	**December Snow Depth (cm) [n, IQR]**	**January Snow Depth (cm) [n, IQR]**
V1	2 [80, 1.5]	5 [160, 1]	8 [160, 4]	11 [79, 4]
V2	3 [80, 2.5]	7 [40, 3]	7 [40, 5]	8 [39, 4]
V3	5 [80, 2]	8 [160, 3]	12 [159, 6]	18 [81, 9]
V4	4 [80, 2]	9 [40, 1]	15 [40, 5]	31 [40, 11]
V5	3 [159, 3]	8 [80, 2]	13 [80, 6]	18 [80, 9]
V6	4 [200, 2]	9 [200, 3]	19 [199, 7]	36 [100, 11]
V7	3 [80, 4]	11 [40, 5]	19 [40, 14]	42 [40, 31]
V8	4 [80, 3]	9 [40, 3]	20 [40, 6]	34 [40, 8]
V9	3 [160, 2.5]	6 [80, 2]	15 [159, 2]	26 [80, 4]
V10	3 [225, 4]	7 [121, 2]	16 [240, 6]	31 [120, 7]
R1	5 [500,4]	10 [600, 4]	7 [400, 4]	12 [102, 8]

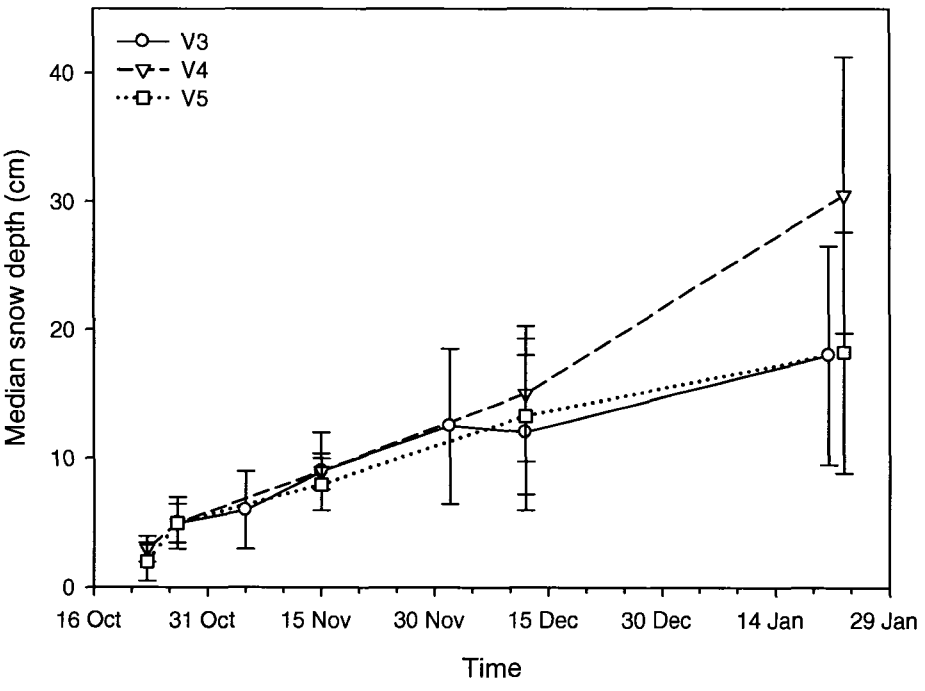

Fig. 5.1 Median snow depth and interquartile range (IQR) at three valley-bottom sites with a vegetation cover characterised by low shrubs and tussocks.

the IQR of snow-depth measurements was observed after November 15th.

The variability rose as the wind began to erode snow from the high points of the microtopography while snow accumulated in the depressions, effectively increasing the variability of the snow depth measurements at the microscale. Figure 5.2 presents a photograph of the snow pack at a low shrub and tussock site in the valley on December 5th, 2006. At sites V3, V4, and V5, the top of the hummocks had a thin snow pack and deeper snow was found in inter-hummock troughs.

Snow-pack variability also increased at the landscape scale between November 15th and December 2nd. Figure 5.3 presents the development of the snow pack at four sites located in the valley bottom which are characterized by four different vegetation covers. There was noticeably less snow at the site with no vegetation (V2) than at the vegetated sites (V3, V6, and V10) from the end of October onwards, and there was no further snow accumulated at V2 after mid-November. At both sites with no vegetation, snow transport began to occur near the end of October, earlier than at the vegetated sites, as snow-pack thickness exceeded 5 cm. The vegetated sites all had a similar median snow-pack thickness until mid-November, when approximately 10 cm had accumulated. Differentiation of the snow pack between vegetated sites began between November 15th and December 2nd, and became more accentuated over the following weeks.

Snow transport begins when the snow pack exceeds the snow-holding capacity of the vegetation cover, and when the shear velocity of the wind at the snow surface exceeds the threshold shear velocity of the snow cover. The observed increase in snow distribution may thus have been due to increased availability of snow for transport, or to

Fig. 5.2 Photograph of the snow pack at a low shrub and tussock valley-bottom site looking north-east on December 5th, 2006.

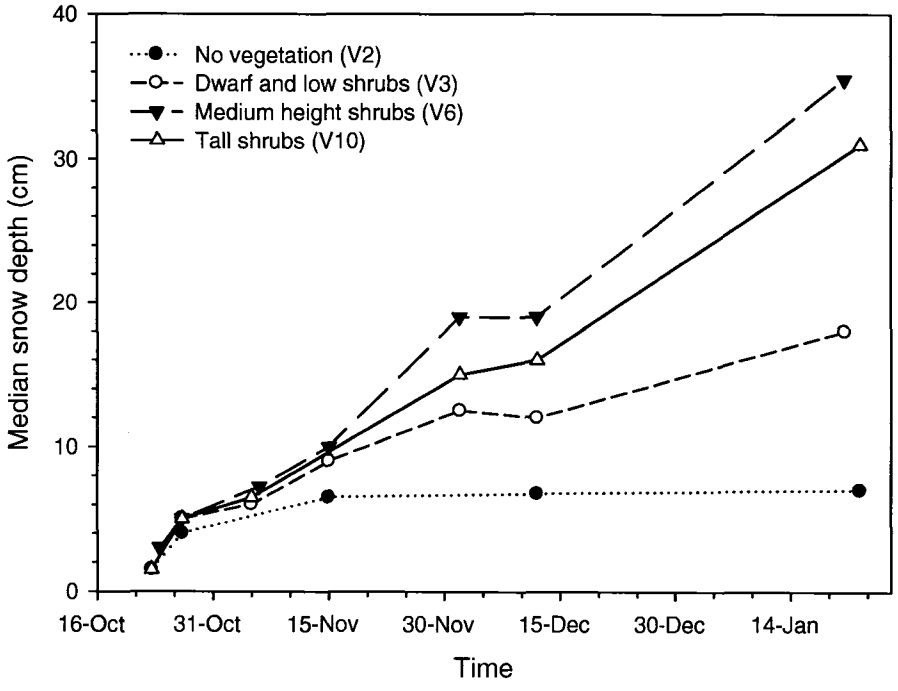

Fig. 5.3 Evolution of snow-pack thickness at four valley-bottom sites characterized by four different vegetation covers.

an increase in wind speed. Figure 5.4 allows an examination of the weather conditions recorded between November 15th and December 2nd, in relation to the evolution of the snow pack at V3 and V6. Wind conditions at 3 m and air temperature at 1.5 m were recorded at the meteorological station within the study area and precipitation events were recorded at Oglivie Camp, 65 km to the north. Due to topographic effects, absolute values of precipitation recorded at Olgivie Camp may not be repeated in the study area. They are included in the diagram as an indication of days where precipitation was recorded in the vicinity of the study area.

On November 19th and 20th, a precipitation event accompanied by daily mean wind speeds of 4 m/s was recorded. Half-hourly wind speeds near 8 m/s were recorded during these two days for the first time since the beginning of snow accumulation. Air temperature generally increased during high-wind and precipitation events, reducing the cohesion of the snow pack and facilitating erosion and transport of snow. As a result of these conditions, the threshold shear velocity of the snow cover was exceeded, leading to the redistribution of snow from vegetated areas with a reduced snow-holding capacity such as V3 to areas with an increased snow-holding capacity such as V6.

This period of increased winds was followed by a snowfall event in relatively calm conditions on November 30th and December 1st, and fresh snow was recorded at V3 and V6 on December 2nd. Despite its high elevation on the valley bottom, no fresh snow was observed on December 2nd at the reference site (R1). A wind slab was observed at the surface of the snow pack. Assuming it had also received snow after the windy

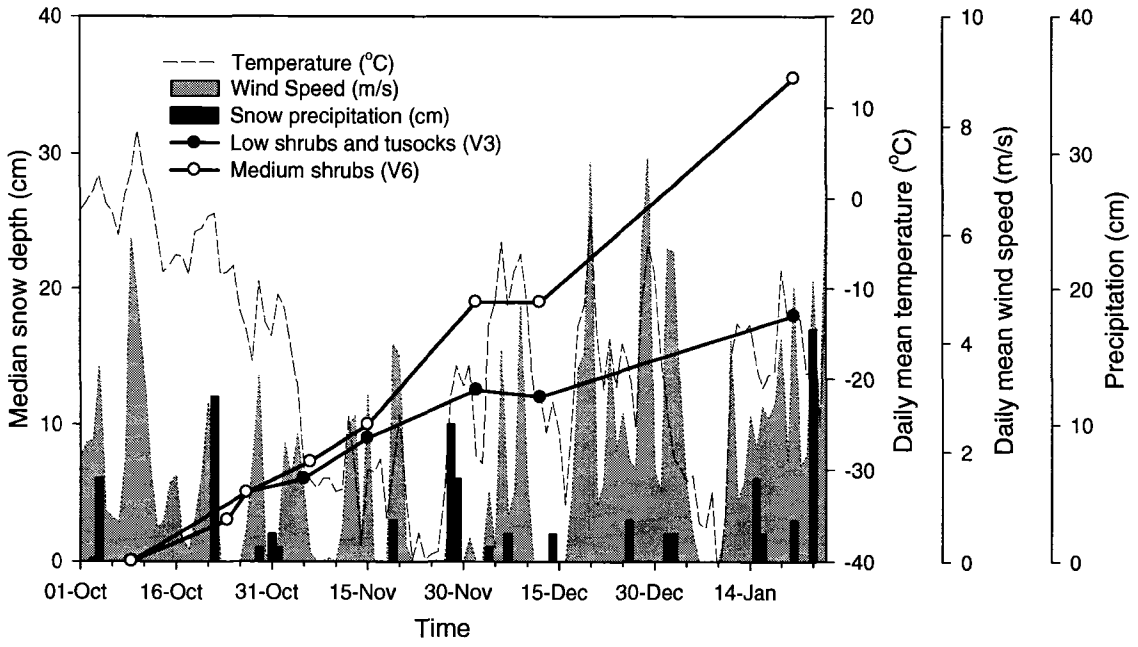

Fig. 5.4 Snow-pack development at two valley-bottom sites in relation to daily mean air temperature and daily mean wind speed 3 m above the ground recorded in the study area, and precipitation events recorded at Ogilvie Camp.

conditions of November 19th and 20th, this observation suggests windier conditions at the reference site than at other valley-bottom sites during that period.

5.3 Snow-pack development at the hill sites

Transect T1, T2, and T5 are all located between 1200 m and 1400 m elevation, and are the closest in elevation to the valley-bottom transects. At these sites, snow accumulation until November 16th was followed by reduced changes in snow-pack thickness, with a slight increase at T1 and T2 and a slight decrease at T5 (Fig. 5.5 and Table 5.2). Transects T1 and T2 have a similar snow-pack thickness until mid-November, and an increasingly different snow pack after the beginning of December (Fig. 5.5). The interquartile range (IQR) of the snow depth measurements at T1, T2, and T5 is also larger in December and January than in October and November (Table 5.2), following a pattern similar to the valley-bottom transects.

In contrast, the IQR of measurements at T3 and T4, located respectively at 1570 m and 1675 m elevation, was more than double that of the lower hill transects in October, and did not increase between November and December. This suggests that substantial redistribution of snow by wind occurred in October and November at these higher sites. The median snow depth at T4 decreased by nearly 60% between October 26th and December 12th before stabilising near 7 cm (Fig. 5.5). The rate of snow accumulation at T3 decreased after October 26th, and between November 17th and December 12th snow thickness was reduced by approximately 20%. This marked decrease in snow thickness suggests that the snow which accumulated at these higher elevations during the first

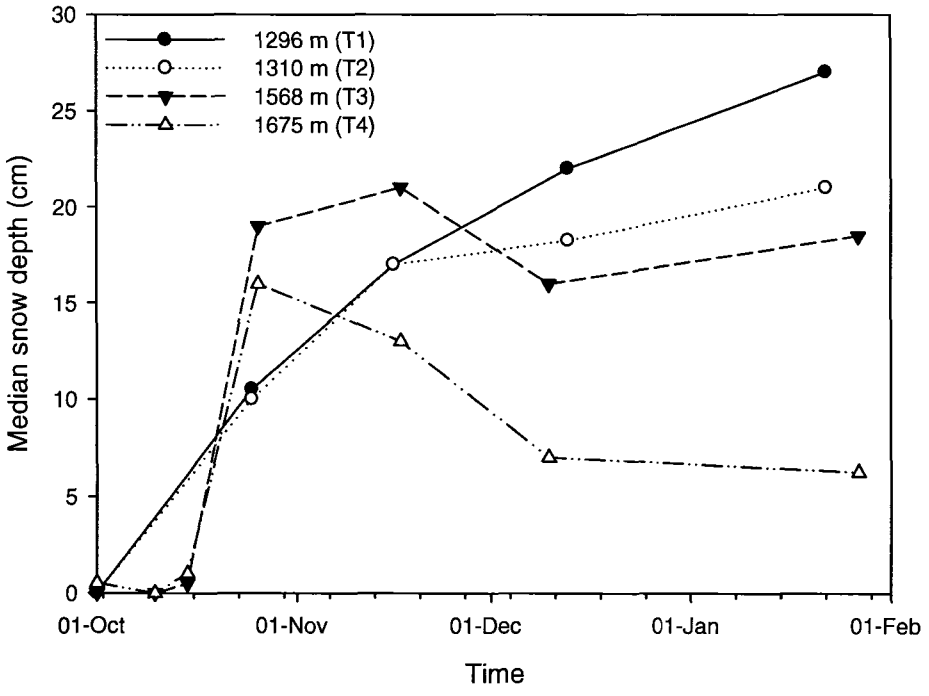

Fig. 5.5 Development of the snow pack at four hill sites.

Table 5.2 Monthly median snow depth and interquartile range for all hill transects.

	October Snow Depth (cm) [n, IQR]	**November Snow Depth (cm) [n, IQR]**	**December Snow Depth (cm) [n, IQR]**	**January Snow Depth (cm) [n, IQR]**
T1	11 [100, 2]	17 [100, 3]	22 [99, 8]	27 [100, 18]
T2	10 [70, 2]	17 [70, 5]	18 [70, 11]	21 [70, 16]
T3	19 [100, 7]	21 [100, 9]	16 [100, 9]	19 [103, 14]
T4	16 [110, 7]	13 [100, 10]	7 [110, 8]	6 [110, 6]
T5	11 [100, 3]	20 [100, 6]	22 [100, 10]	21 [102, 13]

snowfalls exceeded the holding capacity of the vegetation structure and microtopography under windy conditions.

5.4 Controls on snow-pack development

5.4.1 Relations between snow depth and vegetation structure

In the months of October and November, prior to redistribution of snow by wind, snow depth was similar at all valley-bottom transects and showed no statistically significant relation to canopy height or leaf-area index (Fig. 5.6). A positive correlation between snow depth and vegetation structure developed in December and January.

Despite a median canopy height of 0.71, snow depth at V10 did not exceed snow depth at the shrubby sites with a lower canopy. Transect V10 was located at the center of an area covered with tall shrubs. Tall and dense vegetation can act as a wind break, preventing wind-transported snow from reaching the center of the stand. This effect is apparent, for example, along a snow profile extending through V2 and V7 in December (Fig. 5.7). The snow eroded from the area with no vegetation (V2) and blown towards the medium height shrubs (V7) was mostly deposited in the first 25 m of shrubby vegetation.

5.4.2 Vegetation structure and snow-holding capacity

The snow-holding capacity of a specific vegetation cover is the depth of snow that can accumulate and "be held" in the vegetation without being susceptible to erosion by wind (Liston and Sturm, 1998). When snow depth exceeds this capacity, excess snow is available for transport by wind (Liston and Sturm, 1998). The majority of the Blackstone Uplands is covered with tundra vegetation typically characterised by a low snow-holding capacity (Table 2.2) due to its minimal structure. In areas with a snow-holding capacity

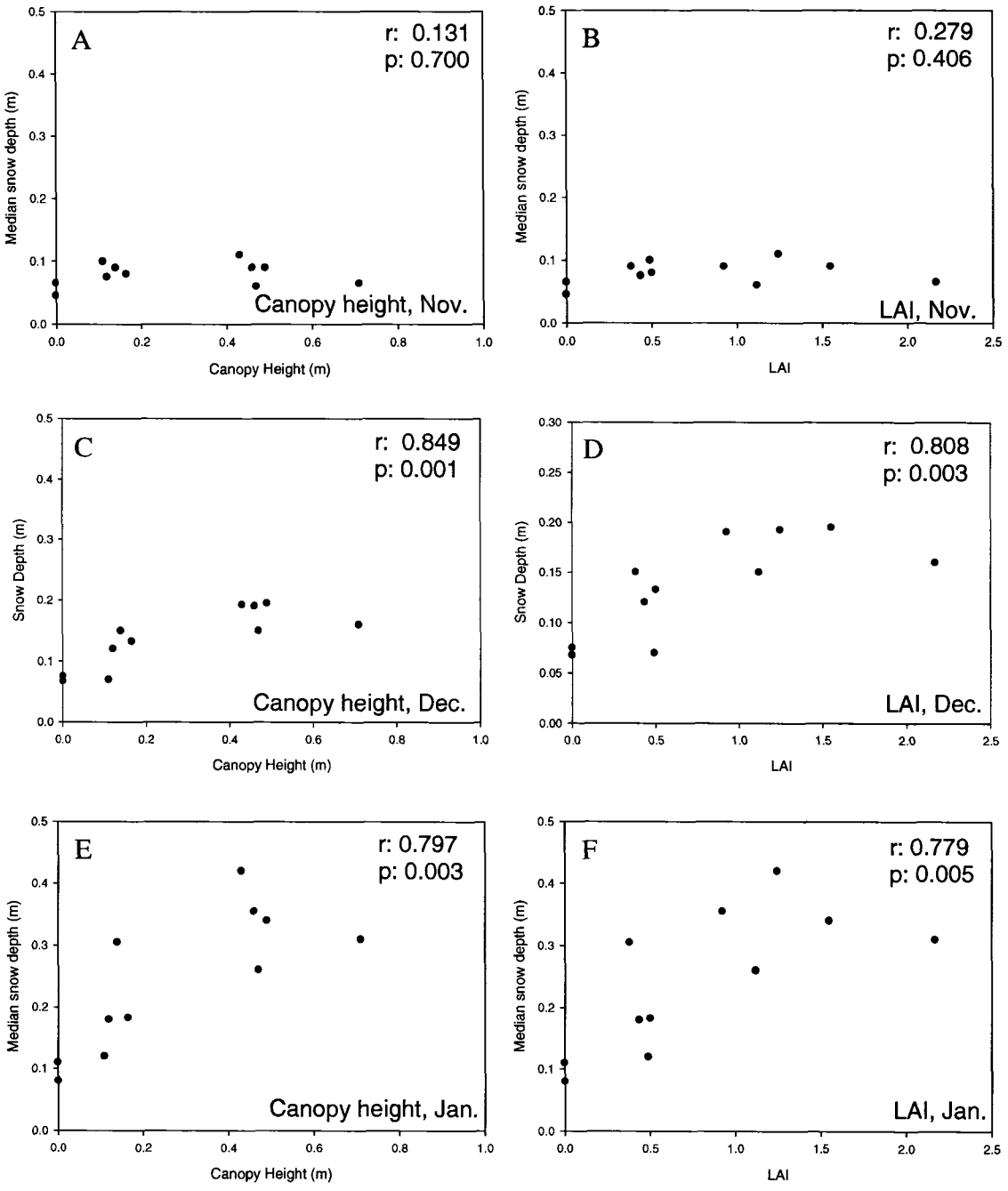

Fig. 5.6 Scattergrams of November snow depth in relation to (A) canopy height and (B) LAI; December snow depth in relation to (C) canopy height and (D) LAI; January snow depth in relation to (E) canopy height and (F) LAI. Only valley-bottom transects are included. Spearman's rank order correlation coefficient (r) and p-value (2-tail) are indicated in each corner.

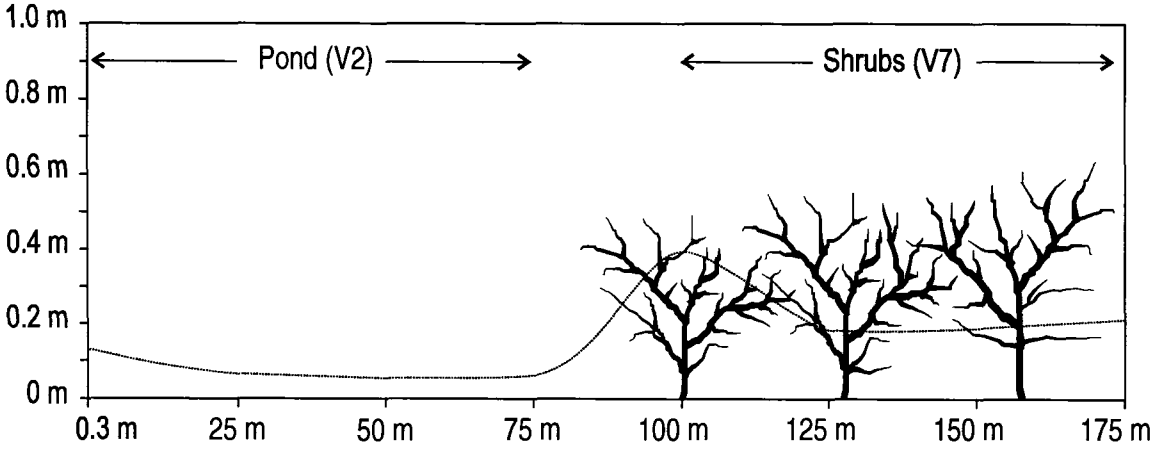

Fig. 5.7 December snow depth profile (dotted line) along two adjoining transects. Shrub height to scale.

below 15 cm the snow cover may decrease below the required snow depth of 15 cm under windy conditions.

Snow-holding capacity along the transects was examined using the minimum snow depth held by the vegetation after wind erosion had occurred. This is based on the assumption that windy events resulted in the erosion of all excess snow, reducing the snow thickness to the vegetation snow-holding capacity. Sampling stations where a decrease in snow depth was observed after the onset of windy conditions (mid-November 2006) were selected. Only measurements taken when no snowfall events were recorded after the last episode with a mean daily wind speed above 4 m/s were used. To ensure snow-holding capacity had been reached, stations with a canopy height above the maximum snow depth measured along all transects during the study period, 73 cm, were excluded. These minimum measured snow depths occurred in November, December, and January at different sites, and were assumed to correspond to the vegetation cover snow-holding capacity at the corresponding stations (Table 5.3).

The relation between the snow-holding capacity and vegetation structure at these stations was investigated and a strong positive correlation was found with canopy height. Examination of the scattergram reveals a trend up to a canopy height of approximately 20 cm, and considerable scatter above this point (Fig. 5.8). It is noteworthy that, under the conditions of scarce snowfall observed in fall and early winter 2006, sites with a canopy height of 20 cm or more generally 'held' a snow cover of at least 15 cm under windy conditions. It is likely that most medium and tall shrubs did not reach maximum snow-holding capacity in fall and early winter 2006 due to the shallow snow cover. Under snowy conditions, sites with canopy heights above 20 cm may reach maximum snow-

Table 5.3 Selected sampling stations and associated snow-holding capacity.

Sampling Station #	Snow-Holding Capacity (m)
V1-4	0.04
V1-10	0.04
V2-11	0.05
V2-12	0.06
V3-3	0.1
V3-5	0.14
V3-6	0.1
V3-7	0.13
V3-8	0.14
V6-6	0.18
V6-7	0.15
V6-9	0.15
V6-10	0.19
V9-2	0.14
V9-3	0.15
V9-6	0.16
T2-4	0.17
T3-2	0.21
T3-3	0.08
T3-4	0.19
T3-5	0.17
T3-6	0.2
T3-7	0.09
T3-8	0.16
T3-9	0.13
T3-10	0.06
T4-10	0.16
T6-1	0.16
T6-7	0.17
T6-8	0.12
T6-9	0.14
T4-1	0.01
T4-2	0.05
T4-3	0.03
T4-4	0.08
T4-5	0.06
T4-6	0.06
R1-7	0.06
R1-8	0.06

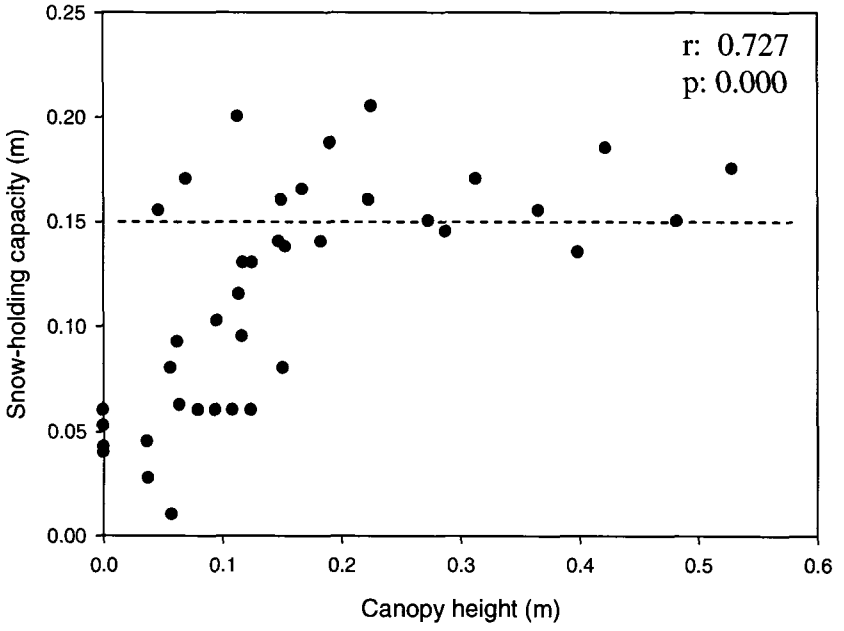

Fig. 5.8 Scattergrams of vegetation snow-holding capacity against canopy height. Spearman correlation coefficient and p-value (two-tailed) are indicated in the corner of the graph. The minimum snow depth required for the opening of the snowmobile season is indicated with a dashed line.

holding capacity at a higher snow thickness, possibly extending the observed trend beyond 20 cm. Further investigation under conditions of abundant snowfall would help clarify this relation for taller vegetation.

5.4.3 Relation between elevation and snow depth

The relation between snow depth and elevation was strong and positive in October and deteriorated as winter progressed (Fig. 5.9). In December and January, after redistribution by wind had gained in importance at the sites located below 1400 m, no significant correlation was found between snow depth and elevation. Correlations were assessed using all the hill transects, except T5 which includes tall shrubs, and R1, V3, V4, and V5 which have a low vegetation cover similar to the hill transects.

5.4.4 The influence of aspect, slope, and topographic sheltering on snow depth

The transects surveyed for this study were mostly located in open, flat areas and as a result the narrow range of topographic sheltering observed in this dataset did not allow for the examination of the relation between topographic sheltering and snow-pack development.

5.5 Assessing snow-pack development in the Blackstone Uplands

5.5.1 Snow-depth at the highway camps

Snow depth on the ground is recorded weekly at Klondike Camp, 30 km to the south of the study area, and at Ogilvie Camp, 65 km to the north. Snow depth at Klondike Camp generally exceeded snow accumulation at the valley-bottom and hill sites during the entire study period (Fig. 5.10a). Snow-pack thickness at Ogilvie Camp was similar to the snow depths observed in the Blackstone Uplands (Fig. 5.10b), but it exceeded

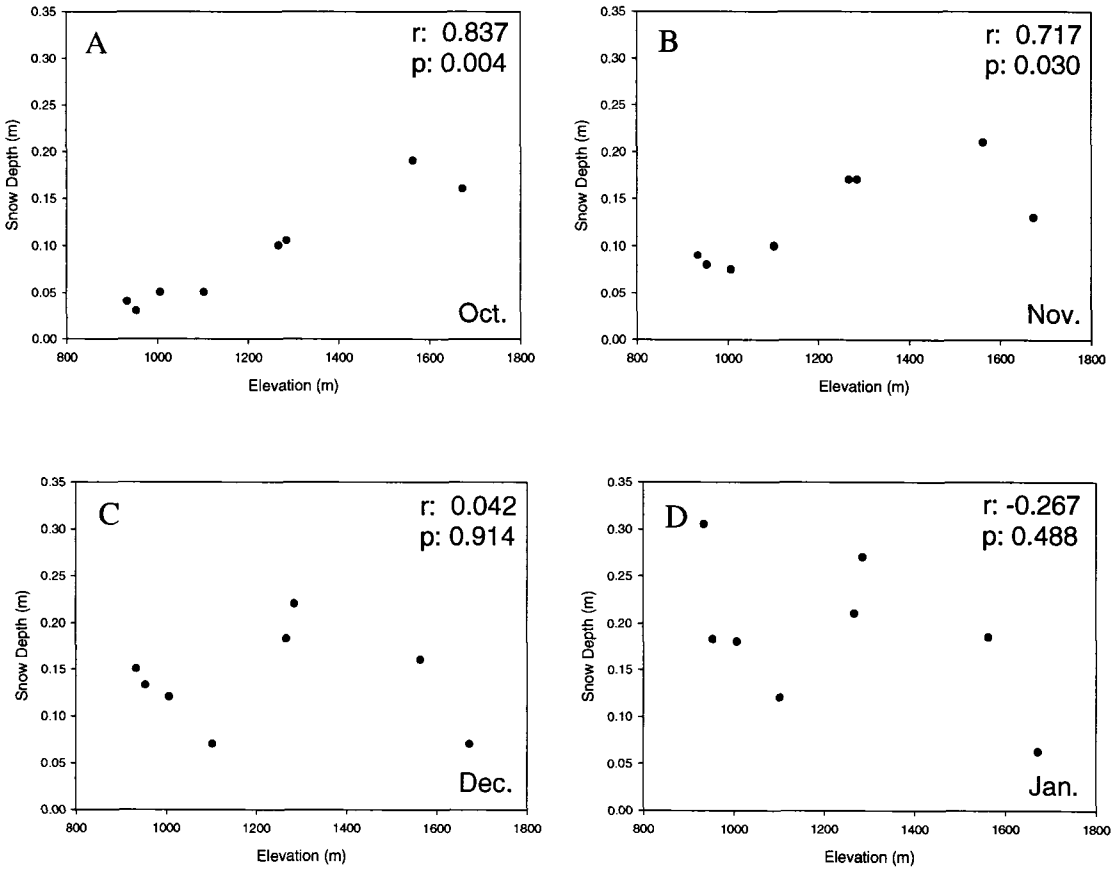

Fig. 5.9 Scattergrams of snow depth in relation to elevation at nine sites with a structurally similar vegetation cover in (A) October, (B) November, (C) December, and (D) January. The Spearman correlation coefficients (r) and p-values (2-tailed) are indicated in the corner of each graph.

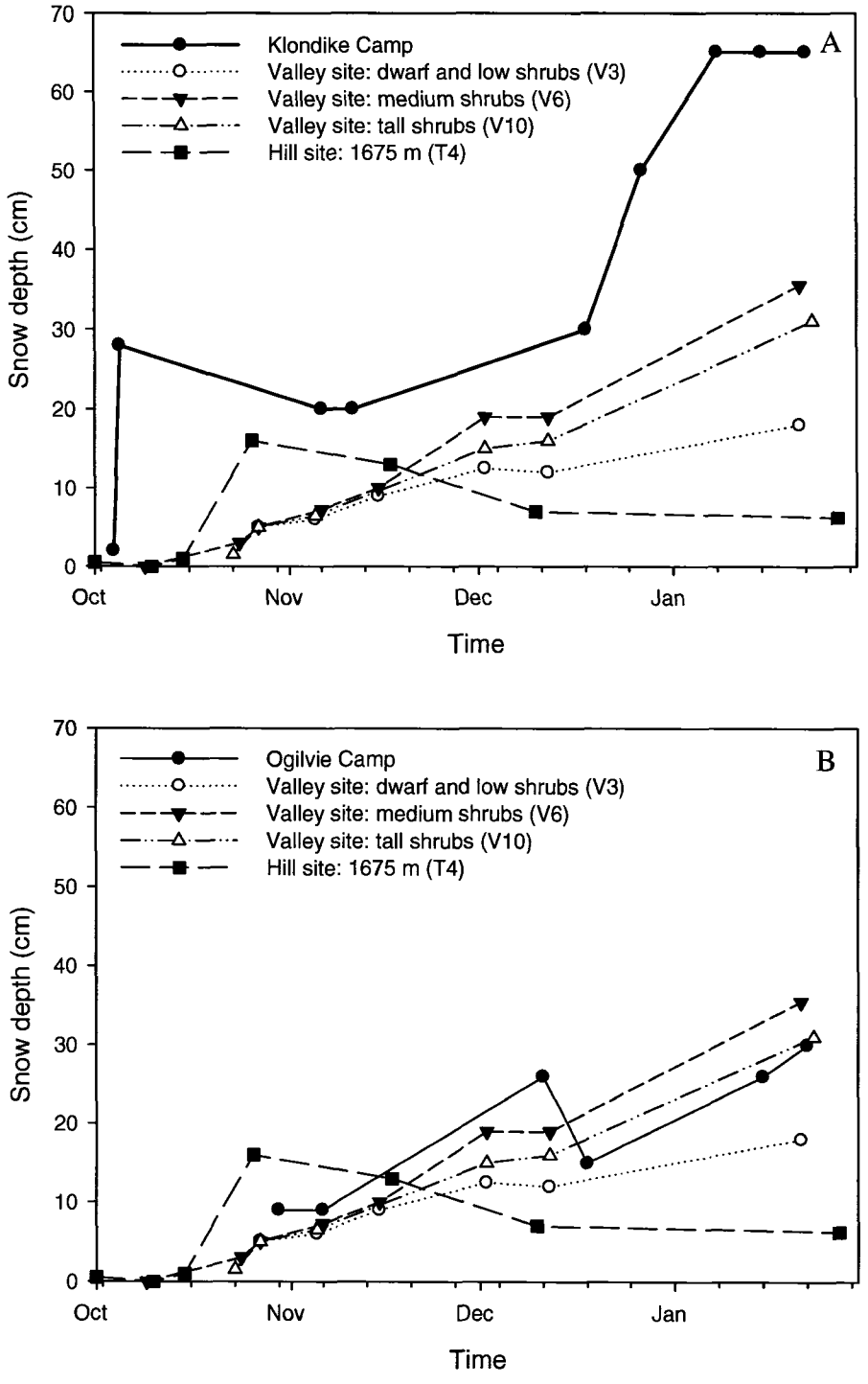

Fig. 5.10 Snow depth on the ground measured at (A) Klondike Camp and (B) Ogilvie Camp compared to median snow depths along representative valley-bottom and hill transects.

snow depth at all valley-bottom sites with dwarf and low shrubs. This vegetation type covers the majority of the high intensity snowmobile-traffic corridor. Using Ogilvie Camp as a reference for snow depth may lead to an overestimation of snow-pack thickness in critical portions of the Blackstone Uplands, and the use of at least one reference site located within the Blackstone Uplands is necessary.

5.5.2 Effectiveness of the reference site as an indicator of snow depth in the area

The reference site is located near the southern boundary of the study area, where the East Blackstone River valley is at approximately 1100 m elevation. Northwards through the study area the elevation decreases to near 920 m. Snow depth at the reference site was 15 cm when the redistribution of snow began, but it remained below 15 cm afterwards (Fig. 5.11), suggesting that the snow-holding capacity of the reference site may be less than to the minimum snow depth required for the opening of the snowmobile season.

The evolution of the snow pack at R1 does not seem to follow the sequence of wind and precipitation events recorded at the meteorological station and at Ogilvie Camp (Fig. 5.11). For example, snow accumulated at R1 between November 16th and 22nd while high winds were recorded at the meteorological station, and snow-pack thickness abruptly declined between November 22nd and December 2nd while calm conditions were recorded at the meteorological station and snow fall at Ogilvie Camp. On December 2nd, a wind slab was observed at R1 while fresh snow was noted at V3 and V6, and freshly deposited snow was still observed on branches at V9 and V10. This suggests that the sequence of wind and precipitation events at the reference site was different from the other valley-bottom sites.

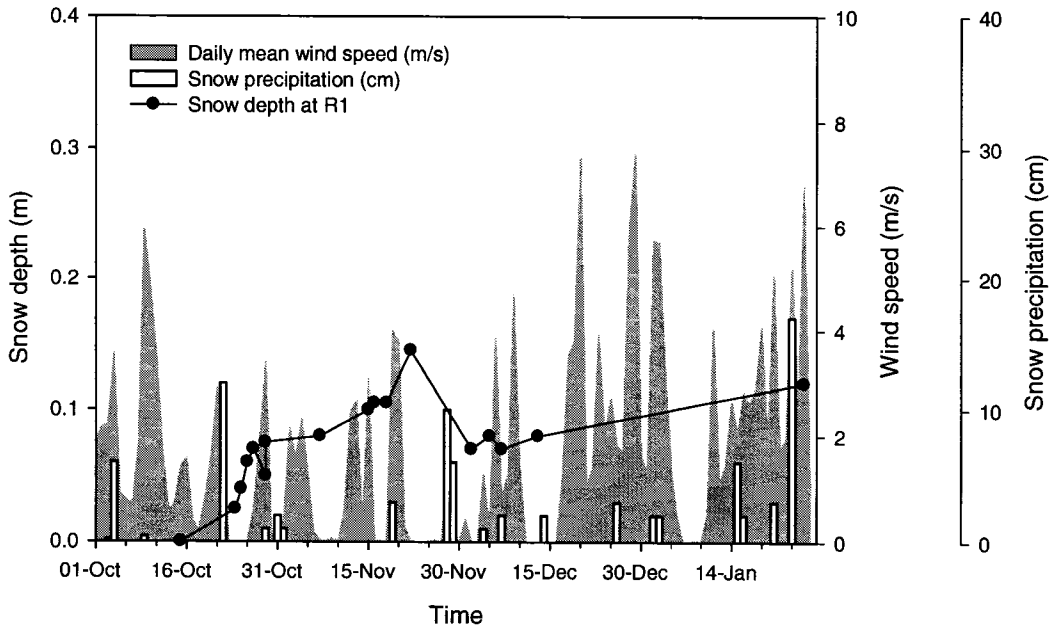

Fig. 5.11 Development of the snow pack at the reference site, with wind events recorded in the study area and precipitation events recorded at Ogilvie Camp.

Spearman correlation coefficients were used to examine the relation between median snow depth at the reference site and at the other transects. For each survey date at a given transect, the reference-site survey date closest in time was selected. Only one date where the snow depth at both sites was zero was included for each series, to avoid bias due to more frequent surveying of certain sites prior to snow accumulation. All valley-bottom sites except V1 are significantly correlated to the reference site at the 0.05 confidence level (Table 5.4a) indicating that, despite possible differences in wind-regime and precipitation, valley-bottom sites generally followed a pattern of snow accumulation and erosion similar to R1. Amongst the hill sites, only T1 and T2 followed a pattern similar to R1 for snow-pack development (Table 5.4b). The two highest sites (T3 and T4) and the site with the highest topographic sheltering (T5) were not significantly correlated to R1 for snow-pack development. The valley bottom (925 m to 1200 m) and intermediate elevations (1200 m to 1400 m) represent the majority of the study area and all of the high-intensity snowmobile traffic is included in these zones. It is reasonable to assume that the development of the snow pack at the reference site is correlated to the development of the snow pack over the majority of the area of interest for snowmobile-management purposes.

The relation between the reference site and other transects was further examined using ratios of the median snow depth along each transect to the median snow depth at the reference site. For survey dates where no measurements were collected at the reference site, the median snow depth from the closest reference site survey date was used. A ratio above 1 indicates that a site has more snow than the reference site on that date.

Table 5.4a Spearman correlation coefficients and p-values (2-tailed) for the relation between snow-pack development at the reference site (R1) and at all valley-bottom sites.

	V1	V2	V3	V4	V5	V6	V7	V8	V9	V10
R1	0.70	**0.94**	**0.96**	**0.94**	**0.94**	**0.80**	**0.94**	**0.94**	**0.90**	**0.94**
p	0.08	0.00	0.00	0.00	0.00	0.02	0.00	0.00	0.01	0.00
n	7	6	7	6	6	8	6	6	7	7

Table 5.4b Spearman correlation coefficients and p-values (2-tailed) for the relation between snow-pack development at the reference site (R1) and at all hill sites.

	T1	T2	T3	T4	T5
R1	**0.90**	**0.90**	0.70	0.63	0.70
p	0.04	0.04	0.12	0.13	0.19
n	5	5	6	7	5

At the hill sites, the snow-depth ratio to R1 generally decreased over time (Fig. 5.12) while it generally increased over time at the valley-bottom sites (Fig. 5.13). In both cases, the relation to the reference site changed in mid-November, when the snow depth was approximately 15 cm at the reference site (Fig. 5.13) and redistribution by wind began to affect snow depth in the valley.

From the beginning of snow precipitation up to this point, snow depth was primarily controlled by elevation. During this period all hill sites had a ratio above 1 indicating a snow pack thicker than at R1, while valley-bottom sites, which are located lower on the valley floor, generally maintained a ratio below 1. The reference site thus provided a reduced level of information on snow-pack thickness at elevations below R1 (1115 m), which represent 48% of the study area and 68% of the zone of high-intensity snowmobile traffic. If an abundant snow fall followed by calm conditions would lead to the opening of the snowmobile season prior to the onset of redistribution by wind, the use of a reference site at a lower elevation would help avoid overestimation of the snow-pack thickness in the valley. Site V5, for example, is located at an elevation of 950 m, near the meteorological station, and may be more representative of valley-bottom snow-pack thickness.

Following the onset of snow distribution by wind in the valley, the snow-depth ratio remained above 1 at all hill sites except at T4, the highest site. At T4 the ratio decreased to 0.9 by December 10th and was down to near 0.5 at the end of January, with a median snow depth of 6 cm. Areas above 1600 m, such as T4, represent less than 1% of the study area. At the end of January other hill sites had ratios between 1.5 and 2.25

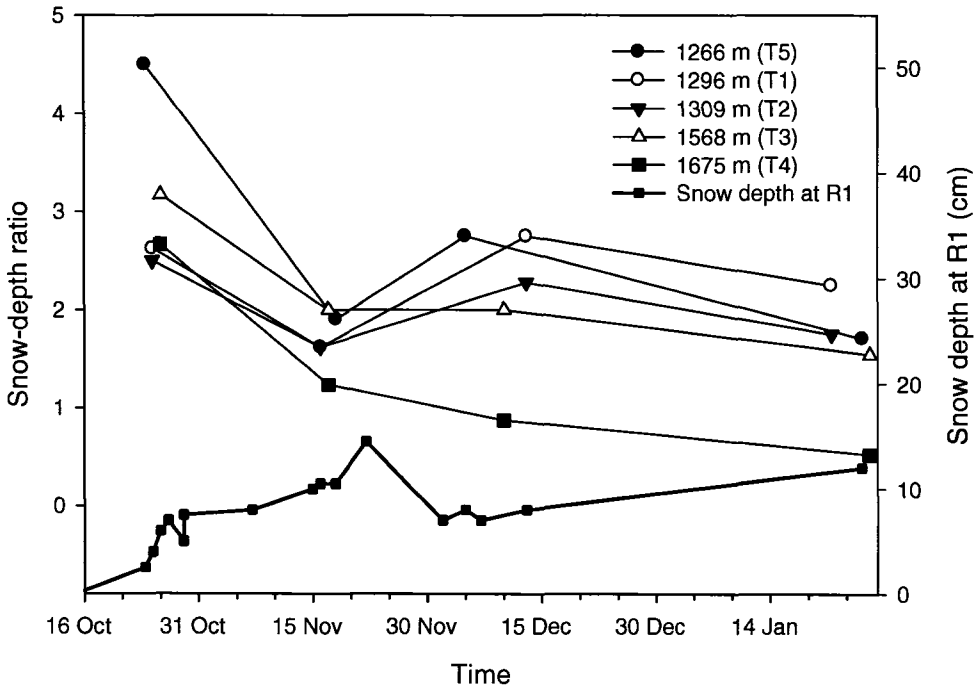

Fig. 5.12 Snow-depth ratios over time at all hill sites.

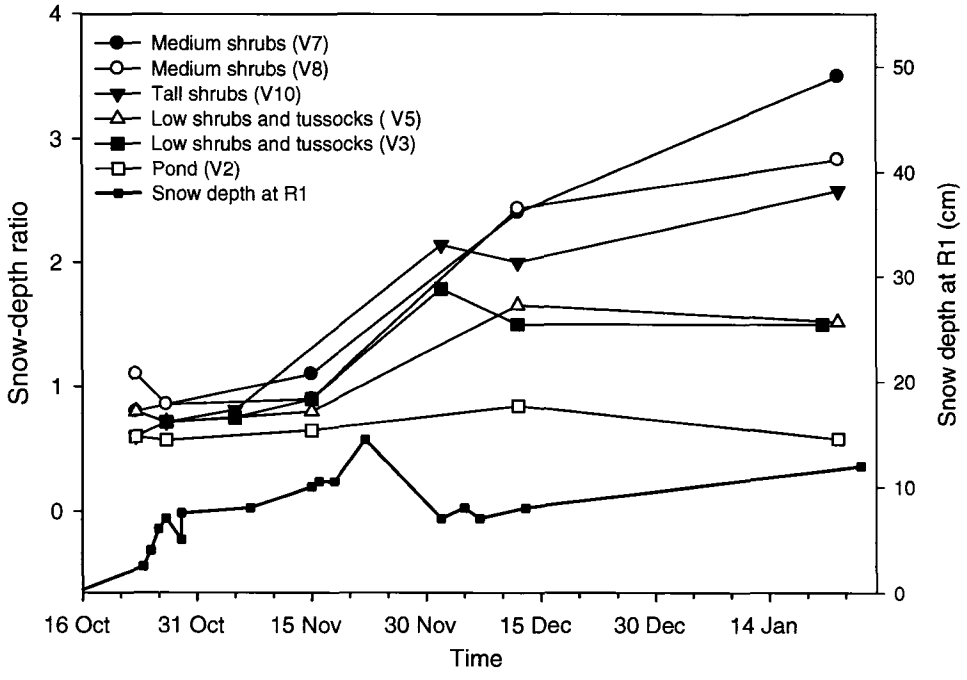

Fig. 5.13 Snow-depth ratio over time at representative valley-bottom transects.

corresponding to snow depths between 19 and 27 cm. These sites represent a greater proportion of the Blackstone Uplands, and over 30% of the study area ranges between 1200 m and 1600 m elevation.

At all valley-bottom sites the snow-depth ratio increased above 1 with the onset of wind distribution. The only exceptions were the two sites with no vegetation, V1 and V2, with snow-depth ratios of 0.9 and 0.8 respectively. All vegetated valley-bottom sites maintained a snow-depth ratio between 1.5 and 3.5 after this point. Fig 5.14a presents snow-depth ratios against median canopy height for valley-bottom transects in December, when the Blackstone Uplands were open to snowmobile traffic. Vegetated sites had median ratios between 1.6 and 2.5, and median snow depths between 11 and 18 cm. Consistent with observations described above, the relation between median snow-depth ratio to R1 and median canopy height appears curvilinear as increases in canopy height beyond 25 cm (dwarf and low shrubs) only result in small increases in snow depth. The range of snow-depth ratios measured along V10 (tall shrubs) is entirely included within the range of ratios observed along the three transects characterised by medium height shrubs (Fig. 5.14b).

In the Blackstone Uplands, dwarf and low shrubs over grass tussocks and moss characterize the dominant vegetation cover, and constitute preferred snowmobiling terrain when snow depth is low. Snow-depth ratios measured along valley-bottom transects located within these vegetation types ranged between 1.2 and 2.7, with a median of 1.9 (Fig. 5.14b). This suggests that snow depth ranged between 8 cm and 19 cm (with a median value of 13 cm) over the majority of the high-intensity snowmobile traffic corridor when the snowmobile season was open in 2006.

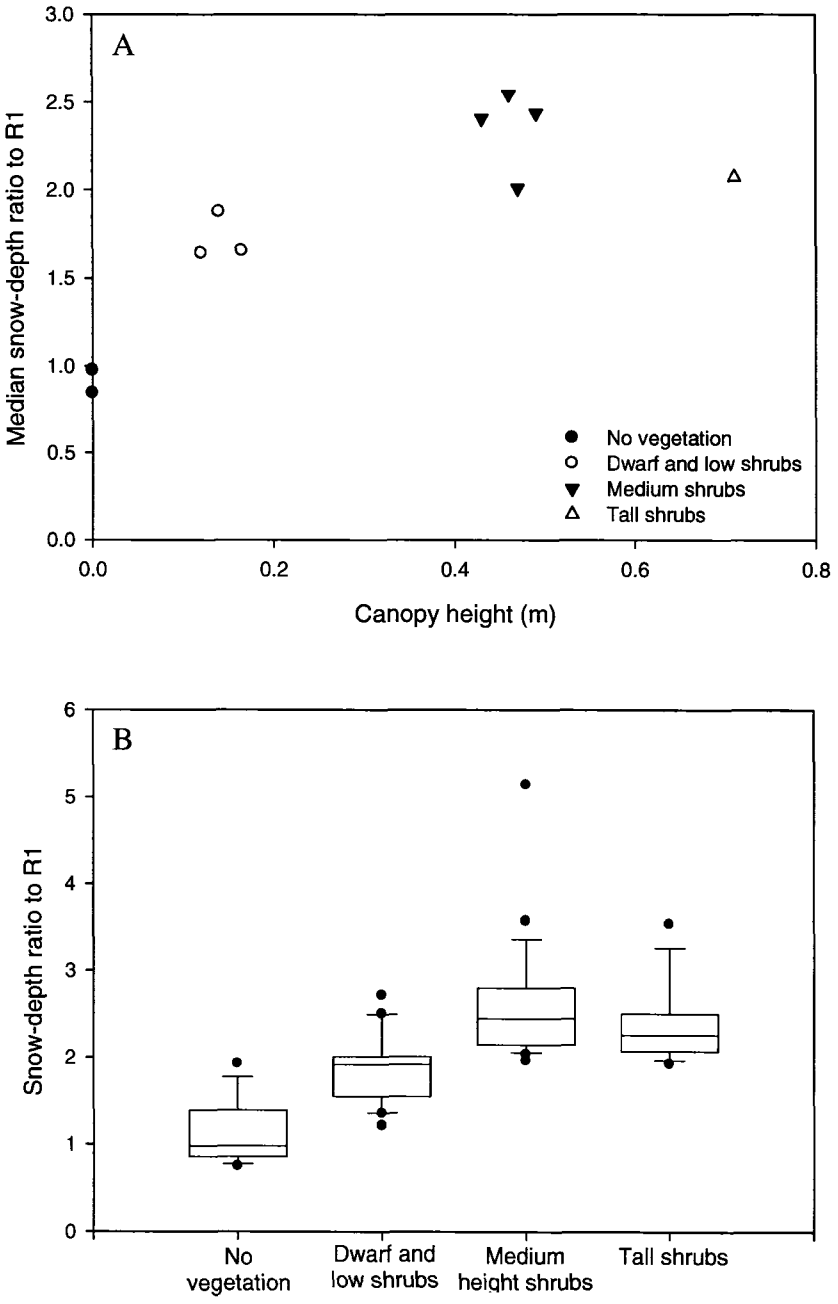

Fig. 5.14 (A) Median snow-depth ratio to R1 against canopy height for valley-bottom transects in December. (B) Range of snow-depth ratios observed along the transects included in each vegetation cover category.

5.5.3 Extrapolating field relations to the landscape scale

Prior to redistribution by wind, snow-pack development in the study area was chiefly controlled by elevation and transects located in similar elevation ranges generally had similar ratios to R1 (Fig. 5.15). Fig. 5.16 presents a map of the three elevation classes included in Figure 5.15 with snow-depth ratios to R1 assigned to each class. Snow-depth ratios were assigned based on the median value of snow-depth ratios at all sampling stations (Fig. 3.10) included in each elevation class. The variability encountered in each elevation class is presented in Figure 5.17. All valley-bottom transects are included in the first class. More variation is observed at higher elevations, where wind erosion of the snow pack began earlier than in the valley bottom (Fig. 5.5).

After the onset of snow transport by wind at lower elevations, the main control on snow-pack thickness in the valley bottom was vegetation height, and the greatest variation in snow-pack thickness was observed between canopy heights of 0 m and 0.5 m. This narrow range of vegetation heights is difficult to differentiate with satellite imagery (Sylvain Leblanc, personal communication, June 2007; Ian Olthof, personal communication, June 2007). Two vegetation maps developed by the Canadian Centre for Remote-Sensing were considered to extrapolate the relation between canopy height and snow depth in December. The first image represents leaf area index along the Dempster corridor. It was developed with cloud-free and atmospherically corrected composites of SPOT VEGETATION red, near infra-red, and shortwave infrared bands combined with Landsat-7 images and has a resolution of 30 m^2. The second image represents above-ground biomass (tons/ha) along the Dempster corridor. It was developed using a combination of Landsat-7 images (infrared ratio TM4/TM5) combined with L-band

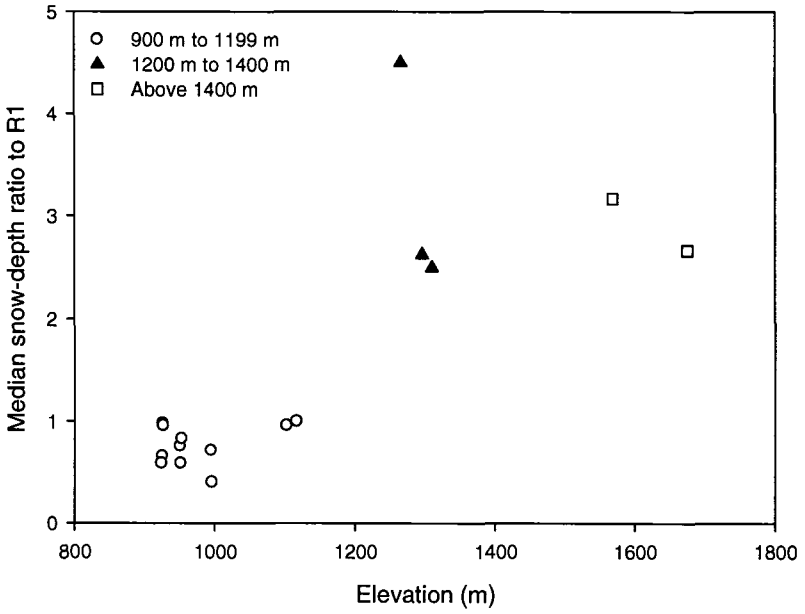

Fig. 5.15 Scattergram of the ratios of snow depth along each transect to snow depth at R1 against elevation.

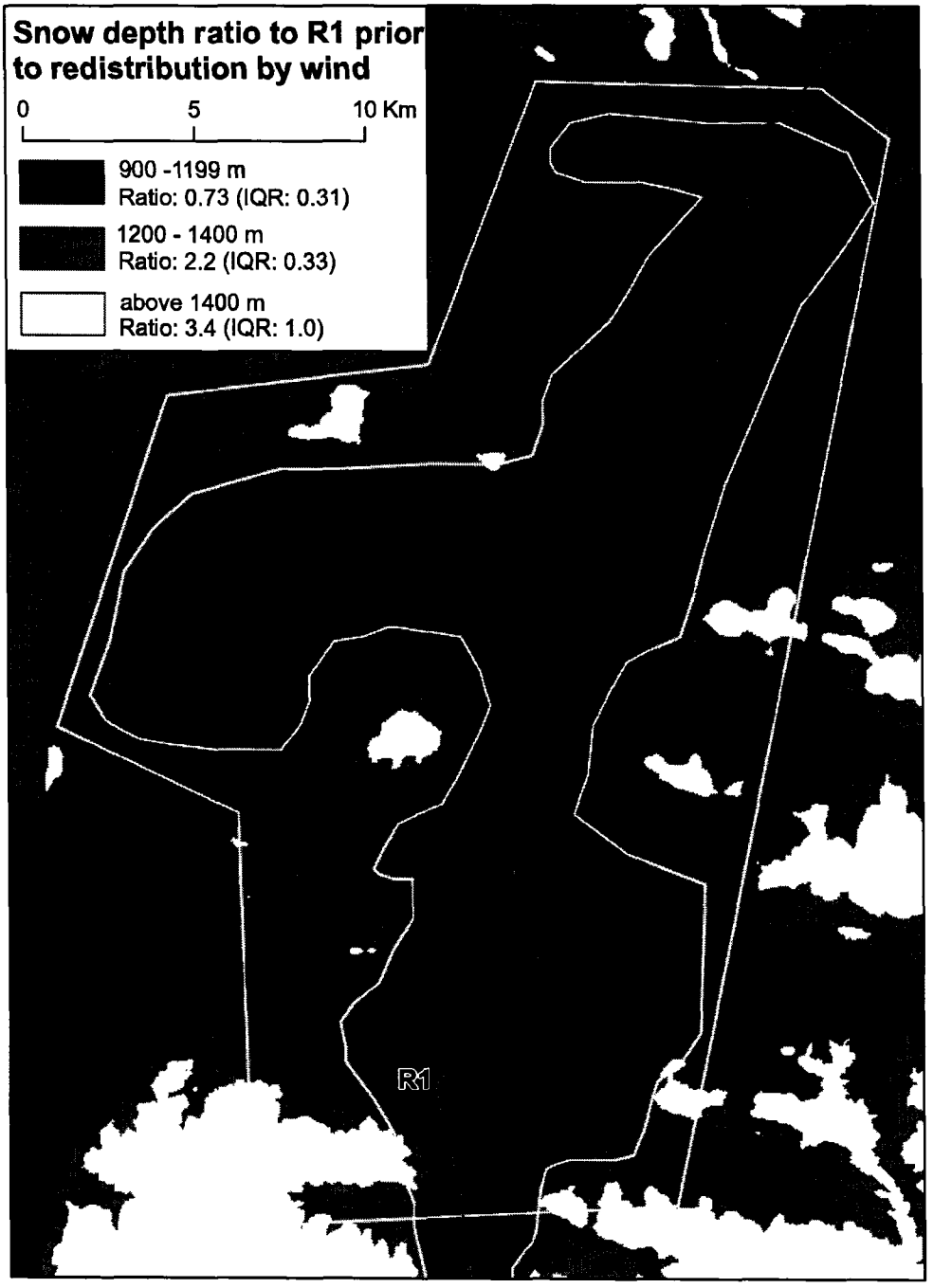

Fig. 5.16 Map of elevation classes with assigned snow-depth ratios based on the median snow-depth ratio of all stations included in each class prior to the onset of redistribution of snow by wind in the valley bottom. The interquartile range is indicated in parenthesis in the legend. The boundaries of the study area and high intensity snowmobile-traffic corridor are represented in white.

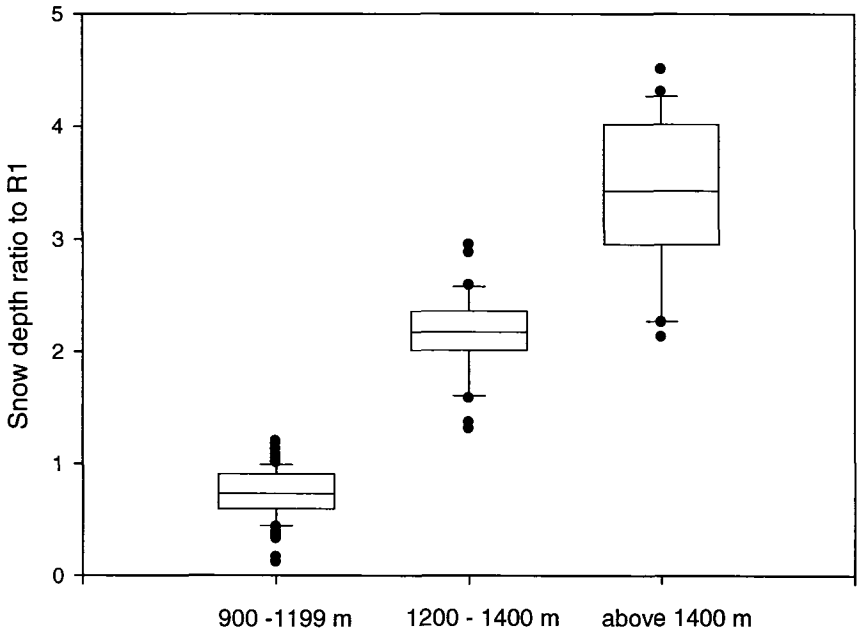

Fig. 5.17 Variation in snow-depth ratios observed within each elevation class included in Figure 5.16.

JERS-1/SAR images (Chen et al. 2006). This image is coarse, with a resolution of 100 m^2.

LAI and biomass values extracted from these vegetation maps were compared to measured canopy heights using all transects and all secondary dataset points. Best results were obtained when using the mean of values extracted within a 50-m buffer around each point. Canopy height and biomass values were log-transformed to improve the distribution of the data and a linear regression analysis was conducted on both sets of data. Points further than four standard deviations from the mean were considered outliers and excluded from the analysis (1 point). The results are presented with scattergrams in Figure 5.18. There was considerable scatter in both relations, and the information on vegetation cover structure extracted from these satellite-derived vegetation maps did not allow differentiation of canopy heights below 0.5 m, a range of heights critical to development of the snow pack in a low snow year. As a result, attempts to use satellite-derived vegetation data to extrapolate the observed field relations to the landscape scale were unsuccessful. This highlights the difficulty of using the currently available satellite-derived vegetation data to extrapolate the observed field relations between vegetation cover and snow depth to the landscape scale in the Blackstone Uplands.

5.6 Summary of findings on snow-pack development

In the Blackstone Uplands, fall and early winter 2006 were characterised by scarce snowfall and generally calm conditions. Two distinct regimes in snow-pack development were observed: elevation controlled snow depth prior to redistribution of snow by wind, while vegetation structure was the main control on snow depth after the onset of blowing snow. Redistribution by wind began to occur when snow depth was 15 cm at the

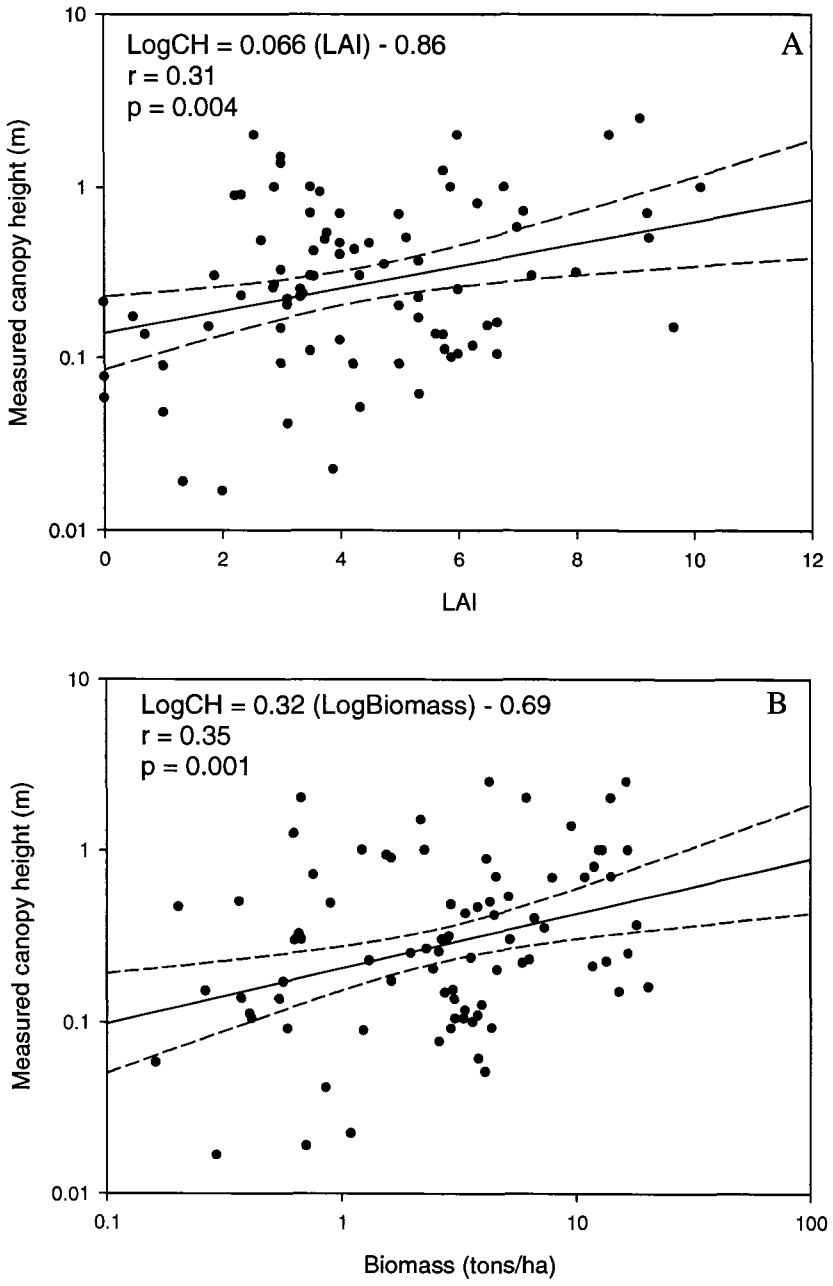

Fig. 5.18 Scattergrams of (A) measured canopy height (CH) against mean LAI values extracted from a satellite-derived image of the vegetation cover, and (B) measured canopy height (CH) against mean above ground biomass extracted from a satellite-derived image of the vegetation cover. The equation of the principal axis and the coefficient of determination are indicated in the corner of each graph. The 95% confidence interval is represented with dashed lines.

reference site and daily wind speeds of 4 m/s with maximum speeds up to 8 m/s were recorded within the study area. Under the observed scarce snowfall conditions, sites with a canopy height of 20 cm or more retained a snow thickness of 15 cm or more under windy conditions. It was not possible to extrapolate field relations between canopy height and snow-pack development to the landscape scale using the available satellite-derived vegetation data for the Blackstone Uplands. Critical variations in snow depth occur over a narrow range of low canopy heights, which current satellite imagery and processing techniques cannot differentiate.

Snow-pack development at the reference site was significantly correlated to all surveyed sites located within the high-intensity snowmobile-traffic corridor. Prior to the onset of redistribution of snow by wind, all hill sites had more snow than the reference site, while the snow pack was thinner at all valley-bottom sites than at the reference site. During this period, the use of a reference site located at a lower elevation in the valley would help avoid overestimation of snow-pack thickness over the high intensity snowmobile-traffic corridor. After the onset of redistribution of snow by wind, the ratio of snow depth to R1 decreased at the hill sites but remained above 1. The snow-depth ratio in the valley bottom increased above 1 at all vegetated sites and the reference site appeared to offer a conservative estimate of snow depth in the Blackstone Uplands.

5.7 Frost penetration at the monitored sites

Ground temperature was monitored by data logger at nine sites in order to compare the rate of frost penetration under different snow packs. Temperature sensors were installed in the ground at depths of 5 cm, 15 cm, 30 cm and at the top of the permafrost (Table 5.5). *Initiation of the zero curtain* was defined at the time when temperature throughout the active layer was recorded at -0.16°C, the first interval below 0°C. The *freezing front* was considered to have passed a specific depth on the first day when the temperature at that depth dropped below -0.61°C (the next level below -0.16°C) prior to a steady decrease in temperature. The *duration of the zero curtain* is the time between the initiation of the zero curtain and the first day when the temperature at the top of the permafrost (TTOP) dropped below -0.61°C prior to a steady decrease in temperature. For the purpose of this study, the ground was considered frozen to a given depth when the freezing front passed that depth, and the active layer was considered frozen when the temperature at the top of the permafrost (TTOP) dropped below -0.61°C prior to a steady decrease in temperature.

The initiation of the zero curtain occurred between September 16th (T3) and October 2nd (V10), prior to any snow accumulation in the area. The freezing front reached 15 cm at most sites near the beginning of snow accumulation on the valley bottom. Figure 5.19 presents the timing of frost penetration at four representative sites in comparison to snow-pack development in the valley bottom (V10) and at the highest site (T4). Frost penetration was most rapid at T4, while it was generally slowest at R1. V10 was the last transect to reach the end of the zero curtain, in part due to the depth of its

Table 5.5 Summary of the active-layer freezing dates for all sites equipped with temperature sensors.

Site	Initiation of zero curtain	Freezing front passes 5 cm	Freezing front passes 15 cm	Freezing front passes 30 cm	Freezing front at T.O.P.	Zero curtain duration (days)
V3	25 Sep	13 Oct	23 Oct	05 Nov	08 Nov	44
V4	26 Sep	14 Oct	24 Oct	11 Nov	14 Nov	49
V6	24 Sep	13 Oct	23 Oct	06 Nov	11 Nov	47
V7	01 Oct[1]	13 Oct	26 Oct	N/A	25 Nov	55[2]
V10	02 Oct	14 Oct	22 Oct	02 Nov	28 Nov	58
T1	29 Sep	13 Oct	23 Oct	02 Nov	20 Nov	51
T3	16 Sep	13 Oct	16 Oct	27 Oct	30 Oct	44
T4	22 Sep	30 Sep	14 Oct	18 Oct	28 Oct	41
R1	01 Oct	23 Oct	26 Oct	09 Nov	10 Nov	46

[1] : Latest possible date.
[2] : Shortest possible duration.

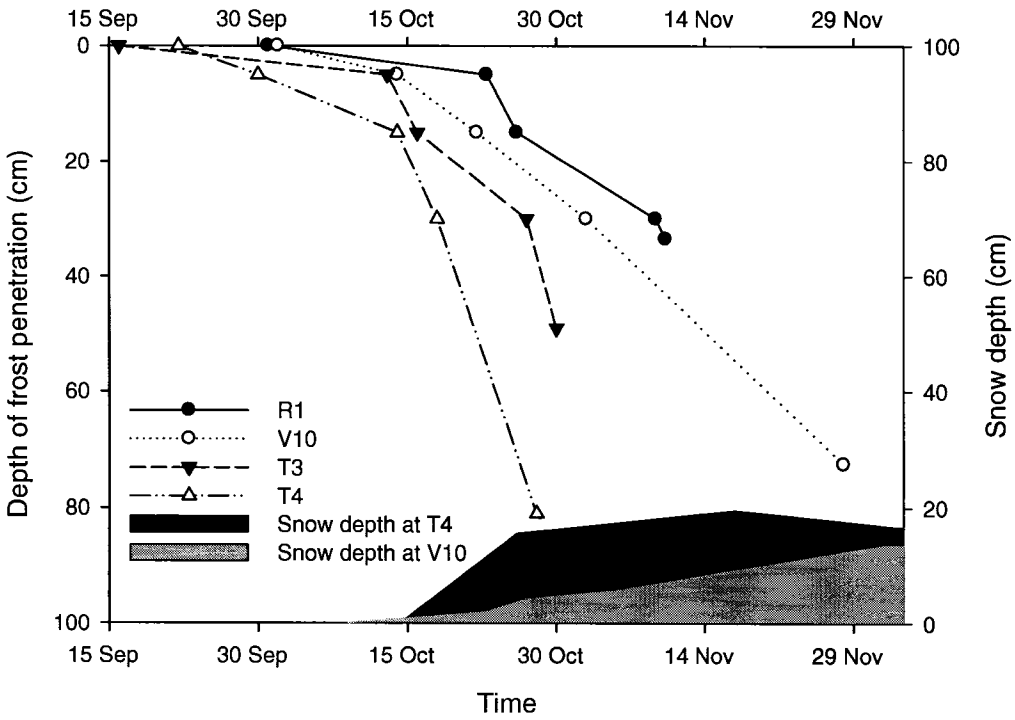

Fig 5.19 Frost penetration at four representative sites and snow pack development in the valley bottom (V10) and at the highest site (T4).

active layer. Hill sites generally froze before valley-bottom sites. Snowfall occurred later than usual in 2006, and the snow cover remained thin through freeze-up, with a maximum accumulation of approximately 15 cm at T1, T3, T4 and V10 during the last days of the zero-curtain. The insulating effect of the snow cover on the freezing of the active layer was therefore very limited in 2006. The following sections discuss the observed rates of frost penetration at different elevations and under different types of vegetation cover, before discussing the effectiveness of the reference site as an indicator of frost penetration over the area.

5.8 Air temperature and velocity of the freezing front

Table 5.6 presents the mean freezing-front velocity between each temperature sensor at the monitored sites. The average freezing rate is weighted by the length of the associated portions of the active layer. At the nine monitored sites, the velocity of the freezing front increased over time, with the exception of T3 and R1, where the freezing front progressed from a depth of 5 cm to a depth of 15 cm in 3 days during cold weather. This general acceleration in the velocity of the freezing front is inconsistent with Stefan's solution applied to frost penetration in the ground, which predicts a decrease in the velocity of the freezing front with the square root of time (eq. 2.5). The Stefan solution assumes uniform thermal properties and constant surface temperature during freezing. It is unlikely that thermal conductivity systematically increased with depth at all sites, or that latent heat systematically decreased with depth, given that the base of the active layer is commonly wetter than the ground surface. The assumption of constant surface temperature during freezing may be acceptable under a thick snow cover, when the surface temperature is affected by the release of latent heat below and relatively warm

Table 5.6 Freezing-front velocity between temperature sensors at each site.

T	Rate to 5 cm (cm/day)	Rate to 15 cm (cm/day)	Rate to 30 cm (cm/day)	Rate to T.O.P. (cm/day)	Average rate (cm/day)
V3	0.3	1.0	1.2	3.7	1.7
V4	0.3	1.0	0.8	1.5	0.9
V6	0.3	1.0	1.1	2.6	1.4
V7	0.4	0.8	N/A	0.9[1]	0.8
V10	0.4	1.3	1.4	1.6	1.4
T1	0.4	1.0	1.5	2.7	2.1
T3	0.2	3.3	1.4	6.3	3.6
T4	0.6	0.7	3.8	5.1	4.0
R1	0.2	3.3	1.1	3.5	1.9

[1]: Rate from 15 cm to top of permafrost.

surface conditions are maintained (Burn 2000; Karunaratne and Burn 2004). In the absence of an insulating snow cover, fluctuations in air temperature directly affect surface temperature.

As mentioned above, the snow cover provided very little insulation through active-layer freeze-up in 2006. Air temperature decreased progressively between September 15th and October 25th (Fig. 5.20). Following the beginning of snow-pack development, air temperature dropped and remained below -20°C from November 4th to November 28th 2006. The acceleration of the freezing front between September 15th and November 28th likely reflected the decreasing air temperature observed during the freeze-up period, and indicates that Stefan's solution is inappropriate for modelling the rate of frost penetration in the ground under these conditions.

5.9 Rate of frost penetration near the bottom of the active layer

Examination of a scattergram of the rate of freezing between 30 cm and the top of permafrost (Fig 5.21) reveals that the valley-bottom sites are grouped along a line suggesting a decrease in freezing rate with increasing snow depth. Median snow depth at these sites varied between 7 and 10 cm when the freezing front passed 30 cm, a variation which is not sufficient to explain the observed differences in freezing rates. However, snow depth at the valley-bottom sites generally ranked in the same order as canopy height, consistently with the relations identified above. This leads to the hypothesis that areas which tend to develop a thicker snow pack may have increased moisture at the bottom of the active-layer, resulting in a reduced freezing rate near the permafrost table.

The hill sites (T1, T3, T4) are grouped to the right as they received more snow in October and November. The insulating effect of the snow cover did not control the rate of

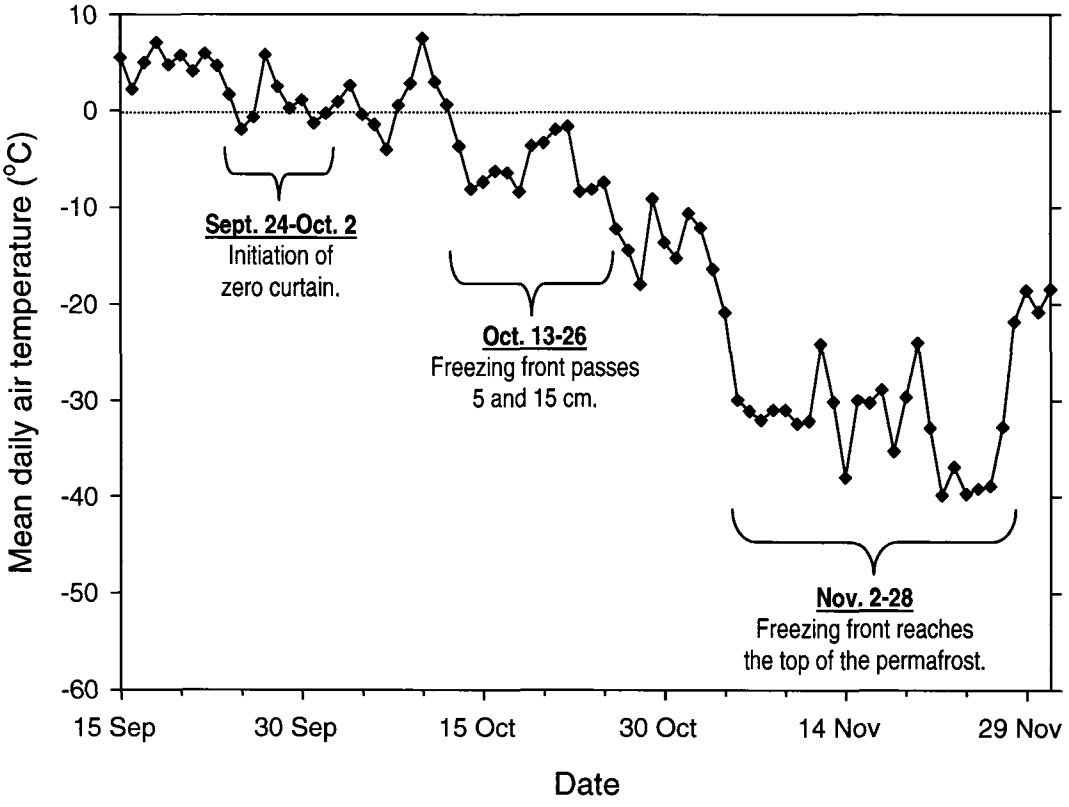

Fig. 5.20 Mean daily air temperature during active-layer freeze-up at valley-bottom sites, recorded near site V5, approximate elevation 960 m.

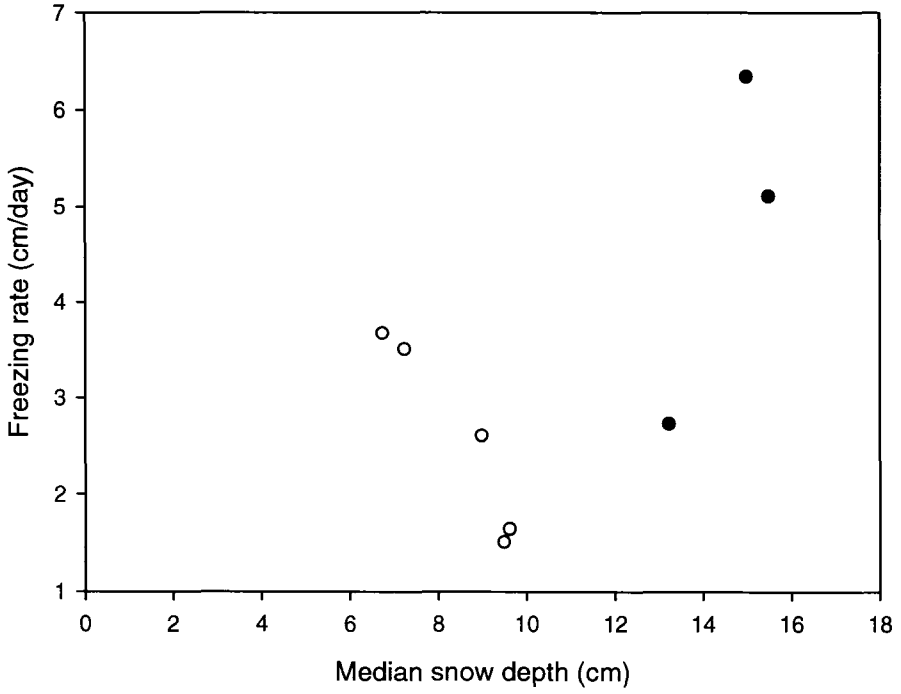

Fig. 5.21 Scattergram of the rate of freezing between 30 cm and the top of permafrost against snow depth at the valley bottom sites (open circles) and at the hill sites (filled circles).

freezing at these sites. On the contrary, freezing rate at the hill sites appears controlled by elevation.

5.10 Frost penetration and elevation

Amongst the hill sites, freezing of the active layer occurred most rapidly at higher elevations (Table 5.7). This accelerated progression of the freezing front may be due to lower air temperatures, or to variations in the thermal properties of the ground. While the lowest hill site, T1, was located on morainal deposits, the two highest sites were located on colluvial deposits, which tend to be better drained.

5.11 Frost penetration and vegetation structure in the valley-bottom

In the valley bottom, the duration of the zero curtain generally increased with canopy height, resulting in the later completion of active-layer freeze-up in areas with tall and dense vegetation (Table 5.8). The average freezing-front velocity, and timing of freezing to depths of 15 cm or 30 cm, on the other hand, did not appear related to vegetation structure. Variations in the duration of the zero-curtain and timing of freeze-back completion under different canopy covers appeared to result from increased active-layer depths under taller and denser vegetation (Table 5.8).

5.12 Effectiveness of the reference site to assess ground freezing in the study area

The progression of the freezing front from the ground surface to a depth of 30 cm was slow at the reference site in comparison to the other monitored sites (Fig. 5.22). However, the active layer was shallow at R1, and the freezing front reached the top of the permafrost shortly after passing 30 cm, on the 10th of November, earlier than five other

Table 5.7 Elevation and ranks for average freezing rate and the time of zero-curtain initiation and frost penetration to 15 cm, 30 cm, and to the top of the permafrost at the three hill sites.

Site	Elevation (m)	Average freezing-front velocity	15 cm	30 cm	Top of permafrost
T4	1676	3	1	1	1
T3	1566	2	2	2	2
T1	1300	1	3	3	3

Table 5.8 Vegetation types and ranks for characteristics of the vegetation-cover structure, active-layer depth, average freezing-front velocity, and the time of frost penetration to 15 cm, 30 cm, and to the top of the permafrost at the three hill sites.

	Vegetation Type	Canopy Height	LAI	Active-layer depth	Average freezing-front velocity	15 cm	30cm	TOP	Zero-curtain duration
V3	Low shrubs & tussocks	1	3	3	5	2.5	2	1	1
V4	Low shrubs & tussocks	2	2	2	2	4	5	4	4
R1	Low shrubs & tussocks	3	1	1	6	5.5	4	2	2
V6	Medium shrubs	4	4	5	3	2.5	3	3	3
V7	Medium shrubs	5	6	4	1	5.5	NA	5	5
V10	Tall shrubs	6	5	6	4	1	1	6	6

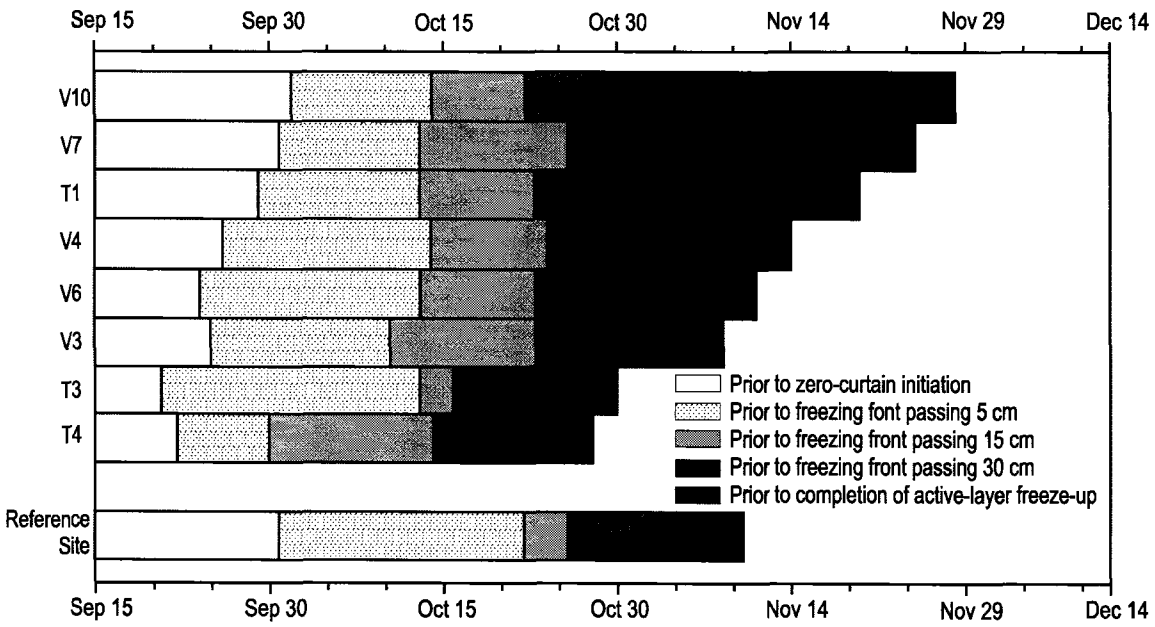

Fig. 5.22 Progression of the freezing front at each site in comparison to the reference site.

sites. The delayed penetration of the freezing front in the upper 30 cm at R1 in comparison to all other monitored sites suggests that R1 offers a conservative reference for monitoring frost penetration in the Blackstone Uplands when snow-pack development is minimal.

5.13 Summary of findings on frost penetration in the Blackstone Uplands

Despite the reduced snow-cover during active layer freeze-up, considerable variability was observed in the progression of the freezing front, particularly past depths of 15 cm. Approximately two weeks separated the first and last sites to initiate the zero curtain and to freeze to depths of 5 cm and 15 cm, while a full month separated the first and last sites to complete freeze-back. Freezing occurred most rapidly at higher elevations. In the valley-bottom, sites with a vegetation cover favourable to the development of a thicker snow pack had reduced freezing rates near the bottom of the active layer, suggesting increased moisture contents. When the snow-pack development is minimal, the reference site offers a conservative reference to monitor the depth of frost penetration in the Blackstone Uplands.

Chapter 6

Summary and Conclusions

The objectives of this research were to (1) investigate the effects of topography and vegetation structure on snow-pack development during early winter in the Blackstone Uplands, Y.T., (2) examine the rate of active-layer freezing under different snow packs, and (3) assess whether snow-pack development and frost penetration in the portion of the Blackstone Uplands which receives a high-intensity of snowmobile traffic can be effectively monitored using an accessible reference site.

Scarce snowfall and calm conditions until mid-November 2006 allowed a careful examination of snow-pack development near the 15 cm snow-depth criterion for the opening of snowmobile access to the Blackstone Uplands. Delayed snow precipitation and cold November temperatures resulted in near completion of active-layer freeze-up prior to the development of the snow cover. The next sections summarize findings for snow-pack development and ground freezing, highlight possibilities for future research, and present management recommendations for the effective use of the reference site.

6.1 Development of the snow pack

Two distinct regimes in snow-pack development were observed. Elevation controlled snow depth prior to the onset of redistribution by wind in the valley-bottom. Redistribution by wind began to occur when snow depth was 15 cm at the reference site, and daily wind speeds of 4 m/s with maximum half-hourly speeds up to 8 m/s were recorded within the study area. Variability of the snow cover increased abruptly with the beginning of wind transport as snow was eroded from exposed areas and accumulated in sheltered parts of the landscape.

Vegetation structure controlled snow depth after the onset of snow transport by wind in the valley-bottom. Under the observed scarce snowfall conditions, only sites with a canopy height of 20 cm or more retained a snow thickness of at least 15 cm after wind erosion. It was not possible to extrapolate field relations between canopy height and snow-pack development to the landscape scale using the available satellite-derived vegetation data for the Blackstone Uplands. Critical variations in snow depth occurred for canopies dominated by dwarf, low, and medium shrubs representing a narrow range of canopy heights (0.1 to 0.5 m) which are difficult to differentiate with current satellite imagery. The Canadian Center for Remote Sensing is currently working on the improvement of satellite-derived vegetation maps for the Dempster Highway corridor (Sylvain Leblanc, personal communication, June 2007; Ian Olthof, personal communication, June 2007). This may allow the extrapolation of the results to the landscape scale in the future, and the mapping of areas with a snow-holding capacity below 15 cm which may be left without the required protective snow cover after wind erosion of the snow pack.

6.2 Ground freezing

The thin snow cover and decreasing air temperature observed during ground freeze-up resulted in the acceleration of the freezing front over time. This indicates that Stefan's solution is inappropriate to assess the depth of frost penetration in the ground under the observed conditions.

Despite the reduced snow cover during active-layer freeze-up, considerable variability was observed in the progression of the freezing front, particularly past depths of 15 cm. Penetration of the freezing front to a depth of 30 cm occurred over a period of

three weeks at the monitored sites and a full month separated the first and last sites to complete freeze-back. Freezing occurred most rapidly at higher elevations. Despite a thin snow cover, valley-bottom sites with a vegetation cover favourable to the development of a thicker snow pack had reduced freezing rates near the active layer, suggesting increased moisture contents.

6.3 Effectiveness of the reference site and implications for snowmobile management

Snow-pack development at the reference site was significantly correlated to all surveyed sites located within the high intensity snowmobile-traffic corridor, and can thus provide an effective management tool. Prior to the onset of redistribution of snow by wind, all hill sites had more snow than the reference site, while the snow pack was thinner at all valley-bottom sites than at the reference site. During this period, the use of a reference site located at a lower elevation in the valley would help avoid overestimation of snow-pack thickness over the high intensity snowmobile-traffic corridor.

After the onset of redistribution of snow by wind, snow-pack thickness decreased at the highest sites but it remained greater at all hill sites than at the reference site. In the valley bottom, snow depth at all vegetated sites was greater than snow depth at the reference site. After the onset of snow redistribution by wind in the valley-bottom, the reference site appeared to offer a conservative estimate of snow depth in the Blackstone Uplands.

Frost penetration was delayed at the reference site in comparison to all monitored sites. Despite this delay, frost penetration to the permafrost table occurred at the reference site near the median freeze-up date for all sites. Under conditions of minimal snow-pack

development, the reference site offered a conservative reference to monitor the depth of frost penetration in the Blackstone Uplands.

REFERENCES

Anderton, S.P., White, S.M., Alvera, B. 2004. Evaluation of spatial variability in snow water equivalent for a high mountain catchment. Hydrological Processes, **18**: 435-453.

Andersland, O.B., and Anderson, D.M. 1978. Geotechnical Engineering for Cold Regions. McGraw-Hill Inc., New York, NY.

Barry, R.G. 1992. Mountain Weather and Climate, 2nd Edition. Routledge, London, UK.

Beierle, B.D. 2002. Late quaternary glaciation in the northern Ogilvie mountains: revised correlations and implications for the stratigraphic record. Canadian Journal of Earth Sciences, **39**: 1709-1717.

Benson, C.S., and Sturm, M. 1993. Structure and wind transport of seasonal snow on the Arctic slope of Alaska. Annals of Glaciology, **18**: 261-267.

Berry, M.O. 1981. Snow and climate. *In* Handbook of Snow: Principles, Processes, Management and Use. *Edited by* D.M. Gray, D.H. Male. Pergamon Press, Toronto, ON., pp. 32-58.

Billings, W.D., and Mooney, H.A. 1968. The ecology of arctic and alpine plants. Biological Reviews, **43**: 481-529.

Bostock, H.S. 1961. Physiography and resources of the northern Yukon. Canadian Geographical Journal, **63**: 112-119.

Bradley, R.S., Keimig, F.T., and Diaz, H.F. 1992. Climatology of surface-based inversions in the North American Arctic. Journal of Geophysical Research, **97**: 15,699-15,712.

Brown, R.J.E. 1967. Permafrost in Canada. National Research Council, Geological Survey of Canada, "A" Series Map 1246A, scale 1: 8 426 160.

Brown, J.K. 1976. Estimating shrub biomass from basal stem diameters. Canadian Journal of Forest Research, **6**: 153-158.

Burn, C.R. 1998. The active layer: two contrasting definitions. Permafrost and Periglacial Processes, **9**: 411-416.

Burn, C.R. 2004. The thermal regime of cryosols. *In* Cryosols, Permafrost Affected Soils. *Edited by* J.M. Kimble. Springer, Berlin, Germany, pp. 391-413.

Caine, N. 1975. An elevational control of peak snowpack variability. Water Resources Bulletin, **11**: 613-621.

Caissie, A. 1999. Effects of snowmobile traffic on the vegetation of a coastal plain Sphagnum bog in Gros Morne National Park, Western Newfoundland. M.Sc. Thesis, University of New Brunswick, Fredericton, NB.

Carey, S.K., and Woo, M.K. 2005. Freezing of subarctic hillslopes, Wolf Creek basin, Yukon, Canada. Arctic, Antarctic, and Alpine Research, **37**: 1-10.

Carslaw, H.S., and Jaeger, J.C. 1959. Conduction of Heat in Solids, 2nd edition. Clarendon Press, Oxford, UK.

Chen, J.M., Pavlic, G., Brown, L., Cihlar, J., Leblanc, S.G., White, H.P., Hall, R.J., Peddle, D., King, D.J., Trofymow, J.A., Swift, E., Van der Sanden, and J., Pellikka, P. 2002. Derivation and Validation of Canada-wide coarse-resolution leaf area index maps using high resolution satellite imagery and ground measurements. Remote Sensing of Environment, **80**: 165-184.

Clobeck, S.C. 1983. Ice crystal morphology and growth rate at low supersaturations and high temperatures. Journal of Applied Physics, **54**: 2677-2682.

Colbeck, S.C. 1997. A review of sintering in seasonal snow. CRREL Report 97-10. US Army Corps of Engineers. Hanover, NH.

Côté, M.M. 2002. The influence of elevation and aspect on permafrost distribution in central Yukon Territory. M.Sc. thesis, Carleton University, Ottawa, ON.

Daubenmire, R. 1959. A canopy-coverage method of vegetational analysis. Northwest Science, **33**: 43-66.

Dong, Z., Gao, S., and Fryrear, D. 2001. Drag coefficients, roughness length and zero-plane displacement height as disturbed by artificial standing vegetation. Journal of Arid Environments, **49**: 485-505.

Duk-Rodkin, A. 1996. Surficial geology, Dawson, Yukon Territory. Geological Survey of Canada, Open File 3288, Map, scale 1: 250 000.

Durand, Y., Guyomarc'h, G., Mérindol, L., and Corripio, J.G. 2004. Two-dimensional numerical modelling of surface wind velocity and snowdrift effects over complex mountainous topography. Annals of Glaciology, **38**: 59-70.

Elder, K., Dozier, J., and Michaelsen, J. 1991. Snow accumulation and distribution in an alpine watershed. Water Resources Research, **7**: 1541-1552.

Essery, R., Li, L., and Pomeroy, J. 1999. A distributed model of blowing snow over complex terrain. Hydrological Processes, **13**: 2423-2438.

Essery, R., and Pomeroy, J. 2004. Vegetation and topographic control of wind-blown snow distributions in distributed and aggregated simulations for an arctic tundra basin. Journal of Hydrometeorology-Special section, **5**: 735-744.

Foothills Pipe Lines Yukon Ltd. 1979. The Dempster Lateral Gas Pipeline Project, Vol. 4, Environmental Impact Statement.

Geddes, C.A., Brown, D.G., and Fagre, D.B. 2005. Topography and vegetation as predictors of snow water equivalent across the alpine treeline ecotone at lee ridge, glacier national park, Montana, USA. Arctic, Antarctic, and Alpine Research, **37**: 197-205.

Gill, D. 1973. A spatial correlation between plant distribution and unfrozen ground within a region of discontinuous permafrost. *In* Permafrost: the North American Contribution to the 2nd International Conference, Yakutsk, U.S.S.R. National Academy of Science Press, Washington, D.C., pp. 105-113.

Goodrich, L.E. 1982. The influence of the snow cover on the ground thermal regime. Canadian Geotechnical Journal, **19**: 421-432.

Gordey, S.P., and Makepeace, A.J., 2000. Yukon Digital Geology. Geological Survey of Canada, Open File D3826.

Government of Canada, 2003. Landsat 7 Orthorectified Imagery over Canada. Natural Resources Canada, Earth Science Sector, Data Management and Dissemination Branch. Ottawa, Canada.

Greller, A.M., Goldstein, M., and Marcus, L. 1974. Snowmobile impact on three alpine tundra plant communities. Environmental Conservation, **1**: 101-110.

Gross, M.F., Hardisky, M.A., Doolittle, J.A., and Klemas, V. 1990. Relationships among depth to frozen soil, soil wetness, and vegetation type and biomass in tundra near Bethel, Alaska, U.S.A. Arctic and Alpine Research, **22**: 275-282.

Heginbottom, A.J., Dubreuil, M.A., and Harker, P.A. 1995. Canada-Permafrost. *In* The National Atlas of Canada, 5th Edition. National Atlas Information Service, Natural Resources Canada, Ottawa. Plate 2.1. MCR 4177.

Jackson, M.C. 1978. Snow cover in Great Britain. Weather, **33**: 298-309.

Johnstone, J.F., and Kasischke, E.S. 2005. Stand-level effects of soil burn severity on postfire regeneration in a recently burned black spruce forest. Canadian Journal of Forest Research, **35**: 2151-2163.

Kaimal, J.C., and Finnigan, J.J. 1994. Atmospheric Boundary Layer Flows. Oxford University Press, New York, NY.

Karunaratne, K.C., and Burn, C.R. 2003. Freezing n-factors in discontinuous permafrost terrain, Takhini River, Yukon Territory, Canada. *In* Proceedings of the 8th International Conference on Permafrost, Zurich, Switzerland, 21-25 July 2003. *Edited by* M. Phillips, S.M. Springman, L.U. Arenson, A.A. Balkema, Lisse, The Netherlands. Vol. 1, pp. 519-524.

Kendrew, W.G., and Kerr, D. 1955. Climate of British Columbia and the Yukon Territories. Queen's Printer, Ottawa, ON.

Kennedy, C.E., and Smith, C.A.S. 1999. Vegetation, terrain, and natural features in the Tombstone area, Yukon Territory. Department of Renewable Resources, Government of the Yukon and Agriculture and Agri-food Canada, Whitehorse, YT.

Kikuchi, T. 1981. A wind tunnel study of the aerodynamic roughness associated with drifting snow. Cold Regions Science and Technology, **5**: 107-118.

Kind, R.J. 1981. Snow Drifting. The distribution of snowcover. *In* Handbook of Snow: Principles, Processes, Management and Use. *Edited by* D.M. Gray, D.H. Male. Pergamon Press, Toronto, ON, pp. 153-190.

Klene, A.E., Nelson, F.E., Shiklomanov, N.I., and Hinkel, K.M. 2001. The n-factor in natural landscapes: variability of air and soil-surface temperatures, Kuparuk River Basin, Alaska, U.S.A. Arctic, Antarctic, and Alpine Research, **33**: 140-148.

Klohn Leonoff Consultants Ltd. 1979. Dempster Lateral Drilling Program, Vol.1.

Lacelle, D., Lauriol, B., Clark, I.D.,Cardyn, R., Zdanowicz, C. 2007. Nature and origin of a Pleistocene-age massive ground-ice body exposed in the Chapman Lake moraine complex, central Yukon Territory, Canada. Quaternary Research, **68**: 249-260.

Lapen, D.R., and Martz, L.W. 1993. The measurement of two simple topographic indices of wind sheltering-exposure from raster digital elevation models. Computers and Geosciences, **19**: 769-779.

Langham, E.J. 1981. Physics and properties of snowcover. *In* Handbook of Snow: Principles, Processes, Management and Use. *Edited by* D.M. Gray, D.H. Male. Pergamon Press, Toronto, ON, pp. 275-237.

Lettau, H. 1969. Note on aerodynamic roughness-parameter estimation on the basis of roughness-element description. Journal of Applied Meteorology, **8**: 828-832.

Leverington, D.W., and Duguay, C.R. 1996. Evaluation of three supervised classifiers in mapping "depth to late-summer frozen ground", central Yukon Territory. Canadian Journal of Remote Sensing, **22**: 163-174.

Li, L., and Pomeroy, J.W. 1997a. Estimates of threshold wind speeds for snow transport using meteorological data. Journal of Applied Meteorology, **36**: 205-213.

Li, L., and Pomeroy, J.W. 1997b. Probability occurrence of blowing snow. Journal of Geophysical Research, **102D**: 21,955-21,964.

LI-COR inc. 1990. LAI-2000 Plant Canopy Analyser, for rapid, non-destructive, leaf area index measurements. Lincoln, NE, PCA2-1190.

LI-COR inc. 1992. LAI-2000 Plant Canopy Analyser, Operating Manual. Lincoln, NE, p.F-1.

Liston, G., McFadden, J.P., Sturm, M., and Pielke, R.A.Sr. 2002. Modelled changes in arctic tundra snow, energy and moisture fluxes due to increased shrubs. Global Change Biology, **8**: 17-32.

Liston, G.E., and Sturm, M. 1998. A snow-transport model for complex terrain. Journal of Glaciology, **44**: 498-516.

Lunardini, V.J. 1981. Heat transfer in cold climates. Van Nostrand Reinhold Co., New York, NY.

Mackay, J.R. 1977. Probing for the bottom of the active layer. *In* Report of Activities, Part A. Geological Survey of Canada, Paper 77-1A, pp. 327-328.

Mackay, J.R. 1997. A full-scale field experiment (1978-1995) on the growth of permafrost by means of lake drainage; western arctic coast: a discussion of the method and some results. Canadian Journal of Earth Sciences, **34**: 17-33.

Mackay, J.R., and MacKay, D.K. 1974. Snow cover and ground temperatures, Garry Island, N.W.T. Arctic, **27**: 287-296.

Marks, D., Winstarl, A., and Seyfried, M. 2002. Simulation of terrain and forest shelter effects on patterns of snow deposition, snowmelt and runoff over a semi-arid mountain catchment. Hydrological Processes, **16**: 3605-3626.

Martinez, A.J. and Lopez-Portillo, J. 2003. Allometry of *Prosopis glandulosa* var. *torreyana* along a topographic gradient in the Chihuahuan desert. Journal of Vegetation Science, **14**: 111-120.

McKay, G.A., and Gray, D.M. 1981. The distribution of snowcover. *In* Handbook of Snow: Principles, Processes, Management and Use. *Edited by* D.M. Gray, D.H. Male . Pergamon Press, Toronto, ON, pp. 153-190.

McMicheal, C.E., Hope, A.S., Stow, D.A., and Fleming, J.B. 1997. The relation between active layer depth and a spectral vegetation index in arctic tundra landscapes of the North Slope of Alaska. International Journal of Remote Sensing, **18**: 2371-2382.

Meiman, J.R. 1970. Snow accumulation related to elevation, aspect, and forest canopy. Proceedings, Workshop Seminar on Snow Hydrology. Queen's Printer of Canada, Ottawa, ON, pp. 35-47.

Meteorological Services of Canada. 2007. Historical Canadian Climate Database, Version 2; Monthly Rehabilitated Precipitation and Homogenized Temperature Data Sets. Climate Monitoring Research Branch, Meteorological Service of Canada. http://www.cccma.bc.gc.ca/hccd/. Accessed May 16, 2007.

Michel, F.A. 1984. Isotope geochemistry of frost-blister ice, North Fork Pass, Yukon, Canada. Canadian Journal of Earth Sciences, **23**: 543-549.

Morrissey, L.A., and Strong, L.L. 1986. Mapping permafrost in the boreal forest with thematic mapper satellite data. Photogrammetric Engineering and Remote-Sensing, **52**: 1513-1520.

Mueller-Dombois, D., and Ellenberg, H. 1974. Aims and Methods in Vegetation Ecology. John Wiley & Sons, New York, NY.

Muller, S.W. 1947. Permafrost or Permanently Frozen Ground and Related Engineering Problems. J. W. Edwards Inc., Ann Arbor, MI.

Nelson F.E., and Outcalt, S.I. 1983. A frost index number for spatial prediction of ground-frost zones. Proceedings, Fourth International Conference on Permafrost, Fairbanks, AK, pp. 907-911.

Nelson, F.E., Shiklomanov, N.I., and Mueller, G.R. 1997. Estimating active-layer thickness over a large region: Kuparuk River Basin, Alaska, U.S.A. Arctic and Alpine Research, **29**: 367-378.

Niklas, K.J. 1994. Plant Allometry. The University of Chicago Press, Chicago, IL.

Norris, D.K. and Dyke, L.D. 1997. Proterozoic. *In* The Geology, Mineral, and Hydrocarbon Potential of Northern Yukon Territory and Northwestern District of Mackenzie. *Edited by* D.K. Norris, Geological Survey of Canada, Bulletin 422, pp.65-84.

Olsson, L., and Pilesjö, P. 2002. Approaches to spatially distributed hydrological modelling in a GIS environment. *In* Environmental Modelling with GIS and Remote-Sensing. *Edited by* A. Skidmore. Taylor and Francis, London, UK, pp.166-199.

Osterkamp, T.E., and Romanovsky, V.E. 1997. Freezing of the active layer on the coastal plain of the Alaskan arctic. Permafrost and Periglacial Processes, **8**: 23-44.

Peddle, D.R., and Franklin, S.E. 1993. Classification of permafrost active layer depth from remotely-sensed and topographic evidence. Remote Sensing of Environment, **44**: 67-80.

Pollard, W.H., and French, H.M. 1983. The occurrence of seasonal frost mounds, North Fork Pass, Ogilvie Mountains, Yukon Territory. *In* Proceedings of the 4th International Conference on Permafrost, July 17-22 1983. National Academy Press, Washington, D.C. Vol. 1, pp.1000-1004.

Pollard, W.H., and French, H.M. 1984. The groundwater hydraulics of seasonal frost mounds. North Fork Pass, Yukon Territory. Canadian Journal of Earth Sciences, **21**: 1073-1081.

Pomeroy, J.W., and Gray, D.M. 1990. Saltation of snow. Water Resources Research, **26**: 1583-1595.

Pomeroy, J.W., Gray, D.M., and Landine, P.G. 1993. The prairie blowing snow model: characteristics, validation, operation. Journal of Hydrology, **144**: 165-192.

Pomeroy, J.W., Marsh, P., and Gray, D.M. 1997. Application of a distributed blowing snow model to the arctic. Hydrological Processes, **11**: 1451-1464.

Prasad, R., Tarboton, D.G., Liston, G.E., Luce, C.H., and Seyfried, M.S. 2001. Testing a blowing snow model against distributed snow measurements at Upper Sheep Creek, Idaho, United States of America. Water Resources Research, **37**: 1341-1359.

Purves, R.S., Barton, J.S., Mackaness, W.A., and Sugden, D.E. 1998. The development of a rule-based spatial model of wind transport and deposition of snow. Annals of Glaciology, **26**: 197-202.

Raupach, M.R. 1994. Simplified expressions for vegetation roughness length and zero-plane displacement as functions of canopy height and area index. Boundary-Layer Meteorology, **71**: 211-216.

Ricker, K.E. 1959. An investigation of morphological, periglacial, pedological,and botanical criteria for possible use in the chronology of morainal sequences. M.Sc. thesis, University of British Columbia, BC.

Riseborough, D.W. 2001. An analytical model of the ground surface temperature under snow cover with soil freezing. Proceedings, 58th Eastern Snow Conference, Ottawa, Ontario. http://www.easternsnow.org/proceedings/2001/Riseborough. Accessed May 16, 2007.

Roe, G.H. 2005. Orographic precipitation. Annual Review of Earth and Planetary Sciences, **33**: 645–71.

Romanovsky, V.E. and Osterkamp, T.E. 1997. Thawing of the active layer on the coastal plain of the Alaskan arctic. Permafrost and Periglacial Processes, **8**: 1-22.

Schaerer, P.A. 1981. Avalanches. *In* Handbook of Snow: Principles, Processes, Management and Use. *Edited by* D.M. Gray, D.H. Male. Pergamon Press, Toronto, ON, pp. 475-516.

Schimel, J.P., Bilbrough, C., and Welker, J.M. 2004. Increased snow depth affects microbial activity and nitrogen mineralization in two Arctic tundra communities. Soil Biology and Biochemistry, **36**: 217–227.

Scorer, R.S. 1978. Environmental Aerodynamics. Ellis Horwood Ltd., Chichester, UK.

Sheskin, D.J. 2000. Handbook of Parametric and Nonparametric Statistical Procedures. Chapman & Hall/CRC, Boca Raton, FL.

Shippert, M.M., Walker, D.A., Auerbach, N.A., and Lewis, B.E. 1995. Biomass and leaf-area index maps derived from SPOT images for Toolik Lake and Imnavait Creek areas Alaska. Polar Record, **31**: 147-154.

Slatyer R.O., Cochrane, O.M., and Galloway, R.W. 1984. Duration and extent of snow cover in the Snowy mountains and a comparison with Switzerland. Search, **15**: 327-331.

Smith, M.W., 1975. Microclimatic influences on ground temperatures and permafrost distribution, Mackenzie Delta, Northwest Territories, Canadian Journal of Earth Sciences, **12**: 1421-1438.

Sturm, M., and Benson, C.S. 1997. Vapour transport, grain growth and depth-hoar development in the subarctic snow. Journal of Glaciology, **43**: 42-59.

Sturm, M., Holmgren, J., König, M., and Morris, K. 1997. The thermal conductivity of seasonal snow. Journal of Glaciology, **43**: 26-41.

Sturm, M. and Johnson, J.B. 1992. Thermal conductivity measurements of depth hoar. Journal of Geophysical Research, **97**: 2129-2139.

Sturm, M., McFadden, J.P., Liston, G., Chapin, S. III, Racine, C.H., and Holmgren, J. 2001. Snow-shrub interactions in arctic tundra : a hypothesis with climatic implications. Journal of Climate, **14**: 336-344.

Takeuchi, M. 1980. Vertical profile and horizontal increase of drift-snow transport. Journal of Glaciology, **26**: 481-492.

Taras, B., Sturm, M., and Liston, G.E. 2002. Snow-ground interface temperatures in the Kuparuk River basin, arctic Alaska: measurements and model. Journal of Hydrometeorology, **3**: 377-394.

Tarnocai, C., Smith, C.A.S., and Fox, C.A. 1993. International Tour of Permafrost Affected Soils: The Yukon and Northwest Territories of Canada. Centre for Land and Biological Resources Research, Research Branch, Agriculture Canada, Ottawa.

Tenhumen, J.D., Lange, O.L., Hahn, S., Siegwolf, R., and Oberbauer, S.F. 1992. The ecosystem role of poikilohydric tundra plants. *In* Arctic Ecosystems in a Changing Climate, and Ecophysiological Perspective. *Edited by* F.S.III Chapin, R.L. Jefferies, J.F. Reynolds, G.R. Shaver, J. Svoboda. Academic Press, San Diego, CA, pp. 213-237.

Thomas, R., and Rampton, V. 1982. Surficial geology and geomorphology, Blackstone River, Yukon Territory. Geological Survey of Canada. Map 7-1982, scale 1: 100 000.

Wahl, H.E., Fraser, D.B., Harvey, R.C., and Maxwell, J.B. 1987. Climate of Yukon. Atmospheric Environment Service, Environment Canada, Climatological Studies No. 40.

Wahl, H.E. 2004. Climate. *In* Ecoregions of Yukon Territory: Biophysical properties of Yukon landscapes. *Edited by* C.A.S. Smith, J.C. Meikle and C.F. Roots, Agriculture and Agri-Food Canada, PARC Technical Bulletin No. 04-01, pp. 19-23.

Walker, D.A., Epstein, H.E., Jia, G.J., Balser, A., Copass, C., Edwards, E.J., Gould, W.A., Hollingsworth, J., Knudson, J., Maier, H. A., Moody, A., and Raynolds, M. K. 2003. Phytomass, LAI, and NDVI in northern Alaska: relationships to summer warmth, soil pH, plant functional types, and extrapolation to the circumpolar Arctic. Journal of Geophysical Research, **108D2**, 8169, doi: 10.1029/2001JD000986.

Weiss, M., Baret, F., Smith, G.J., Jonckheere, I., and Coppin, P. 2004. Review of methods for in situ leaf area index (LAI) determination Part II. Estimation of LAI, errors and sampling. Agricultural and Forest Meteorology, **121**: 37-53.

Welles, J.M. 1990. 3. Some indirect methods of estimating canopy structure. Remote Sensing Reviews, **5**: 31-43.

Welles, J.M., and Norman, J.M. 1991. Instrument for indirect measurement of canopy architecture. Agronomy Journal, **83**: 818-825.

Whiteman, C.D. 2000. Mountain meteorology: fundamentals and applications. Oxford University Press, New York, NY.

William, P.J., and Smith, M.W. 1989. The Frozen Earth: Fundamentals of Geocryology. Cambridge University Press, Cambridge, UK.

Winstral, A., Elder, K., and Davis, R.E. 2002. Spatial snow modeling of wind-redistributed snow using terrain-based parameters. Journal of Hydrometeorology, **3**: 524-538.

Winstral, A., and Marks, D. 2002. Simulating wind fields and snow redistribution using terrain-based parameters to model snow accumulation and melt over a semi-arid mountain catchment. Hydrological Processes, **16**: 3585–3603.

Yoshino, M.M. 1975. Climate in a small area : An introduction to local meteorology, Tokyo University press, Tokyo, Japan.

Yosida, Z. 1955. Physical studies on deposited snow I: thermal properties. Contributions from the Institute of Low Temperature Science, **7**: 19-74.

Yukon Ecoregions Working Group, 2004. North Ogilvie Mountains. *In* Ecoregions of Yukon Territory: Biophysical properties of Yukon landscapes. *Edited by* C.A.S. Smith, J.C, Meikle and C.F. Roots, Agriculture and Agri-Food Canada, PARC Technical Bulletin No. 04-01, pp. 123-130.

Yukon Territorial Government. 2006. Snow depth and density along the Dempster Highway, 1991 to 2004. Department of Environment, Report to file.

Zhang, T., Osterkamp, T.E., Stamnes, K. 1996. Influence of the depth hoar layer of the seasonal snow cover on the ground thermal regime. Water Resources Research, **32**: 2075-2086.

Zinko, U., Seibert, J., Dynesius, M., and Nilsson, C. 2005. Plant species numbers predicted by a topography-based groundwater flow index. Ecosystems, **8**: 430-441.